

SPATIAL AND TEMPORAL CHARACTERISTICS OF RUNOFF PROCESSES
ON A PUERTO RICAN WATERSHED REPRESENTATIVE OF THE HUMID
MONTANE TROPICS

By

ROBERT A. SWETT

A DISSERTATION PRESENTED TO THE GRADUATE SCHOOL
OF THE UNIVERSITY OF FLORIDA IN PARTIAL FULFILLMENT
OF THE REQUIREMENTS FOR THE DEGREE OF
DOCTOR OF PHILOSOPHY

UNIVERSITY OF FLORIDA

1999

To the memory of Dr. Leonard Zabler.

ACKNOWLEDGMENTS

First and foremost, my gratitude is extended to God for blessings bestowed and strength imparted.

I wish to express appreciation to my supervisory committee. Dr. Gustavo Antonini, my chair, for his support and guidance, and for the invaluable lessons garnered under his tutelage. Special thanks are accorded my cochair, Dr. Peter Waylen, whose keen intellect is exceeded only by the generous and giving spirit he displayed as he shepherded me through the process. Drs. Joann Mossa, Ken Campbell, and Paul Zwick were constant sources of encouragement and they provided me with deep insights into the fields of hydrological and information sciences. I thank Dr. Caviedes, chair of the Geography Department, for his generosity. Dr. Leonard Zobler is dearly missed and his contributions to my life extend well beyond this dissertation.

I thank the U.S. Geological Survey in Puerto Rico and Zaida Aquino in particular for graciously providing the necessary hydrologic data to complete this work. I appreciate the generosity of Dr. Matthew Larsen who answered my many questions and took me to visit research sites maintained by the Geological Survey in the Luquillo Experimental Forest. Dr. Ariel Lugo of the U.S. Forest Service facilitated my visit to Puerto Rico and, with Frederick Scatena, provided valuable information and access to bibliographic resources at the International

Institute of Tropical Forestry in Puerto Rico. My thanks go to Dr. Keith Beven of Lancaster University, Lancaster, UK, for providing access to his hydrological model, TOPMODEL. The following entities provided funding and resources, which greatly facilitated the work: the Geography Department, the Center for Latin American Studies and the Graduate School at the University of Florida, and the U.S. Agency for International Development.

My sincere appreciation to the administrative staff of the Geography Department, Julia Williams, Desiree Price, and Carolyn Hall, for their help and good will. Thanks and appreciation are owed to my fellow students and co-workers, David Fann and Drs. Paul Box, Rene Ledesma, and Charles Sidman. Their support, guidance, and fellowship have been a source of tremendous comfort.

To my family, the rock that sustained me during my journey, I wish to express my deep and heartfelt gratitude. Antonieta, my wife, is a font of understanding, wisdom, patience, and love. I am blessed and enhanced because of her. My children, Miguel, Elizabeth, and Christopher, are continual sources of joy and delight. Their spirit rejuvenates and strengthens mine. My parents, together with my brothers and sisters, laid the foundation for any success I may enjoy, and I thank them.

TABLE OF CONTENTS

	page
ACKNOWLEDGMENTS	iii
TABLE OF CONTENTS	v
LIST OF TABLES	viii
LIST OF FIGURES	ix
ABSTRACT	xii
CHAPTERS	
1. INTRODUCTION	1
Background	1
Objectives	3
Structure of Presentation	5
2. LITERATURE REVIEW	7
Conceptual Framework	7
The Historical Context of Hillslope Hydrology	8
Runoff Generating Mechanisms	11
Subsurface Flow	13
Preferential Flow	15
Translatory Flow	15
Groundwater Ridging	16
Principal Controls of Hydrologic Behavior	16
Effective Precipitation	18
Baseflow Analysis and Hydrograph Separation Techniques	21
3. SITE DESCRIPTION AND CHARACTERIZATION	28
The Caribbean Region	28
Puerto Rico	30

Characteristics of Río Icacos Basin and Northeastern Interior	
Puerto Rico.....	33
Río Icacos Basin	35
Land Use / Land Cover	36
Geology and Soils	36
Hydrologic Controls and Processes	38
Precipitation and runoff.....	40
Interception, throughfall, and stemflow	43
Evapotranspiration and temperature.....	43
Soil water and groundwater	45
Hypothesized Runoff Generating Mechanisms Operative in	
Río Icacos Basin	47
4. TOPOGRAPHY-BASED HYDROLOGIC MODEL	48
TOPMODEL Theory	49
Model Structure	53
5. RESEARCH METHODS	58
Data Processing	59
GIS Coverages	59
Precipitation and Discharge	61
Data Limitations.....	61
Storm Events	62
Hydrograph Separation.....	62
Determination of Net Precipitation	66
Selection of Individual Precipitation and Discharge Events	70
Statistical Analysis of Storm Event Descriptors.....	72
Topographic Analysis	75
6. RESULTS AND DISCUSSION	82
Recession Curve Analysis.....	82
Description of Storm Events.....	85
Statistical Analysis	87
Maximum Precipitation Intensity Versus Peak Instantaneous	
Runoff Rate	87
Quickflow Versus Basin Wetness.....	93
Discussion of Statistical Analysis	102
Topographic Analysis	109
TOPMODEL Parameter Determination	117
Event Simulation	120
Discussion of TOPMODEL Simulations	125

7. SUMMARY AND CONCLUSIONS.....	133
LIST OF REFERENCES.....	139
BIOGRAPHICAL SKETCH.....	150

LIST OF TABLES

Table	page
5-1. Name, parameter, identifier, and period of record for 15-minute interval precipitation and discharge stations located in the vicinity of Río Icacos basin.	61
5-2. Storm parameters derived for each event.	72
5-3. Cross-sectional area and channel velocity calculations for a range of discharges recorded at the outlet of Río Icacos.	81
6-1. Storm descriptors used in the analysis of 35 events that occurred on Río Icacos basin: 1993-1997.	86
6-2. Regression results of log peak instantaneous runoff rate versus log maximum precipitation intensity for Río Icacos basin.	93
6-3. Pearson Product-Moment Correlations for quickflow proportion, mean baseflow, antecedent baseflow, and gross precipitation for Río Icacos basin.	100
6-4. Pearson Product-Moment Correlations for quickflow proportion, mean baseflow, antecedent baseflow, and gross precipitation for Geebung Creek.	100
6-5. Regression results of quickflow proportion versus log mean baseflow and log gross precipitation for Río Icacos basin.	102
6-6. Comparison of average monthly precipitation and runoff at the Río Icacos and Guabá basin outlets during wet and dry periods: 11/1993 - 9/1997.	114

LIST OF FIGURES

Figure	page
2-1. Principal runoff generating mechanisms.	12
3-1. Location of Río Icacos basin in eastern Puerto Rico.	29
3-2. Locations of meteorological stations, discharge gages, and U.S. Army Corps of Engineers study sites in the vicinity of the Río Icacos basin.	34
3-3. Land cover in the Río Icacos basin and Guabá subcatchment.	37
3-4. Soil types in the Río Icacos basin and Guabá subcatchment.	39
3-5. Río Icacos basin: mean monthly precipitation and runoff: 1983-1995; mean monthly runoff: 1945-1997.	42
3-6. Probabilities associated with precipitation intensity for northeast Puerto Rico.	44
4-1. TOPMODEL program structure.	54
6-1. Determination of the quickflow termination point using baseflow recession curves from Río Icacos basin and Quebrada Blanca.	84
6-2. Boxplot showing the distribution of maximum precipitation intensity values recorded at Guabá during 35 storm events.	89
6-3. Histogram showing the distribution of maximum precipitation intensity values recorded at Guabá during 35 storm events.	89
6-4. Boxplot showing the distribution of peak instantaneous runoff rates recorded for Río Icacos during 35 storm events.	91
6-5. Histogram showing the distribution of peak instantaneous runoff rates recorded for Río Icacos during 35 storm events.	91
6-6. Log-Log regression plot of peak instantaneous runoff rate versus maximum precipitation intensity for Río Icacos basin.	92

6-7. Log-Log regression plot of peak instantaneous runoff rate versus maximum precipitation intensity for Geebung Creek.	92
6-8. Boxplot showing the distribution of mean baseflow values recorded for Río Icacos during 35 storm events.	95
6-9. Histogram showing the distribution of mean baseflow values recorded for Río Icacos during 35 storm events.	95
6-10. Boxplot showing the distribution of antecedent baseflow recorded for Río Icacos prior to 35 storm events.	96
6-11. Histogram showing the distribution of antecedent baseflow recorded for Río Icacos prior to 35 storm events.	96
6-12. Boxplot and histogram showing the distribution of the quickflow proportion recorded for Río Icacos during 35 storm events.	97
6-13. Boxplot showing the distribution of gross precipitation values recorded at Guabá during 35 storm events.	98
6-14. Histogram showing the distribution of gross precipitation values recorded at Guabá during 35 storm events.	98
6-15. Regression plots of quickflow versus mean baseflow and gross precipitation for Río Icacos basin and Geebung Creek.	101
6-16. Comparison of the water level rise in two floodplain wells with the stream level rise during a storm event.	106
6-17. Sixty day moving average of daily runoff for Río Icacos: 1992-1997.	108
6-18. Regression plot of quickflow proportion versus mean baseflow for 11 storm events that occurred during a dry hydrologic period on the Río Icacos basin.	110
6-19. Mean monthly precipitation and runoff recorded at the Río Icacos and Guabá basin outlets from 11/1993 to 9/1997.	111
6-20. Average monthly precipitation and runoff recorded at the Río Icacos and Guabá basin outlets during wet and dry periods: 11/1993 - 9/1997.	113

6-21. September 7, 1994 storm event calibration: observed versus simulated runoff from Guabá basin.....	121
6-22. June 11, 1994 storm event validation: observed versus simulated runoff from Guabá basin.....	123
6-23. October 28, 1996 storm event calibration: observed versus simulated runoff from Guabá basin.....	124
6-24. January 7, 1996 storm event validation: observed versus simulated runoff from Guabá basin.....	126
6-25. Slope ranges, 10-meter contours, and topographic index values for Guabá subcatchment.....	127
6-26. Water table response to daily rainfall at USACE site A.....	129
6-27. Change in water table elevation at USACE site A with respect to the initial water table depth and the daily rainfall	131

Abstract of Dissertation Presented to the Graduate School
of the University of Florida in Partial Fulfillment of the
Requirements for the Degree of Doctor of Philosophy

**SPATIAL AND TEMPORAL CHARACTERISTICS OF RUNOFF PROCESSES
ON A PUERTO RICAN WATERSHED REPRESENTATIVE OF THE HUMID
MONTANE TROPICS**

By

Robert Swett

May, 1999

Chair: Dr. Gustavo A. Antonini

Cochair: Dr. Peter R. Waylen

Major Department: Geography

Humid tropical steeplands contain fragile environments prone to natural disturbances and often subject to anthropogenic activities. These factors can upset the tenuous physical balance of steepland areas and result in system disturbances, such as erosion and slope movements. System responses are coupled to the pathways that precipitation receipts follow en route to the drainage basin outlet. The spatial and temporal distribution of potential surface and subsurface runoff generating mechanisms on a watershed has important implications for management practices. The objective of this research is to differentiate mechanisms and source areas that, together, define the characteristics of storm water runoff from a tropical steepland environment.

A well-instrumented, undisturbed 3.26-km² watershed located in the Luquillo Experimental Forest of Puerto Rico was selected for analysis. A literature review was conducted to determine physical and climatic characteristics associated with particular runoff generating mechanisms. Preliminary inferences were made as to the spatial and temporal characteristics of runoff processes in the study watershed, based on information derived from maps of topography, geology, vegetation, and soils, climate and discharge records, and field observations. Thirty-five hydrologic events were selected from 15-minute precipitation and discharge records to test for the inferred runoff mechanisms. Statistical analysis of precipitation and hydrograph parameters was compared with results for a basin well described by the variable source area concept.

A topography-based hydrologic computer simulation model was used to simulate the hydrographs for a subset of the 35 storm events. Model parameterization was based on field data and calibration and validation was performed on separate events. Comparison of timing, shape, and magnitude characteristics of predicted and observed storm event hydrographs provided additional evidence of the prevalent runoff processes and of the existence and spatial distribution of runoff source areas.

The research advances knowledge of runoff processes and contributes to a more effective management of tropical steep-land landscapes. Land use management and accurate assessment of the impact of human activities require an understanding of the spatial and temporal characteristics of drainage basin

runoff. Awareness of these physical relationships contributes to sustainable yield and to the social and economic stability of rural areas.

CHAPTER 1 INTRODUCTION

Background

The inherent beauty of montane regions of the humid tropics is attributed, in part, to steep slopes and a highly dissected topography blanketed with diverse vegetation. Unfortunately, these same ingredients often contribute to the fragility of steepland hillslopes. Exogenous events further exacerbate the tenuous physical balance that exists in steepland areas. Precipitation in tropical and subtropical steepland areas may occur as intense convectional storms, often concentrated during a short season or in conjunction with tropical waves or hurricanes. These events provide potent energy inputs that profoundly impact the form and function of the steepland ecosystem.

The sustainable use of tropical steeplands is dependent on both anthropogenic and natural factors. Land use decisions are applied to the basic geomorphic unit: the hillslope, which may be viewed as a delicately balanced system that adjusts to exogenous energy inputs and to internal and external slope processes, as in mass wasting. Anthropogenic activities, such as agriculture, forestry, and construction, often disturb this balance. System responses, such as erosion and slope movements, are an attempt to restore steady-state equilibrium conditions (Pethick, 1984). These system responses

are intimately linked to the pathways that precipitation receipts follow while in transit to the basin outlet.

No consensus or unifying theory exists that can explain or predict the hydrologic behavior of basins at various scales (Pearce et al., 1986). Current knowledge of the mechanisms of runoff generation has been derived almost exclusively from research conducted in temperate regions and relatively few intensive field investigations have been conducted in tropical humid areas (Bonell and Balek, 1993). Most information concerning hydrologic behavior of tropical basins is largely qualitative or anecdotal in nature. This situation stems, partly, from the relative paucity of data sets that are sufficient to adequately describe and model basin hydrology. The management of resources in tropical areas requires a sound understanding of hydrologic processes on undisturbed basins and their relation to foreseen and unforeseen alterations in land use and land cover. The utilization of hydrologic models to manage tropical resources necessitates the selection of models that adequately describe runoff generating mechanisms and which can be operationalized with the data available in tropical regions.

Puerto Rico offers a bridge to our understanding and modeling of hydrologic responses in tropical environments. Various entities, such as the U.S. Geological Survey, the U.S. Forest Service, the University of Puerto Rico, and other Commonwealth agencies have long-term environmental monitoring programs and research projects, particularly in the tropical humid montane regions of the northeast. Major research initiatives in Puerto Rico include the

Water-Energy-Biogeochemical Budgets Program of the U.S. Geological Survey (Larsen et al., 1992) and a National Science Foundation funded Long Term Ecological Research Site, both located in the Luquillo Mountains of northeast Puerto Rico. A long established, well-equipped research facility at El Verde in the Luquillo Mountains has helped attract a steady stream of scientists and researchers to the Island. A wealth of information, generated by investigations dating back 100 years to the present, has added considerable detail to existing, island-wide survey programs, such as the National Cooperative Soil Survey (Boccheciampi, 1977; National Soil Survey Center, 1998). Inferences and conclusions regarding runoff mechanisms that are drawn from this relatively data rich environment will extend baseline knowledge and should be transferable to similar environments.

Objectives

This research proposes to characterize the runoff generating mechanisms that predominate in a tropical steeppland environment. Various mechanisms may contribute to storm runoff during and following precipitation events on watersheds. The degree to which a particular process contributes to the shape of the discharge hydrograph is a function of several primary factors, including soil characteristics, topography, antecedent moisture conditions, ground water levels, and precipitation characteristics. The spatial and temporal distribution of runoff processes on a watershed has important implications for management practices. This research applies a methodology to identify the physical

hydrology of water fluxes and to represent spatial and temporal patterns of runoff processes on a tropical steepland watershed.

The methodology is applied to a representative watershed in Puerto Rico. The candidate watershed was chosen based on the availability of information needed to characterize hydrologic response, including climatic and stream discharge records and physical characteristics, such as land cover, topography, geomorphology, and soil parameters. The results of this research should lead to a better understanding of the runoff processes that occur on tropical steepland watersheds and elsewhere. Results could then be incorporated into models and management decisions to more accurately reflect the effects of land use modification on tropical steepland watersheds.

The specific research objectives are to

- 1) Ascertain, from the literature, the physical and climatic characteristics of a site or region that are associated with specific runoff generating mechanisms.
- 2) Inventory and assess the attributes associated with hydrologic behavior within the humid montane region of Puerto Rico in general, and for the study basin in particular.
- 3) Based on the characterizations derived from 1 and 2 above, conjecture as to the prevailing runoff mechanisms that are operative within the study basin.
- 4) Examine statistical relationships among hydrologic parameters derived from a sample of storm events occurring on the study basin. Compare

the results with similar relationships for a basin whose runoff generating mechanisms are well described and amply documented.

- 5) Apply topographic analysis to the study basin and assess its ability to model the runoff generating mechanisms that were conjectured in step 3 and revealed in step 4.

Structure of Presentation

Chapter 2 reviews the literature to determine known relationships between specific runoff generating mechanisms and the physical or climatic characteristics of a site or region. Particular attention is paid to research conducted in humid, montane areas similar to that of the study region. Chapter 3 details the principal hydrologic controls and the physical and climatic characteristics associated with the study basin. The characteristics of the study basin are compared to research results presented for similar basins, and hypothesized runoff generating mechanisms are proposed. Chapter 4 describes the theory and structure of TOPMODEL, a topography-based hydrologic model designed for basins with characteristics similar to those of the study basin. Statistical tests designed to verify the hypothesized runoff mechanisms are presented in Chapter 5 and further verification is provided through implementation of the topography-based hydrologic model. The statistical and topographic analyses are conducted on individual storm events. Chapter 6 presents and discusses the results obtained from the statistical and topographic

analyses. Chapter 7 summarizes the research and provides some conclusions and recommendations.

CHAPTER 2

LITERATURE REVIEW

Conceptual Framework

This chapter presents the historical context that has led to our current knowledge of hillslope runoff processes. Important theoretical milestones and field investigations are reviewed and the climatic and basin characteristics associated with particular runoff generating mechanisms are examined. The review will provide a basis to infer which runoff generating mechanisms predominate in the study basin. Inferences will be tested by examining hydrologic parameters extracted from a subset of storm events, and by the application of a topographic analysis.

The examination of runoff mechanisms, within a research framework, requires an adequate accounting of the precipitation inputs and outputs to a basin or hillslope. The basin, when treated as a hydrological system, may be characterized by the partitioning of water into separate flows by interconnected, controlling processes (Veen and Dolman, 1989). To aid research, it is useful to compartmentalize these partitioning processes into three distinct spatial levels: 1) aboveground, within the vegetative layer, 2) at the soil surface, and 3) within the soil. Methods to identify and quantify the potential abstractions from effective precipitation are reviewed and the runoff mechanisms above and below

the surface are examined. The identification of specific runoff mechanisms depends, partly, on the ability to separate the hydrograph into distinct components, such as quickflow and baseflow. Hydrograph separation requires the isolation of discrete precipitation and discharge events from the period of record. Methods of hydrograph separation and event delineation are reviewed.

The Historical Context of Hillslope Hydrology

Researchers have expended considerable effort to catalog and quantify the full range of runoff mechanisms that are involved in the transformation of precipitation receipts from hillslope to streamflow. Kirkby (1988) underscores the significance of this research when he indicates that approximately 95% of effective precipitation either passes through or over a hillslope while en route to a channel segment. Our current understanding of hillslope hydrologic processes, though incomplete, is built on theoretical studies and on field investigations conducted at various scales, including on plots, hillslopes, and in basins. This research thread extends back to the early 1930's, when R. E. Horton began publishing ideas that led to the infiltration theory of overland flow.

Horton (1933), in a classic paper, suggested that the soil surface partitions precipitation between overland flow and vertical drainage to groundwater. Horton postulated that the storm event hydrograph is dominated by overland flow generated uniformly over the basin surface area, and that infiltrated water serves to recharge the groundwater reservoir. Infiltrated water was assumed to contribute solely to long-term recession discharge, given its

inherently low flux rate (Dunne, 1983). Infiltration-excess overland flow, or so-called Hortonian overland flow, occurs when rainfall or snowmelt rates exceed the infiltration capacity of a soil. Horton's concept of infiltration-excess overland flow complemented Sherman's (1932) unit hydrograph theory, the most widely utilized model of surface hydrology (Hromadka, 1987). Both theories provided very successful tools for solving hydrologic problems and, as a result, research into hillslope runoff processes was dampened until the 1960's (Anderson and Burt, 1990a).

C. R. Hursh, a contemporary of Horton, noted that infiltration-excess overland flow rarely occurred on the experimental basins of the Coweeta Hydrologic Laboratory in North Carolina (Crossley and Swank, 1988). His observations were corroborated during the 1960's, by several researchers working primarily in undisturbed, humid, temperate watersheds (Hewlett and Hibbert, 1967). Numerous storm hydrographs were observed that exhibited the classic shape associated with surface flow in the absence of any recorded overland flow (Tischendorf, 1969; Rawitz et al., 1970). Additional investigations revealed that the rainfall intensity in these humid temperate areas seldom exceeded infiltration capacity and storm runoff originated from areas of limited spatial extent, commonly located adjacent to stream channels.

The increasing lack of evidence for basin-wide overland flow led Betson (1964) to propose the 'partial area' concept as a modification of Horton's infiltration theory (Betson and Marius, 1969). Betson suggested that runoff issued from a relatively consistent and small portion of a basin, the spatial extent

of which varied minimally with precipitation intensity and antecedent moisture conditions. Partial areas in the southern Appalachians were noted to comprise approximately 5% of basin area in light-to-moderate storms and 40% during heavier storms (Chorley, 1978; Ponce, 1989).

Betson's partial area concept, in conjunction with frequent observations of contributing areas that expanded and contracted both seasonally and during storms, led to the 'variable source area' concept of hillslope hydrology (Hewlett and Hibbert, 1967) and to subsequent variations of that model (Freeze, 1974; Bonell and Balek, 1993). Source areas commonly occur 1) at slope bases adjacent to streams, 2) in association with topographic features such as concavities and hollows, where fluxes converge, and 3) in conjunction with thin soils (Kirkby and Chorley, 1967). The variable source area concept became the dominant model for hillslope hydrology in undisturbed basins, and subsurface flow was the assumed delivery mechanism of upslope infiltrated moisture to the source areas (Anderson and Burt, 1990b).

Hortonian overland flow, or infiltration-excess overland flow, largely was dismissed as a significant runoff mechanism with the ascendance of the variable source area concept (Van de Griend and Engman, 1985; Kirkby, 1988). Initially, infiltration-excess overland flow was assumed to be restricted to sparsely vegetated, arid regions. Subsequent studies have shown that infiltration-excess overland flow occurs under a wider variety of circumstances, including on degraded, eroded, or thin soils. Significantly, Bruijnzeel (1983) did not observe Hortonian overland flow in an undisturbed tropical rainforest, even with

precipitation intensities of 200 mm/hr. The infiltration capacity of soils in humid temperate regions is, in general, high enough to eliminate infiltration-excess runoff as a major contributor (Dunne et al., 1975; Anderson and Burt, 1978b). Infiltration-excess overland flow is assumed to occur rarely under natural conditions in humid tropical environments (Van de Griend and Engman, 1985).

Runoff Generating Mechanisms

The widespread acceptance of the variable source area concept generated a proliferation of field investigations and theoretical studies designed to isolate the mechanisms of individual runoff processes that supply source areas, and to devise methods to delineate source areas (Anderson and Burt, 1990b). The principal storm runoff mechanisms recognized today include partial-area or Hortonian overland flow, saturation-excess overland flow, and subsurface flow, including rapid throughflow of new water or displacement of old water (Pearce et al., 1986; Anderson and Burt, 1990b). Subsurface flow can further be distinguished as Darcian (e.g. soil matrix flow) or non-Darcian, including macropore flow and pipe flow (Anderson and Burt, 1990b). Return flow, the exfiltration of subsurface water, is associated with topographic concavities, flow convergence zones, and shallow soil profiles (Kirkby, 1988). Figure 2-1 presents a broad compartmentalization of the various runoff mechanisms.

Variable source areas, frequently observed adjacent to stream channels in undisturbed basins, expand and contract in sync with hydrometeorological

conditions, thus dynamically altering the hydrologic behavior of a basin. The dynamic nature of source areas, both within storms and between storms, has made their inclusion in hydrologic models difficult (Van de Griend and Engman, 1985). Most studies have resorted to the tedious application of field techniques in order to map the spatial extent of source areas (Anderson and Burt, 1978b; Dunne, 1983).

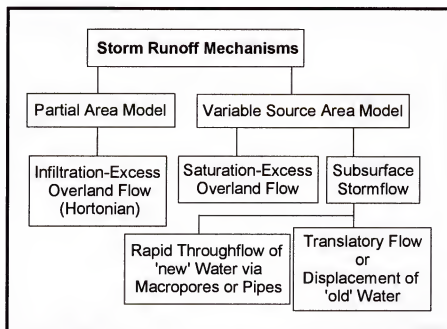


Figure 2-1. Principal runoff generating mechanisms (Burt, 1989).

Variable source areas commonly are associated with saturation-excess overland flow or with saturated subsurface flow. Saturation-excess overland flow occurs when soil moisture storage capacity is filled, thus shunting subsequent direct precipitation to overland flow. Profile saturation may occur from above or below. One mechanism of profile saturation, that leads to

saturation-excess overland flow, is by *in situ* accumulation of infiltrated precipitation in conjunction with subsurface flow that originates upslope. Upon saturation, subsequent precipitation receipts onto the saturated areas are shunted to overland flow, and subsurface flow inputs exfiltrate as return flow (Dunne and Black, 1970). Alternatively, source areas may be attributed to a saturated wedge of moisture that is fed by subsurface flow originating upslope and moving laterally above a restricting layer (Weyman, 1973).

Bonell and Gilmour (1978) noted that saturation-excess overland flow is a common occurrence in humid tropical environments, but the general mechanism differs significantly from that of humid temperate regions. They indicated that soils in humid tropical environments commonly decline in permeability with depth and that tropical areas are characterized by high rainfall intensities. The higher precipitation intensities tend to exceed subsoil transmission rates, which leads to soil saturation and, thus, saturation-excess overland flow (Gilmour and Bonell, 1979; Bonell et al., 1981). They also observed subsurface stormflow in the topsoil of steeper slopes and the occurrence of perched water tables, which often induced saturation-excess overland flow.

Subsurface Flow

Subsurface flow, or throughflow, is considered the dominant path by which precipitation receipts on upland slopes are transported to source areas and to stream channels (Burt, 1986). The optimum conditions for lateral subsurface flow include deep, permeable, vegetated soils that decline in permeability with depth, or that overlie an impermeable layer such as bedrock

(Hewlett and Nutter, 1972; Weyman, 1970). A horizontal conductivity that is significantly greater than the vertical conductivity also will induce lateral moisture flow. Slope steepness determines the relative magnitude of the lateral, downslope component of gravitational potential and convergent topographic features enhance lateral flow.

Early research indicated that subsurface velocities, even for saturated throughflow, normally are too low to allow for direct contribution to runoff peaks (Freeze, 1972). It is useful to compare approximate velocities of subsurface and surface runoff as reported in the literature. Whipkey (1965) reported a relatively rapid saturated throughflow velocity of 0.20 m/hr; Dunne (1978) noted overland flow velocities ranging from 10-500 m/hr; and Pilgrim (1966) reported an average channel velocity of 1620 m/hr. Dunne and Black (1970, p. 1303) concluded that, normally, "subsurface stormflow alone is too small, too late, and too insensitive to fluctuations in rainfall intensity to contribute significantly to the storm hydrograph". Exceptions may occur where a thick humus or litter layer exists and where layering may provide for rapid lateral flow. Subsurface flow does have the capacity to maintain high moisture content downslope and, thus, increase the runoff in downslope source areas. Throughflow may provide a substantial and prolonged contribution to baseflow in areas where deep soil overlies impermeable bedrock (Carson and Kirkby, 1972). In some areas throughflow may be the sole source of baseflow (Hewlett, 1961).

Preferential Flow

Concentrated lateral soil-water movement in the form of preferential flow offers a possible mechanism by which subsurface flow may exceed the normal velocities encountered in the soil matrix (Pearce et al., 1986; Sklash et al., 1986). Non-Darcian flows can occur in a variety of soil structures, such as macropores, pipes, root holes, soil cracks, and faunal cavities, and thus bypass the soil matrix. Macropores are non-capillary pores while pipes are slightly larger and usually have been enlarged by erosion. Pipes are further distinguished in that they often occur as interconnected networks, which may offer uninterrupted flow paths from remote locations to source areas or stream channels. Few studies have demonstrated direct contribution to the storm hydrograph from preferential flow mechanisms. Rather, indications are that preferential flow pathways serve to deliver infiltrated water more rapidly to the water table, thus increasing the hydraulic head and contributing to translatory flow.

Translatory Flow

The theory of translatory flow maintains that 'old', or pre-event soil water, is displaced downslope by 'new' water (Pierson, 1980). Translatory flow helps explain the seemingly anomalous occurrence of greater proportions of 'old' water than 'new' water noted in hydrograph studies using conservative tracers (Sklash et al., 1976). Logic dictates that runoff from a storm event would be dominated by current, net precipitation rather than by basin moisture with a longer residence time. Newly infiltrated water acts to 'push' previously infiltrated water

downslope and into the stream channel during translatory flow. The mechanisms of translatory flow have yet to be validated.

Groundwater Ridging

Groundwater ridging is a phenomenon believed to occur in areas adjacent to streams, in association with fine-textured soils and a capillary fringe or tension-saturated zone that is close to the surface (Bonell and Balek, 1993). Theory holds that small inputs of moisture quickly convert small negative potentials into positive pressures leading to a rapid rise in the water table and to a significantly steeper hydraulic gradient. With sufficiently rapid hydraulic conductivities, large volumes of subsurface flow move through stream banks and into the channel (Sklash and Farvolden, 1979; Abdul and Gillham, 1984; Abdul and Gillham, 1989). As with translatory flow, the theory of groundwater ridging is relatively recent and has not been fully corroborated.

Principal Controls of Hydrologic Behavior

Climate (rainfall intensity, storm size), soils (thickness, conductivities, antecedent wetness) and topography (convergence, valley floor slope) are principal controls on runoff processes (Anderson and Burt, 1990b). Based on available evidence, Dunne (1978) associated specific characteristics of basins, in humid temperate regions, with the relative dominance of saturation-excess overland flow and subsurface flow. Accumulated evidence tends to support his view that saturation-excess overland flow is associated with thin soils, gentle terrain, concave lower slopes, and wide valley bottoms while subsurface flow

favors areas with steep, straight or convex slopes, narrow valley bottoms, incised channels, and very permeable slopes (Pearce et al., 1986).

In undisturbed basins of temperate humid areas it has been demonstrated that soil infiltration and percolation rates commonly exceed prevalent rainfall intensities. Few investigations have been conducted in tropical areas, but anecdotal observations indicate that a similar situation holds. One noteworthy exception is a field study conducted with runoff troughs in a wet tropical forest located on the coast of Queensland, Australia. Soils in the basin consist of clays and the mean annual precipitation is 4175 mm (Bonell and Gilmour, 1978). The basin exhibited characteristics normally associated with lateral subsurface flow towards source areas located on lower slopes. Mean hydraulic conductivities of surface soils greatly exceeded rainfall intensities and yet the basin was dominated by overland flow. Analysis revealed that short-term precipitation intensities (6-minute) often exceeded percolation rates of lower soil layers, leading to the development of a perched water table. The soil above the perched water table quickly saturated during storm events and subsequent precipitation was shunted to overland flow.

Beven (1978) demonstrated the importance of local topographic configuration within basin contributing areas, particularly in relation to spatial variations in runoff contributions. When hydraulic conductivity decreases with depth on sloping soils a lateral moisture flux is induced (Anderson and Burt, 1978a) and where topographic convergences occur lateral flows tend to concentrate (O'Loughlin, 1986). With sufficient moisture accumulation the

above conditions may lead to areas of saturation, especially on lower slopes. During a 5-day period, which included two major precipitation events, Anderson and Burt (1978b) made hourly measurements of soil-water potential at a series of locations in a hollow and on an adjacent spur with 25° slopes. Results from this study showed that, in steeply sloping areas, elevation potential dominates over soil water potential in determining the direction of soil water movement downslope.

Research continues into the investigation of hillslope runoff processes. Investigative themes vary and include such topics as preferential flow mechanisms and hydrograph separation via chemical analysis. Progress is iterative, with field studies complementing the development of mathematical models of hillslope processes. Understanding hillslope mechanisms is important, as is understanding the conditions under which they likely occur, in order to facilitate their incorporation into physically-based models (Beven and Kirkby, 1979).

Effective Precipitation

Effective or net precipitation is that portion of incoming rainfall that contributes to streamflow. In order to quantify effective precipitation it is necessary to account for abstractions, such as vegetative cover, which may reduce the amount of incoming precipitation that reaches the ground. A proportion of precipitation will pass directly to the ground as throughflow and another portion is intercepted by vegetation and will subsequently pass to the

ground as stemflow or drip. The remainder is stored on the vegetative surface and evaporates. The controls on the interceptive process consist of meteorological factors, including rainfall intensity and wind speed; and vegetative characteristics such as storage capacity, which is a function of vegetation type and seasonal characteristics. Vegetation also can greatly influence meteorological controls, such as wind turbulence.

Many interception models have been formulated as regression equations characterized by the following general form (Gash, 1979):

$$I = aP_g + b \quad (2-1)$$

where I = interception loss
 P_g = gross rainfall incident on vegetation
 a, b = regression coefficients

In order to place interception modeling on a physical foundation, Rutter et al. (1971) proposed the following formulation (Bonell and Balek, 1993):

$$(1 - p - p_i)P = E_p + D \pm \Delta C \quad (2-2)$$

where P = rainfall rate
 p = throughfall proportion
 p_i = stemflow proportion
 E_p = evaporation rate of water stored on vegetation
 D = drain rate of canopy by drip
 ΔC = change in amount of water stored

The evaporative term in the Rutter equation was determined using the Penman-Monteith equation:

$$\lambda E_p = \frac{[\Delta A + \rho c_p \delta_q g_a]}{[\Delta + \gamma(1 + g_a / g_s)]} \quad (2-3)$$

where λE_p	= evaporative flux
λ	= latent heat of vaporization
A	= available energy
δ_q	= specific humidity deficit
g_a	= aerodynamic conductance
g_s	= surface conductance
Δ	= change of saturation vapor pressure with temperature
ρ	= moist air density
c_p	= specific heat of air at constant pressure
γ	= psychrometric constant

The difficulties in obtaining the necessary meteorological data for the Rutter model led Gash (1979) to devise a model based on fewer parameters. Gash associated a physical meaning with the regression coefficients (a, b) in equation 2-1 above as follows:

$$a = \bar{E} / \bar{R} \quad (2-4)$$

$$b = (S + \int_0^{t'} E dt) \{1 - (\bar{E} / \bar{R})(1 - p - p_t)^{-1}\} \quad (2-5)$$

where \bar{E}	= mean evaporation rate
\bar{R}	= mean rainfall rate
S	= canopy storage capacity
t'	= time interval for saturation of the canopy to occur

Gash determined values for mean evaporation and rainfall rates from a series of storms whose rainfall amounts and intensities exceeded that necessary to saturate the vegetation. The Gash interception model has been used widely and shown to give reasonable estimates of interception losses (Veen and Dolman, 1989; Bonell and Balek, 1993).

Baseflow Analysis and Hydrograph Separation Techniques

The discharge hydrograph represents the integration of all processes that affect and transform precipitation receipts within a basin and it is an obvious evidentiary source to distinguish between potential runoff pathways. The form of the hydrograph partly is a function of the spatial and temporal distribution of various processes, such as the amount and intensity of rainfall, infiltration, evapotranspiration, groundwater flow, and runoff pathways. Hydrograph relationships, such as timing and volume, can be analyzed for evidence of the quickflow runoff pathways that prevail on a particular basin or during a particular storm event. The tools by which a hydrograph is separated into distinct components fall within the domain of hydrograph analysis. The following discussion reviews techniques that are utilized to analyze a hydrograph and, in particular, techniques used to determine baseflow recession rates and to separate a hydrograph into components.

To study any inherent relationships between quickflow pathways and the discharge hydrograph it is necessary to isolate that portion of the hydrograph that is attributed to quickflow. The discharge hydrograph is composed of two major components, baseflow and quickflow. Baseflow is defined as that portion which sustains streamflow during dry periods or during periods of minimal precipitation (Ponce, 1989). Baseflow traditionally has been associated with infiltrated moisture that reaches the water table and slowly discharges into the stream (Singh, 1988). A more inclusive definition incorporates any slow-draining

moisture reserve that provides baseflow under certain conditions, such as from unsaturated soil moisture (Hewlett, 1961; Tallaksen, 1995). Quickflow, or direct runoff, has a relatively fast response time and is defined as that portion of streamflow that occurs during and immediately following a precipitation event. Quickflow may include channel precipitation, overland flow derived from either Hortonian or saturation-excess overland flow, and subsurface flow or interflow.

Recession curve analysis, one aspect of hydrograph analysis, treats the depletion of moisture from a basin, particularly during dry periods or following a precipitation event that results in significant basin recharge. The recession portion of the hydrograph normally will reflect drainage from multiple moisture stores, each of which depletes at its own unique rate (Bras, 1990). Baseflow, the component with the slowest depletion rate, predominates during dry periods or during minimal precipitation events (Tallaksen, 1995). The baseflow recession rate reflects slow drainage from soil and groundwater, and the rate can be significantly affected by evapotranspiration. Recession rates may vary in time and space, which tends to make their characterization more difficult.

For predictive and modeling purposes it is desirable to derive an analytical expression that can be applied to the recession characteristics of a basin. The majority of analytical techniques are derived from the basic nonlinear differential equation that governs unsteady flow to a stream channel from a large unconfined aquifer (Hall, 1968). This theoretical equation is valid under idealized conditions of no evapotranspiration, leakage or recharge and its application requires the simplifying assumption of a homogenous, isotropic

aquifer. The basic flow equation can be linearized to general forms such as the following (Bras, 1990; Tallaksen, 1995):

$$Q_t = Q_o e^{-\alpha t} \quad (2-6)$$

$$Q_t = Q_o k^t \quad (2-7)$$

where Q_t = the flow at time t
 Q_o = the flow when $t = 0$
 α, k = constants that define recession behavior
 e = base of natural logarithms

The time unit, t , is usually expressed in days for large basins and hours or minutes for small basins (Viessman et al., 1989). Variations of these equations form the basis for a majority of baseflow analytical techniques.

It has been conjectured that variability in recession characteristics may reflect contributions to the storm hydrograph from different storage reservoirs or from pathways associated with different runoff mechanisms (Linsley et al., 1982; Singh, 1988). Barnes (1939) suggested that three principal components of the discharge hydrograph, quickflow, interflow, and baseflow, could be identified by examining a semi-logarithmic plot of the recession flow versus time. He proposed that, in general, each component would conform to equations 2-6 and 2-7 above, though distinguished by different parameter values. Daily recession constants, k , typically have been found to correspond to the following ranges: 0.2-0.8 for surface runoff, 0.7-0.94 for interflow, and 0.93-0.995 for baseflow (Nathan and McMahon, 1990). The overlap in ranges is an indication of the difficulty involved in separating out discharge components in an objective manner.

Short-term and seasonal physical factors may further complicate recession analysis by introducing nonlinearities into the recession characteristics of a basin. Nonlinear recession behavior may be attributed to a variety of factors, including spatial and temporal variations in the recharge of moisture storage; the presence of channel, bank, and flood plain storage; or the heterogeneity of aquifer characteristics (Nathan and McMahon, 1990). A nonlinear analytical expression, or an appropriate conceptual model, may better accommodate this variability and other variations that are manifested over the range of flow stages. One method to capture recession nonlinearity is to express equation 2-6 as a superposed exponential formulation in which the constant varies by recession segment, i (Tallaksen, 1995):

$$Q_t = \sum_{i=1}^n Q_{0_i} e^{-\alpha_i t} \quad (2-8)$$

A master recession curve is a model of a basin's hydrograph recession and it represents the average basin characteristics. The curve is constructed from several recession curves that are extracted for a full range of flow stages that occur during dry periods (Wilson, 1990). In humid regions, the recession curve is frequently interrupted and short segments must be used, thus complicating the procedure. Another limitation of the master recession curve is that any natural variability that is inherent to recession characteristics will not be retained. Traditional methods to derive the master recession curve are graphical in nature and tedious to apply, and their inherent subjectivity limits their reproducibility (Tallaksen, 1995). Nathan and McMahon (1990) discuss a semi-

automated technique that greatly speeds the process of deriving master recession curves and eliminates a degree of the subjectivity.

A plethora of empirical techniques have been designed to assist in the separation of baseflow and quickflow. Four of the more common techniques are described below. The straight-line method involves extending a horizontal line from the point of initial hydrograph rise to an opposite point on the receding limb (Chow et al., 1988). The fixed-base method relies on the assumption that quickflow ends an established amount of time, usually defined as N days, after the peak discharge (Viessman et al., 1989). The recession segment that occurs before the initial hydrograph rise is extended horizontally to a point under the peak discharge and then connected to a point on the recession curve, the location of which is defined by the parameter N (days). Formulas, commonly based on physical basin characteristics such as area, are used to define the value of N . A third technique, the variable-slope method, involves the tangential extension of the pre-event and the event recession curves to separate points under the hydrograph peak, where they are then connected. A fourth technique involves superimposing the master recession curve on the event recession curve. The point at which the two curves diverge is defined as the termination of quickflow. Bedient and Huber (1989) point out that techniques of baseflow separation, as exemplified above, often involve more art than science. However, as they further indicate, while any particular technique may involve subjectivity and empiricism, it is important that it be applied consistently.

Computer algorithms and programs have been devised to expedite the baseflow separation process and to introduce a greater level of objectivity and repeatability (Bako and Hunt, 1988; Nathan and McMahon, 1990; Tallaksen, 1995; Arnold et al., 1995). Automated techniques allow for the exact replication of separation procedures, thus permitting the verification of experimental results between basins and across regions. In addition, algorithm parameters can be altered in order to adjust output to some *a priori* conceptual model of the baseflow recession characteristics of a basin or region.

A limitation of many automated techniques is their lack of a physical basis (Nathan and McMahon, 1990). Moore et al. (1986) describe a digital filter that is designed to extract the quickflow component from a continuous discharge hydrograph. The filter is common to signal processing where it is used to separate high and low frequency components. A justification for its use in hydrograph separation is that baseflow is analogous to the low frequency component while quickflow is analogous to the high frequency component.

In summary, baseflow analysis largely has been a subjective endeavor that has resulted in an abundance of techniques (Tallaksen, 1995). This situation has limited the application of the procedure in general, and has made it difficult to compare independent results across basins or regions (Tallaksen, 1995). Ultimately, the subjective nature of recession curve analysis results from the fact that no clear physical indication exists as to when a particular discharge component begins or ends. Other inadequacies can be traced to mathematical assumptions that are made, to the difficulty of interpreting a stream hydrograph,

to the often-questionable accuracy of low flow data or an inadequate measurement interval, and to the high variability of recession behavior often exhibited by a watershed (Tallaksen, 1995).

This chapter has provided background information on runoff generating mechanisms and their association with particular site characteristics. The next chapter will describe, in detail, the characteristics of the study basin that are relevant to hydrologic behavior. The description will provide the basis to conjecture as to the prevalent runoff mechanisms that occur on the basin.

CHAPTER 3

SITE DESCRIPTION AND CHARACTERIZATION

Puerto Rico lies in the Caribbean region, sharing many of the characteristics that define this unique land-water resource area. The main island of Puerto Rico occupies a central position in the volcanic island-arc complex that connects North and South America and includes the islands of the Greater and Lesser Antilles (Picó, 1974). This chapter presents relevant physical, climatologic, and hydrologic characteristics of the Caribbean region and of Puerto Rico. Greater detail is provided for the interior montane portion of northeastern Puerto Rico and, particularly, for the Río Icacos basin which is located in this region (Figure 3-1). Río Icacos, an undisturbed, forested basin located in the Luquillo Experimental Forest (LEF) of northeastern Puerto Rico, was chosen based on its characteristics and on the availability of appropriate and adequate data.

The Caribbean Region

The Caribbean region (see inset map in Figure 3-1) is geographically defined by the separation of the Caribbean Sea from the Atlantic Ocean in the north and in the east by the Greater and Lesser Antilles, and from the Pacific Ocean by the Central American Isthmus and the northern coast of South America. The region has diverse landscapes and climatic environments, both

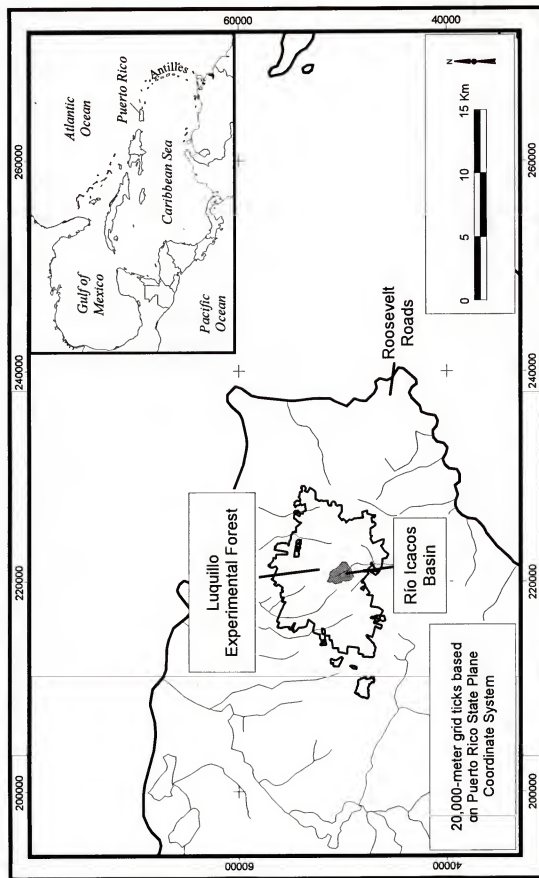


Figure 3-1. Location of Río Icacos basin in eastern Puerto Rico.

tropical and subtropical, humid and subhumid steeplands, areas of rolling hills, and coastal and interior plains and lowlands. The general geologic-geomorphic pattern consists of a coastal or interior mountain range with interior valleys, and a fringing coastal plain.

Puerto Rico

Puerto Rico, the easternmost and smallest island of the Greater Antilles (Briscoe, 1966), is approximately 8,800 square kilometers in size and extends, roughly, 180 kilometers from east to west and 65 kilometers from north to south. The relative small size of Puerto Rico belies its great physical diversity that is due, in part, to its geographic position and east-west orientation. Factors that contribute to the wide diversity of Puerto Rican landforms include the variety of rock types with dissimilar weathering and erosional characteristics, and climatic differences such as humid conditions in the northeast and a semiarid climate in the south and southeast (Monroe, 1980).

A further confirmation of the diversity of Puerto Rican landscapes is the fact that 8 of 11 soil orders in the U.S. Soil Taxonomy system are confirmed to exist on the island, which has not been completely surveyed (Natural Resources Conservation Service, 1999). In one 130-km² area, Augelli (1951) indicated that more than 20 soil types and phases existed, which he attributed to factors such as minute variations in relief, drainage and other microclimatic factors.

Monroe (1980) describes three broad physiographic provinces in Puerto Rico: 1) the northwestern karst region, 2) the discontinuous coastal plains of

varying widths, that consist of alluvial fans, flood plains, and beach and lagoonal deposits and 3), the island's dominant physical feature, the interior mountains and uplands. The interior mountains comprise approximately three-fourths of the island (Beinroth, 1969) and they extend, nearly continuously, from the west to the east coast. The interior mountains consist of several secondary divides and an insular divide, which is composed primarily of the Cordillera Central, the Sierra de Cayey and, in the northeast corner of Puerto Rico, the Sierra de Luquillo, where the study basin is located.

The north coast of Puerto Rico is situated 5° south of the Tropic of Cancer and the island's climate is modified by marine influences and by regional atmospheric and oceanic circulation systems (Augelli, 1951; Calvesbert, 1980). Easterly Trade Winds are a principal climatic control and they occur throughout most of the year. Synoptic-scale disturbances, primarily easterly waves and tropical cyclones, are estimated to produce over 90% of tropical precipitation (Musk, 1988). Subtropical, low-pressure easterly waves, embedded in the Trade Winds and with a period of 3 to 7 days, are a major influence in the Caribbean from June through November (Trewartha and Horn, 1980). These easterly waves are of a large enough spatial extent to affect weather patterns over the entire island (Carter and Elsner, 1996). On average, one-fourth of easterly waves intensify into tropical depressions, and 10% of these become named tropical storms (Musk, 1988). The majority of the more intense disturbances, such as tropical cyclones, occur during the months of August, September and October.

The seasonal migration of the Inter-Tropical Convergence Zone causes a southward shift of the Trade Wind Belt from November to March, allowing occasional invasions of cold air masses from the North American continent (Lugo and Scatena, 1992). The cold fronts that occur in the winter months are often several days in duration and can cause heavy rains.

The orientation of the interior mountains acts as a barrier to moisture-laden Trade Winds and results in considerable orographic precipitation north and east of the interior drainage divides. Annual precipitation amounts can reach over 6000 mm in areas of the Luquillo Mountains. In contrast, areas south and west of the interior mountains lie in a rain shadow and experience a dry climate, as exemplified in the southwest Lajas Valley where annual precipitation amounts of less than 760 mm occur (Lugo-López et al., 1981). Despite the sharp geographic differences in annual totals, precipitation throughout Puerto Rico is fairly well distributed with approximately twice the amount per month from May through October versus January to March (Calvesbert, 1980).

The subtropical maritime climate of Puerto Rico is influenced by global synoptic systems and by mesoscale phenomena, such as local topographic effects and convective precipitation (García-Martínó et al., 1996). Though most precipitation events are sudden intense showers of short duration (15-30 minutes) (Monroe, 1980), longer lasting storms play a very important role.

Characteristics of Río Icacos Basin and Northeastern Interior Puerto Rico

The study basin is located in the northeastern interior of Puerto Rico, in the Luquillo Experimental Forest (LEF) of the Sierra de Luquillo Mountains. This humid montane region lends itself to the objectives of this research because the area is relatively pristine and because several data sets exist that are relevant to the research. Various entities, such as the U.S. Geological Survey (USGS), the U.S. Forest Service, the University of Puerto Rico, and other Commonwealth agencies have long-term research projects in the region. Figure 3-2 shows the location and elevation of environmental monitoring stations in the vicinity of Icacos Basin and of U.S. Army Corps of Engineers (USACE) trafficability study sites. The USACE collected year-long data on soil moisture and groundwater at several sites in Puerto Rico, including three (Figure 3-2, sites A, B and C) within and adjacent to the Icacos basin (Kennedy and Hicks, 1968). The relative uniformity of site characteristics and the robustness and quality of data sources permits the minimization of complicating factors that would tend to obscure the interpretation of analytical results. The conclusions drawn in this study will provide baseline information that may be applicable to other regions.

The 11,491 hectare LEF is largely untouched due to limited access resulting from steep slopes, high annual rainfall, and to 19th century policies of the Spanish Crown (Scatena, 1989; Larsen, 1997). Strategic interests led the Spanish Crown, in 1885, to designate a protected preserve within the mountains and, in 1903, the U.S. established the Luquillo Forest Reserve.

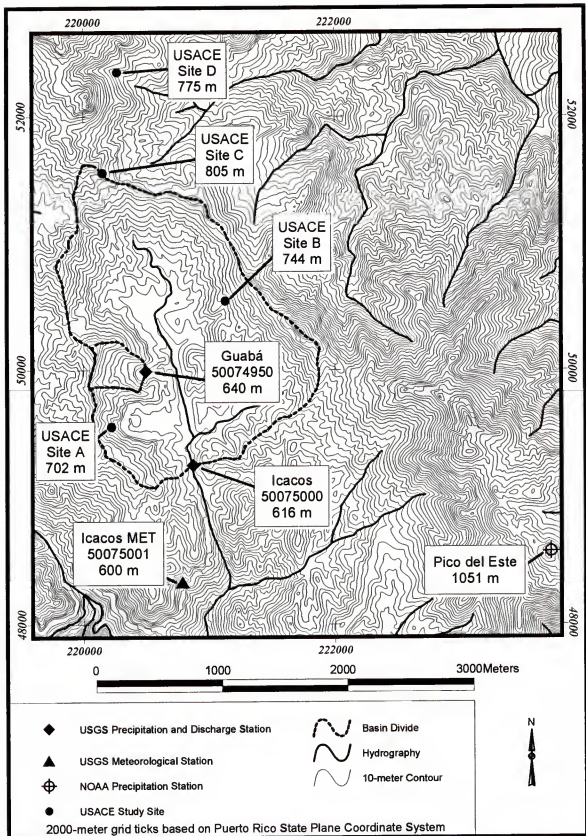


Figure 3-2. Locations of meteorological stations, discharge gages, and U.S. Army Corps of Engineers study sites in the vicinity of the Río Icacos basin.

Río Icacos Basin

Río Icacos basin is 3.26 km² in area with elevations that range from 616 to 840 meters above sea level (224 meters relief). The Río Icacos, a perennial stream with a discontinuous daily discharge record (7/45-3/53; 10/79-9/83; 10/86–present), drains the basin and has a mean annual runoff of 3973 mm. The USGS maintains a crest-stage gage and a sharp-crested weir at the basin outlet for which records are regarded as fair (Díaz et al., 1997). An additional water-stage recorder is maintained on Quebrada Guabá, a small tributary of the Río Icacos that drains an area of 0.13 km² with elevations that range from 640 to 770 m (130 meters relief). Discharge and precipitation records with a 15-minute resolution became available in 1992 at both locations.

The channel characteristics for Río Icacos were determined from 1:24,000 scale topographic maps using techniques that are explained in the research methods (Chapter 5). The main channel of Río Icacos is 2.2 km in length and total channel length is 25.0 km, yielding an approximate drainage density of 7.7 km/km². The average channel width is 2 m (Larsen, 1997) and the channel represents approximately 1.5% of the basin area. The channel has a mean slope of 4.8% and has a sand bottom (McDowell et al., 1992). The average slope in the basin is 24%; approximately 3% of the basin is nearly level (0% to 3% slope), 8% is gently sloping (3% to 8% slope), 14% is strongly sloping (8% to 16% slope), 40% is moderately steep (16% to 30% slope), 25% is steep (30% to 45% slope), and 10% is very steep (>45% slope) (Soil Survey Division staff,

1993). Guabá basin has an average slope of 25% and a slope range distribution similar to that of the whole basin.

Land Use / Land Cover

Four principal forest types are found in the LEF (Wadsworth, 1951) and two of these, the Colorado and Palm forest types, are dominant in the Río Icacos basin (Figure 3-3). The Colorado forest covers approximately 261 ha (80%) of the entire basin and 13 ha (100%) of the Guabá basin. The Palm forest covers approximately 65 ha (20%) of Río Icacos basin. The mountain palm (*Prestoea montana*) is limited to areas of steep slopes or areas of poor drainage and saturated soils, such as in riparian areas along principal channels (Brown et al., 1983; McDowell et al., 1992). Palo Colorado (*Cyrilla racemiflora*), found above the cloud condensation level at approximately 600 meters, is common to well-drained, gently sloping soil and to ridgetops (Larsen, 1997)

Geology and Soils

The Luquillo Mountains are underlain by marine deposited volcanoclastic rocks, including tuffaceous sandstone, siltstone, breccia lavas, and tuff (Meyerhoff, 1933; Guzmán-Rios, 1989). A Tertiary quartz diorite pluton, the Río Blanco Complex, outcrops in the southern section of the Luquillo Mountains, while the northern section consists of bedded volcanoclastic rocks (Scatena, 1989). The bedrock underlying the Icacos basin is quartz diorite (McDowell et al., 1992).

On a regional basis, soil wetness increases with elevation in the Luquillo Mountains and, presumably, the soils remain saturated longer in valleys and at

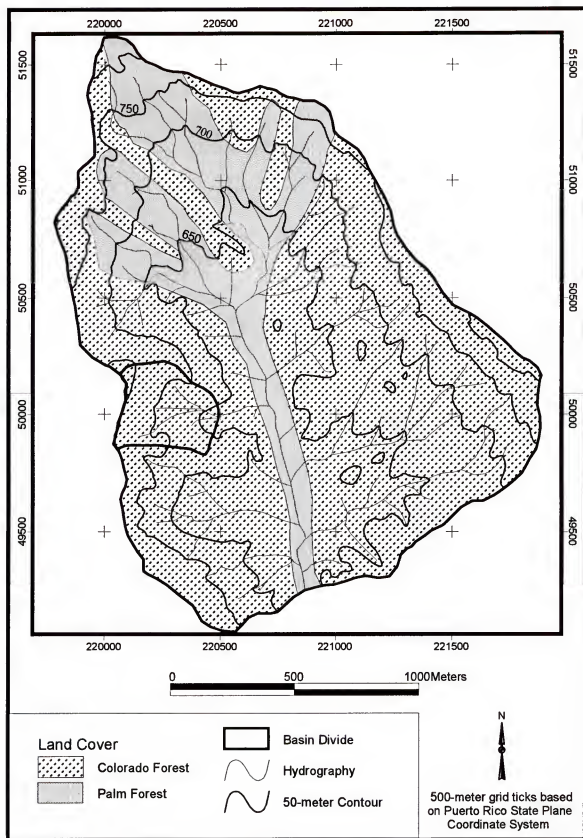


Figure 3-3. Land cover in the Río Icacos basin and Guabá subcatchment.

particular elevations (Wadsworth and Bonnet, 1951). The soils of the Luquillo Mountains are mainly clays, with some silty clay loams and clay loams, and are saturated most of the year. They range in organic matter content from an average of 5% at lower elevations to 15% near the summits (Weaver, 1986).

Three distinct soil complexes are found in the Icacos Basin (Figure 3-4):

1) Picacho Utuado complex covers approximately 269 ha (83%) of the whole basin and 9.8 ha (75%) of the Guabá basin. The Picacho series (Typic Haplohumults) is a very deep (1.8 m), moderately well drained, silty clay loam. The Utuado series (Typic Humitropepts) is a very deep (1.8 m), well drained clay loam. 2) Picacho Ciales complex covers 21 ha (6%) of the entire basin and 3.2 ha (25%) of the Guabá basin. The Ciales series (Aeric Epiaquults) is a very deep (1.5 m), poorly drained, slowly permeable silty clay loam. Ciales is listed as a hydric soil by the National Cooperative Soil Survey. Within the Guabá subcatchment, the Picacho Ciales complex is found on the upper slopes and ridges. 3) Icacos Loam Occasionally Flooded (Typic Fluvaquents) has a fine, loamy texture and occupies 36 ha (11%) of the basin. This is a hydric soil formed under wet conditions and found in the floodplain along the main channel of the basin. Soils overlie saprolite and the maximum combined thickness ranges from approximately 10 meters on ridgetops, a few meters on hillslopes, to 24 meters on lower slopes in floodplain (Larsen, 1997).

Hydrologic Controls and Processes

The disposition of precipitation within a watershed is a function of geologic, topographic, and vegetative characteristics, and of other

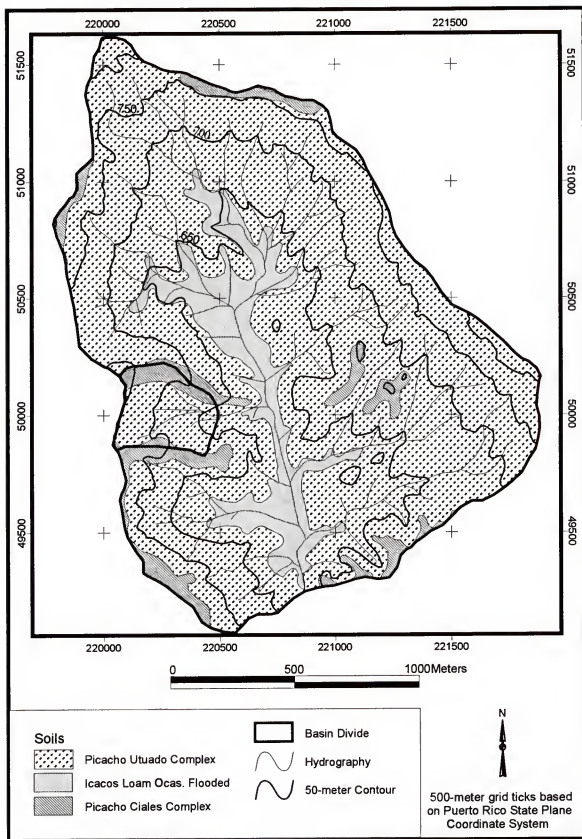


Figure 3-4. Soil types in the Río Icacos basin and Guabá subcatchment.

environmental parameters such as temperature and precipitation patterns and intensity (Riggs and Wolman, 1990). Most studies that relate the above factors to hydrologic behavior have been conducted in temperate regions. The following discussion treats humid montane areas of the tropics and, in particular, the important hydrologic controls that are operative in humid montane sites as exemplified by the LEF.

Precipitation and runoff

In general, precipitation in the northeastern interior highlands increases from north to south, and with increasing elevation. However, the complex relief in the interior of Puerto Rico strongly affects local weather and leads to a diversity of microclimates (Augelli, 1951). Topographic features can modify local exposure to Trade Winds and contribute to variation in slope angles and aspect, thus affecting processes such as evaporation and precipitation. Mesoscale phenomena include diurnal heating of mountain peaks, which may generate considerable convective precipitation, and convergence of sea breezes, easterlies, and of mountain and valley air-flows (Augelli, 1951; Carter and Elsner, 1996). Thus, local topography serves to confound the broad precipitation patterns as exposure and topographic conditions at the immediate site of a station exert an influence nearly as great as orographic effects (Augelli, 1951).

The Luquillo Mountains rise abruptly from sea level to 1074 meters within the short distance of approximately 8 km and, as expected, this steep gradient strongly affects the climate within the LEF. Annual precipitation along the lower,

windward forest border (~100 masl) is approximately 2300 mm and averages about 4500 mm near the summits. The number of days in the year with recorded amounts of precipitation increases with elevation: there are, on average, 97 rainless days at 400 meters and 38 rainless days at 1051 meters (García-Martinó et al., 1996). Ostensibly, there is a wet season from May to December (Figure 3-5), but on average, 5-10% of annual precipitation occurs in each month (Larsen, 1997). Approximately 1,600 to 1,700 rain showers per year occur in the LEF (Briscoe, 1966; Odum et al., 1970) and 78% of these showers are one hour or less in duration.

The National Oceanic and Atmospheric Administration (NOAA) maintains a daily rain station at Pico del Este (Figure 3-2), which is the long-term gage closest to Icacos Basin. The gage is at an elevation of 1051 m and is situated approximately 3.5 km southeast of the center of the Icacos basin. There are approximately 15 years of overlapping record, between 1983 and 1995, with which to compare precipitation to runoff (Figure 3-5). During this period the mean annual runoff and precipitation were 3565 mm and 4318 mm respectively, yielding a runoff ratio of 83 percent. The mean annual runoff for the 23 years of record between 1945 and 1997 was 4085 mm (Figure 3-5).

There are 23 precipitation gages in Puerto Rico for which NOAA publishes 15-minute precipitation values. Twenty-two of these stations employ Fischer-Porter rainfall gages with a resolution of 2.54 mm (0.1 inches). One station, located at San Juan Isla Verde International Airport (3 masl), employs a gage with a resolution of 0.254 mm (0.01 inches). The rainfall intensity

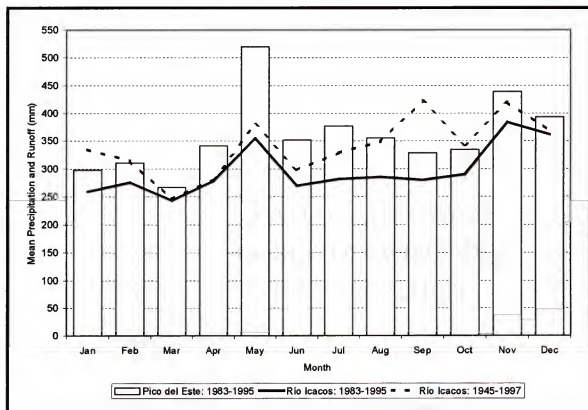


Figure 3-5. Río Icacos basin: mean monthly precipitation and runoff: 1983-1995; mean monthly runoff: 1945-1997.

characteristics were examined for the Isla Verde gage and 5 other gages located in northeastern Puerto Rico. The average period of record for the stations is 19 years. Figure 3-6 shows precipitation intensity relationships measured at the airport gage and at 3 additional stations. Greater than 90% of recorded rainfall rates are 20 mm/hr or less and greater than 80% are less than 10 mm/hr. The significance of precipitation intensities in relation to rates of water movement into and within the soil will be discussed later at greater length.

Interception, throughfall, and stemflow

Throughfall is that portion of precipitation that reaches the ground surface either directly or by dripping from overhead vegetation, while stemflow is the portion that reaches the soil surface by flowing along the tree stem. Scatena (1990) conducted a year-long field study on a basin located in the LEF. He made detailed measurements of the moisture storage capacity for leaves of various species and, based on leaf area indices and relative stem densities, he derived a value of 0.82 mm for interception storage capacity. The throughflow proportion was estimated at 59%, based on random sampling under different vegetation classes. Stemflow measurements yielded an estimated stemflow proportion of 2.8%.

Evapotranspiration and temperature

Mean monthly and diurnal temperatures are less variable along the coast than in the interior valleys. The least variation in temperature is found at higher elevations, above the cloud level of 600 meters (Briscoe, 1966). The mean

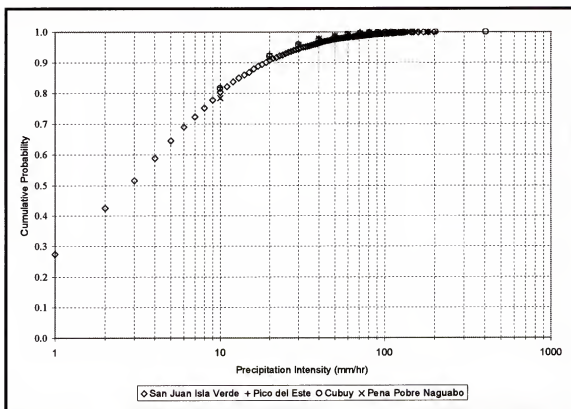


Figure 3-6. Probabilities associated with precipitation intensity for northeast Puerto Rico.

annual temperature is 23°C along the lower, windward border of the LEF and 19°C at the summits. At both elevations, the annual variation in mean monthly temperature is from 3°C to 3.5°C (Brown et al., 1983). Temperature, as a function of elevation, is more predictable than is precipitation (Augelli, 1951), however, Trade Wind influences and local topographic features do alter normal patterns.

The upper slopes and ridges of mountains are usually enveloped in clouds that reduce solar insolation to 60% of that in coastal areas (Briscoe, 1966). Evapotranspiration decreases, and relative humidity and wind velocity increase with elevation (Wadsworth and Bonnet, 1951; Briscoe, 1966). Evapotranspiration is not directly proportional to precipitation receipts but, rather, is strongly influenced by other factors, such as available moisture, temperature, solar radiation, wind, and land cover (Riggs and Wolman, 1990). The mean annual water loss from a basin due to evaporation and transpiration often is approximated as the difference between measured runoff and precipitation, if no significant subsurface loss occurs (Riggs and Wolman, 1990). Larsen (1997) estimated potential evapotranspiration for Icacos basin at 1,123 mm using a model developed by Lugo (1986) and based on 5-m² grid cells.

Soil water and groundwater

Several studies have examined the characteristics of soils in Puerto Rico and their relation to infiltration and water movement. Statistical studies on the results of 740 field infiltration tests demonstrated that rapid 1st hour rates are characteristic of soils throughout Puerto Rico (Lugo-López et al., 1981). The

mean rate of infiltration during the first hour was 21.4 cm/hr. Eighth hour infiltration rates for soil families that are present in the Icacos basin are 7.5 cm/hr for Ultisols, 2.8 cm/hr for Inceptisols, and 2.4 cm/hr for Entisols (Lugo-López et al., 1968). Unusually high infiltration rates (30-60 cm/hr) and low bulk densities ($0.66\text{--}1.18\text{ g/cm}^3$) were observed on undisturbed hillslope soils. McDowell et al. (1992) measured rates of 2-9 cm/minute in Icacos basin and made the observation that the rates are greater than average precipitation intensities. This observation is confirmed by the high frequency of low intensity precipitation present in northeastern Puerto Rico as was demonstrated in Figure 3-6.

McDowell et al. (1992) installed several wells, at depths of 180 cm and 210 cm, along a tributary of the Icacos basin. Measured saturated hydraulic conductivity values ranged from 10^{-4} to 10^{-5} cm/sec. Independent measurements by Larsen (1997) yielded comparable values, from which he estimated an equivalent groundwater flow velocity of 0.1 m/day. Larsen (1997) indicated that bedrock outcrops near the basin outlet and manifests no signs of faults or fracture, and that valley walls are steeply inclined towards the channel. Based on the measured conductivity values and the topographic/geologic relationships, Larsen calculated that deep groundwater loss exceeds no more than a few millimeters per year.

Hypothesized Runoff Generating Mechanisms Operative in Río Icacos Basin

The literature review and an examination of the hydrologic characteristics associated with the LEF and the Río Icacos watershed suggest that the basin likely conforms to the model of variable source areas controlled by topography and fed by subsurface flow. Icacos basin consists of undisturbed forest on steep slopes adjacent to a relatively narrow floodplain. Soils are deep and typified by infiltration rates that exceed average precipitation intensities. Jordan (1970) observed that upper portions of LEF soils tend to be well aggregated with high rates of permeability, and that a decline in density with depth induced lateral flow in the downslope direction. McDowell et al. (1992) and the U.S. Army Corps of Engineers (Kennedy and Hicks, 1968) observed a permanent perched water table, the depth to which decreased from upper to lower slopes. Infiltration-excess overland flow is assumed to occur as a significant runoff generating mechanism, if at all, only during infrequent extreme events.

CHAPTER 4

TOPOGRAPHY-BASED HYDROLOGIC MODEL

The literature review (Chapter 2) highlighted the increased awareness regarding the importance of topographic controls on the spatial and temporal characteristics of basin hydrology; particularly with regard to the occurrence of variable source areas and saturated subsurface flow. This heightened awareness led to the development of topography-based hydrologic models. The evolution of this class of models is particularly important for those areas that lack adequate sources of traditional hydrometric data, which is often the case in humid, montane regions of the tropics. Representations of local and regional topographic features can be generated quickly, and included as input to an appropriate hydrologic model. Elevation information, in the form of contour maps, usually is readily available, and the advent of sophisticated computer programs has facilitated techniques of digital terrain analysis.

The site description and characterization (Chapter 3) suggest that the Río Icacos basin conforms to the assumptions that are inherent to topography-based hydrologic models. The following discussion outlines the assumptions, theory, and structure of one widely utilized model.

TOPMODEL, one of the early topography-based hydrologic models, was conceptualized in 1974 (Kirkby, 1975) and first described by Beven and Kirkby

(1979). TOPMODEL, characterized as a physically-based, semi-distributed hydrologic model, has an extensive research history with over 120 citations to its credit (Beven, 1998). The model is considered a research tool and users are encouraged to modify conceptual elements to match their understanding of the hydrologic behavior of a basin or a region.

TOPMODEL is a simple, parametric model that attempts to represent the heterogeneity of basin processes (Quinn and Beven, 1993), particularly those related to variable source areas fed by saturation-excess overland flow (Durand et al., 1992; Iorgulescu and Jordan, 1994). A basic tenet of the model is that a micro-scale representation of internal state variables is a difficult, if not impossible task, given basin complexities. The spatial distribution of hydrologic processes is represented primarily by basin topography, rather than by the scaling-up of point measurements (Moore et al., 1991). Parameters are physically based, which facilitates 1) application to ungaged basins, 2) the prediction of hydrologic behavior when basin characteristics change and, 3) model calibration utilizing data from similar drainage basins (Kirkby, 1975).

The model was developed originally for humid, temperate basins located in mid-Wales of the United Kingdom, but is deemed appropriate for basins with thin soils, moderate to steep topography, and moderate to high runoff ratios.

TOPMODEL Theory

The principal assumption of TOPMODEL is that basin topography reflects the hydraulic gradient of the saturated zone or the slope of the water table

(Beven et al., 1995a). The subsurface flow through a contour segment of unit length is assumed to be proportional to the local slope and to the upslope contributing area. This gives rise to the topographic index:

$$\ln\left(\frac{a}{\tan \beta}\right) \quad (4-1)$$

where a = upslope contributing area per unit contour length or per cell
 $\tan \beta$ = local surface slope

Locations with a high topographic index value have a greater tendency to develop saturated conditions than do locations with low values. The index is a representation of the physical control that topographic features, such as areas of convergence or divergence, and topographic characteristics, such as slope length, have on soil moisture status and moisture flux.

When adequate information about soil characteristics is available, the topographic index may be extended as follows:

$$\ln\left(\frac{a}{T_o \tan \beta}\right) \quad (4-2)$$

where T_o = lateral transmissivity of a saturated soil profile (m^2/hr)
 (water table intersects surface)

TOPMODEL assumes that the lateral transmissivity of moisture within the soil profile conforms to an exponential decay function of the soil storage deficit, or the depth to the water table:

$$T = T_o e^{-S_t / M} \quad (4-3)$$

where T = lateral transmissivity (m^2/hr)
 S_i = local storage deficit (m)
 M = exponential decay rate of transmissivity with depth (m)

TOPMODEL provides for the inclusion of sub-basins, which facilitates the incorporation of spatial variability of soil properties when known.

The topographic index and the combined soils/topographic index are measures of hydrologic similarity, since locations with comparable values are expected to exhibit equivalent behavior (Beven et al., 1995a). The topographic-index distribution function for a basin typically will consist of 15 to 30 unique values, and each value represents the area of a fractional proportion of the basin (Quinn and Beven, 1993).

The topographic-index distribution is derived from a digital elevation model (DEM). Flow from each DEM cell is distributed proportionally among downslope cells, based on relative slope differences and cell positions (Quinn et al., 1995). A DEM cell size equal to or less than 50 m is recommended to adequately represent the topographic features that are correlated with hydrologic behavior (Beven et al., 1995b). Large cells may provide an adequate macro-scale representation of basin hydrology, but will not provide detail on the spatial and temporal distribution of processes occurring within the basin. Cells that are too small may introduce topographic complexities that unnecessarily complicate and inadequately represent hydrologic pathways.

The assumption that local surface slope reflects the hydraulic gradient combined with the additional assumption that the vertical recharge rate (m/hr), r , is spatially uniform, allows TOPMODEL to link local variations in water table

depth, or moisture deficit, to the topographic index and to soil transmissivity.

The saturated subsurface flow rate per unit contour length (m^2/hr), q_i , at a point (or for a DEM cell) may be expressed as follows:

$$q_i = T_0 \tan \beta e^{-S_i/M} \quad (4-4)$$

$$q_i = ra \quad (4-5)$$

Combining equations 4-4 and 4-5 leads to an expression of the local moisture storage deficit:

$$S_i = -M \ln \frac{ra}{T_0 \tan \beta} \quad (4-6)$$

The integration of the local storage deficit, S_i , over the entire basin area, A , results in a mean value for basin storage deficit, \bar{S} , where i represents individual locations, or cells in a digital elevation model:

$$\bar{S} = \frac{1}{A} \sum_i -M \ln \frac{ra}{T_0 \tan \beta} \quad (4-7)$$

Incorporation of equation 4-6 into 4-7, and the elimination of the spatially uniform (assumed) recharge rate, r , leads to the following relationship between the basin average storage deficit, the local storage deficit, and the basin average values and the local values for the soil and topographic variables:

$$\frac{\bar{S} - S_i}{M} = \left[\ln \frac{a}{\tan \beta} - \lambda \right] - [\ln T_0 - \ln T_e] \quad (4-8)$$

where $\ln T_e$ = basin average saturated transmissivity
 λ = basin average topographic index

Model Structure

Figure 4-1 presents an operational flowchart of TOPMODEL. Model inputs include rainfall (m/hr), potential evapotranspiration (m/hr), and a distribution function of the topographic index for the basin. Observed discharge, expressed as an equivalent depth (m/hr) over the basin during each model time step, may be input for calibration purposes and to provide a statistical comparison with the simulated discharge. Required basin parameters include a storage parameter, M , (equation 4-3), which controls the exponential decline of soil transmissivity with decreasing moisture content (meters); a basin average soil transmissivity value, T_0 , (m^2/hr); a time delay per unit of moisture storage deficit (hr); a channel routing velocity (m/hr); and the maximum available storage capacity of the root zone (m). Two initialization parameters are required: the initial baseflow discharge (m/hr) and the initial value of the root zone deficit (m).

During each model time step, and for each unique topographic index value, a set of conceptual stores accounts for moisture flux at the surface and between the unsaturated and saturated zones. The conceptual stores consist of a root zone storage, a non-active store or unsaturated zone storage, and a saturated zone store. If infiltration-excess overland flow is anticipated, then an optional module can be invoked to simulate infiltration into the root zone according to the Green-Ampt model (Beven, 1984).

Moisture storage in the root zone (SRZ) is modeled as a deficit, with a value of 0 at field capacity and increasingly more positive values as the soil

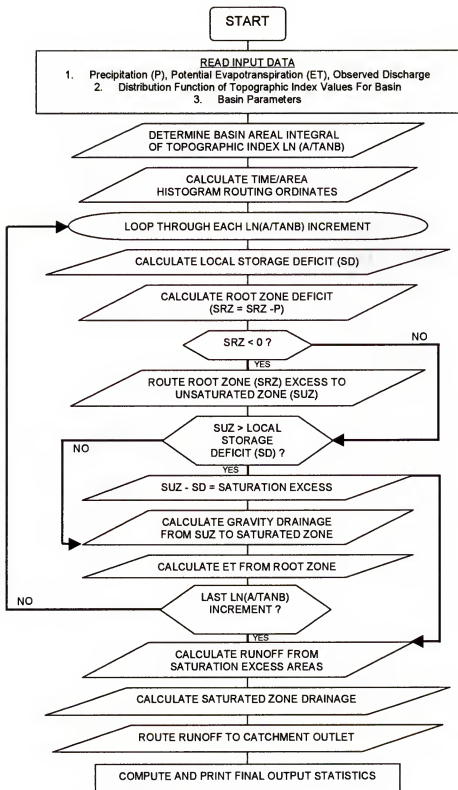


Figure 4-1. TOPMODEL program structure.

approaches the wilting point. Conceptually, the maximum allowable storage deficit in the root zone, $SRMAX$, is equivalent to the moisture content at field capacity minus the moisture content at the wilting point. Evaporation occurs from the root zone store according to the following model:

$$E_a = E_p \left(1 - \frac{SRZ}{SRMAX} \right) \quad (4-9)$$

where E_a = actual evapotranspiration (m/hr)
 E_p = potential evapotranspiration (m/hr)
 SRZ = root zone storage deficit (m)
 $SRMAX$ = maximum allowable storage deficit in root zone (m)

EVAP, an ancillary program provided with TOPMODEL, generates potential evapotranspiration values using the following equation:

$$E_p = E_{\min} + 0.5(E_{\max} - E_{\min}) \left[1 + \sin \left\{ 2\pi \left(\frac{J}{365} - \frac{\pi}{2} \right) \right\} \right] \quad (4-10)$$

where E_{\min} = mean daily potential evapotranspiration at winter low
 E_{\max} = mean daily potential evapotranspiration at summer high
 J = day number after January 1st

Moisture movement from the root zone to the unsaturated zone, SUZ , only occurs when moisture in the root zone exceeds field capacity. In contrast to the root zone, which is modeled as a deficit, the unsaturated zone is modeled as a store and has a value of 0 at field capacity and becomes more positive as it approaches saturation. The rate of vertical drainage, q_v , from the unsaturated store to the saturated zone is a function of the moisture status within the unsaturated zone, the moisture deficit of the saturated zone, S , and the mean residence time per unit of storage deficit, t_d (Beven and Wood, 1983).

$$q_{vi} = \frac{SUZ_i}{S_i t_d} \quad (4-11)$$

where q_{vi} = vertical drainage (m/hr)
 SUZ_i = unsaturated or 'gravity drainage' zone storage (m)
 S_i = saturated zone deficit (m)
 t_d = average residence time per unit of saturation deficit (hr)
 i = topographic index increment

The saturated storage deficit for each topographic index increment is related to the basin average storage deficit, the basin average topographic index, and the local topographic index as follows:

$$S_i = \bar{S} + \frac{M}{A} \int_A \ln \frac{a}{\tan \beta} dA - M \ln \frac{a}{\tan \beta} \quad (4-12)$$

Saturation excess overland flow occurs when the local storage deficit, S_i , is less than zero.

The average storage deficit for the basin is reduced by vertical drainage inputs, q_v , weighted by the fractional basin area that each topographic-index class represents. The basin average saturation zone storage deficit is increased by outflow from the saturated zone as determined by the following equation:

$$Q_b = T_0 e^{-\lambda} e^{(-\bar{S}/M)} \quad (4-13)$$

where Q_b = outflow from the saturated zone
 λ = areal integral of the topographic index

The term, $T_0 e^{-\lambda}$, represents subsurface drainage when the basin average storage deficit, or the basin average water table depth, is zero. Total output from the basin is the sum of subsurface drainage, saturation-excess overland

flow and, if it exists, infiltration-excess overland flow. Runoff may be routed to the basin outlet by a distance-related delay function.

The model outputs include basin average and local soil moisture deficits, surface runoff from saturated areas, and subsurface flow/groundwater discharge (Durand et al., 1992). TOPMODEL also provides graphical outputs that display the spatial distribution of saturated areas for each time step. The numerical fit between observed and simulated hydrographs is evaluated with the Nash and Sutcliffe (1970) efficiency criteria, calculated as follows:

$$E = 1 - \frac{\sum (Q_{obs} - Q_{sim})^2}{\sum (Q_{obs} - \bar{Q})^2} \quad (4-14)$$

where E = efficiency measure
 Q_{obs} = discharge recorded at the basin outlet
 Q_{sim} = simulated discharge
 \bar{Q} = mean observed discharge

The summations are applied over all time steps. The efficiency measure approaches 1 (100%) as the fit improves. The efficiency coefficient allows comparisons between different time periods or basins, and with other models (Beven et al., 1984).

CHAPTER 5

RESEARCH METHODS

The research methodology is based on an examination of individual storm events. An operational definition is required -- one that defines independent and discrete events -- to select a subset of storms from the precipitation and discharge time series. It is common, and intuitive, to think of events in terms of a well-defined meteorological phenomena or weather system, such as the convective thunderstorms prevalent during summer afternoons in the tropics and subtropics. In reality, no standard definition exists but, rather, the nature of the parameters or processes under investigation will determine how an event should be delimited in the hydrologic record.

This study is concerned with the quickflow response of the basin to precipitation receipts. In particular, subsequent statistical and topographic analyses test for the presence or absence of relationships among specific parameters associated with a precipitation event and the related discharge hydrograph, such as peak instantaneous flow, maximum precipitation intensity, measures of basin wetness, and precipitation and flow volumes. To meet the requirements of the analytical steps it is necessary that a discharge response be associated with a well-defined precipitation event. Within this context

precipitation events were selected for inclusion in the study according to the following criteria:

- 1) An independent and discrete event is separated from preceding events and subsequent events by a time period of no rain that is equal to, or greater than, the quickflow recession curve for the basin.
- 2) The total precipitation amount for the event is of sufficient quantity to produce a significant discharge response that is measurable on the hydrograph.

Prior to the delineation and extraction of storm events, pre-processing of the various data sets was necessary. The following discussion outlines the steps involved in the processing of the precipitation and discharge records, and the GIS coverages. Subsequent topics address the procedures for hydrograph separation, the determination of hydrologic abstractions, the selection of individual events, and the methodology involved in the statistical and topographic analyses.

Data Processing

GIS Coverages

Geographic Information System coverages for soils and land cover were obtained for the LEF from the Long Term Ecological Reserve website maintained by University of Puerto Rico (Institute for Tropical Ecosystem Studies, 1997). Soil boundaries were derived from a detailed survey conducted in the LEF for the U.S. Forest Service in 1991 (Olga Ramos, Institute of Tropical Forestry,

Personal Communication, 1999). Ancillary information about soil characteristics was obtained from the National Soil Data Access Facility (National Soil Survey Center, 1998) and greater detail was derived from 3 investigations conducted within Icacos basin (Kennedy and Hicks, 1968; McDowell et al., 1992; Larsen, 1997).

The GIS layer for land cover consists of general forest types as derived from field mapping by the U.S. Forest Service at a scale of 1:20,000 (Olga Ramos, Institute of Tropical Forestry, Personal Communication, 1999). Digital Line Graphs (DLG) of hydrography and hypsography, at a scale of 1:20,000, were obtained from the USGS. A 7.5-minute DEM, with a 30-meter resolution, was obtained from the USGS (U.S. Geological Survey, 1990). The hypsography portrayed in the DLG was derived by photogrammetric methods originally applied to 1941 aerial photos and subsequently revised with 1964 aerial photos.

The drainage divide for Icacos basin was digitized using the hypsography and hydrography GIS layers as guides. Larsen (1997), based on fieldwork, determined that the perennial stream network for Icacos basin is underrepresented on the USGS hydrography layer. The stream channel network for Icacos basin was extended using the crenulation method (Strahler, 1969). A GTCO Digi-Pad Type 5 digitizer with an accuracy of ± 0.010 inches was utilized for the digitization process (GTCO Corporation, 1986) and an RMS error of less than .003 was maintained for all work.

Precipitation and Discharge

Fifteen-minute interval precipitation and discharge measurements were obtained from the U.S. Geological Survey in Puerto Rico. Table 5-1 lists gage names, parameters, identification numbers and the periods of record and Figure 3-2 shows the gage locations.

Table 5-1. Name, parameter, identifier, and period of record for 15-minute interval precipitation and discharge stations located in the vicinity of Río Icacos basin.

Name	Parameter	Identifier	Period of Record
Guabá	Precipitation	50074950	10/7/93 - 9/30/97
Guabá	Discharge	50074950	10/1/92 - 9/30/97
Icacos	Precipitation	50075000	10/1/92 - 9/30/97
Icacos	Discharge	50075000	7/21/92 - 9/30/97
Icacos	Meteorology	50075001	4/15/92 - 9/30/97

These data were provided in a digital text format and a PERL program was written to extract and format dates, times and measurement values from the record. To corroborate the values contained in the 15-minute discharge record, measurements were summed on a daily basis and compared with daily values obtained from EarthInfo, Inc. (1996) and from the USGS website (U.S. Geological Survey, 1998).

Data Limitations

The results and the reliability of research and modeling efforts are dependent on the accuracy of input data and parameter values. The design of an appropriate research methodology is predicated on a thorough understanding of the limitations inherent to data sources. Precipitation is the most widely

recognized error source, since gage precipitation is a point measurement that is extrapolated to a basin area. Spatial, temporal and seasonal factors diminish measurement accuracy to varying degrees. The closer a gage is to a basin center (centroid) the more representative it is of basin precipitation averages (Viessman et al., 1989). Some topographic and convective rainfall patterns are of limited spatial extent and, thus, less likely to be detected by instrumentation. The relatively small size of Icacos basin and the high degree of instrumentation within the basin allow for greater control of potential errors.

The USGS rates streamflow records as excellent, good, fair or poor (Díaz et al., 1997). Excellent signifies that approximately 95% of measured daily discharges are within 5% of the actual value; good within 10%; and fair within 15 percent. The Río Icacos and Guabá records are characterized as fair, except for estimated values, which are classified as poor. Storm events that corresponded with estimated daily streamflow values were not utilized in the research.

Storm Events

Hydrograph Separation

To proceed with subsequent methodological steps it was necessary to extract a number of hydrologic events from the discharge and precipitation records. The literature review revealed that the separation of the discharge hydrograph into distinct components is not a trivial task and that all methods entail varying degrees of subjectivity. The utility of any particular method is enhanced if it is repeatable and if it allows for the comparison of results across

basins and regions. The following section outlines the trial and error application of procedures discussed in the literature review. The end result was a hydrograph separation methodology applicable to Icacos basin.

Operational definitions are necessary in order to clearly and objectively demarcate the starting and ending points of a particular discharge event. The task of differentiating the beginning point is more direct than is the selection of the point at which direct runoff ends and baseflow becomes the sole contributor to the hydrograph. Given a significant precipitation input to a basin, the initial point at which direct runoff commences normally is defined to occur when the slope of the pre-event baseflow recession curve transitions from a negative to a positive value. If the direct runoff recession period of a prior event has not ceased, then the pre-event recession curve will include direct runoff components that are not derived from the current event.

General guidelines available in the literature, as well as observations specific to the study region, are helpful in determining a characteristic duration for the quickflow recession curve. Ponce (1989) indicates that the time period between peak discharge and the quickflow-to-baseflow transition point is approximately 2 to 4 times that of the hydrograph time-to-peak. For large basins, the lag between the peak discharge and the transition point normally will be greater than 4 days (Ponce, 1989). Time-to-peak is defined as the interval between initiation of effective precipitation and the peak discharge. In a baseflow separation study based on analytical solutions of the Boussinesq equation, the estimated time to the transition point varied from approximately 1

day for a 114 km² basin, to 2 days for a 522 km² basin (Szilagyi and Parlange, 1998). Empirical evidence shows that streamflow within the study region is flashy and that baseflow to peak discharge occurs in a matter of minutes to hours, while the duration of the recession limb usually is no more than a few hours (Larsen, 1997).

A determination of the transition point from quickflow to baseflow is more difficult to assess than is the inception point of the event hydrograph. Brutsaert and Nieber (1977) proposed that, since the baseflow depletion rate is the slowest of all hydrograph components, slope analysis could be utilized to determine the transition point according to the following function:

$$\frac{dQ}{dt} = f(Q) \quad (5-1)$$

where Q = discharge

They approximated this function, using low stage discharge observations, as follows:

$$\frac{Q_t - Q_{t-1}}{\Delta t} = f\left(\frac{Q_t + Q_{t-1}}{2}\right) \quad (5-2)$$

Brutsaert and Nieber (1977) suggested that a log-log plot of the slope differentials versus average flow could be utilized to determine the characteristic recession behavior of a catchment or region. They applied the technique graphically to six basins, ranging in size from 80 km² to 326 km², and their results yielded a line with a slope of 1.5 that was common to all basins. Szilagyi and Parlange (1998) applied a variation of Brutsaert and Nieber's technique to four watersheds and reported similar results. Slope analysis was applied to the

Icacos basin with inconclusive results. The validity of the technique depends on numerous observations extracted from baseflow recession segments from across the range of flow stages. The 15-minute discharge record available for Icacos is relatively short, and extended, uninterrupted recession segments at higher stages are infrequent.

A master recession curve was derived for Icacos basin utilizing a methodology adapted from Wilson (1990) and Nathan and McMahon (1990) which includes the following steps:

1. Plot concurrent sequences of discharge and precipitation over an extended time period.
2. Across a range of stages, extract several recession curves that are uninterrupted by precipitation and which include segments of quickflow that transition into 100% baseflow.
3. Create a semi-logarithmic graph containing each recession curve plotted in descending order according to lowest discharge value. Discharge (ordinate) versus time (abscissa).
4. Apply a time offset to each recession curve, such that the lower portions are coincident with a line drawn tangential to the first and last curves.
5. Extract the data points from the lower tangential segments and apply linear regression to define the master recession curve.
6. Regressed line plotted on a linear scale produces the master recession curve.

Before applying the above procedure, the USGS discharge values were adjusted in order to account for the resolution limitations that are inherent to the data. USGS streamflow values are reported with the following precision (Dingman, 1984):

Less than 1 CFS to the nearest 0.01 CFS
1 - 9.9 CFS to the nearest 0.1 CFS
10 - 999 CFS to the nearest 1 CFS
Over 1000 CFS to three significant figures

The limitation in data precision results in rounded measurement values and extended hydrograph segments, during which a constant discharge is reported. This produces a characteristic stair-step plot that is particularly apparent when streamflow is dominated by delayed sources. The steps of the plot are increasingly elongated during periods of low flow. The measurement artifacts that result from the resolution limitations were removed to facilitate the construction of the master recession curve. Given that each hydrograph recession segment utilized in the analysis was abstracted from a dry period, streamflow under each step was assumed to decrease in a linear fashion. As such, duplicate discharge measurements were eliminated and only the first unique measurement that occurred during a period of constant flow was retained.

Determination of Net Precipitation

Components of the Rutter and Gash models were combined in order to account for losses due to interception and evaporation during each time step of a storm. The following continuous storm-event water balance equation is a modified version of that presented by Moore et al. (1986):

$$\frac{dC}{dt} = (1 - p - p_t)P - \frac{C}{S}\bar{E} \quad (5-3)$$

- where C = current status of canopy storage (mm)
 p = throughfall proportion
 p_t = stemflow proportion
 P = gross precipitation rate (mm/hr)
 S = interception storage capacity (mm)
 \bar{E} = mean evaporation rate (mm/hr)

The interception storage capacity and the throughflow and stemflow proportions were based on the year-long field study conducted by Scatena (1990) on a comparable watershed located in the LEF. Recording gage measurements by Scatena indicated that no throughfall occurred when rainfall was less than or equal to 0.51 mm/hr and a one-year study of soil trafficability indicated that storms smaller than 2.54 mm did not appreciably wet the soil and did not contribute to soil moisture accretion (Kennedy and Hicks, 1968). As previously discussed in Chapter 3, Scatena derived a value of 0.82 mm for interception storage capacity, an average throughflow value of 59%, and an average stemflow value of 2.8%. These values were assumed to be representative of conditions in the Río Icacos basin.

A mean evaporation rate was determined for each hour utilizing two years of meteorological data (1990-1991) collected by the University of Puerto Rico at the El Verde Field Station (Institute for Tropical Ecosystem Studies, 1997). Measurements of precipitation (gage resolution 0.254 mm), wet and dry temperature, global solar radiation, and wind speed were taken every 15-minutes in a 0.3 ha forest clearing located approximately 5 kilometers to the northwest of the Icacos basin. The meteorological sensors are located at an elevation of 356 meters above sea level and are 6 meters above the ground on the roof of the field station.

The Penman-Monteith equation (Equation 5-4) was used to determine evaporation rates during time periods when the canopy was assumed to be saturated (Gash, 1979; Bras, 1990; Shuttleworth, 1993). Precipitation volumes

for consecutive 15-minute time periods were tallied and each time period during which the interception capacity was equaled or exceeded, and during which rainfall occurred, was extracted for evaporation analysis.

$$E = \frac{1}{\lambda} \left[\frac{\Delta R_n + \rho_a c_p D / r_a}{\Delta + \gamma} \right] \quad (5-4)$$

- where E = evaporation rate ($\text{kg m}^{-2} \text{s}^{-1}$)
 λ = latent heat of vaporization (MJ kg^{-1})
 Δ = slope of saturation vapor pressure function, de_s / dT_a
 T_a = air temperature ($^{\circ}\text{C}$)
 e_s = saturation vapor pressure (kPa)
 R_n = net radiation ($\text{MJ m}^{-2} \text{s}^{-1}$)
 ρ_a = moist air density (kg m^{-3})
 c_p = specific heat capacity of moist air ($1.013 \times 10^{-3} \text{ MJ kg}^{-1} ^{\circ}\text{C}^{-1}$)
 D = vapor pressure deficit (kPa)
 r_a = aerodynamic resistance (s m^{-1})
 γ = psychrometric constant ($\text{kPa } ^{\circ}\text{C}^{-1}$)

Each component of the Penman-Monteith equation was determined following the steps outlined below. The saturation vapor pressure and gradient of the saturation vapor pressure-air temperature function (Bras, 1990):

$$\Delta = \frac{4098e_s}{(237.3 + T_a)^2} \quad (5-5)$$

$$e_s = 0.6108 \exp \left(\frac{17.27T_a}{237.3 + T_a} \right) \quad (5-6)$$

The net radiation is the sum of net shortwave and longwave radiation. Other potential energy sources such as ground flux, biomass storage, and photosynthesis are considered negligible (Shuttleworth, 1993).

$$L_n = -f\varepsilon'\sigma(T_a + 273.2)^4 \quad (5-7)$$

$$\varepsilon' = a_e + b_e \sqrt{e_d} \quad (5-8)$$

$$f = a_c \frac{S_t}{S_{to}} + b_c \quad (5-9)$$

- where L_n = net longwave radiation ($\text{MJ m}^{-2} \text{s}^{-1}$)
 f = adjustment for cloud cover
 ε' = net emissivity between atmosphere and ground
 σ = Stefan-Boltzman constant ($5.67 \times 10^{-14} \text{ MJ m}^{-2} \text{K}^{-4} \text{s}^{-1}$)
 e_d = vapor pressure (kPa)
 calculated using equation 5-6 using wet-bulb temperature
 a_e, b_e = correlation coefficients (humid conditions:
 $a_e = 0.34, b_e = -0.14$ (Shuttleworth, 1993))
 S_t = measured global solar radiation
 S_{to} = clear sky radiation
 a_c, b_c = longwave radiation coefficients for clear skies
 (humid areas: $a_c = 1.00, b_c = 0.00$ (Shuttleworth, 1993))

The clear sky radiation value, S_{to} , was assumed equal to the maximum observed global radiation value for each daylight hour extracted from the two year record from El Verde. Moist air density, defined by equation 5-10, is a function of atmospheric pressure and air temperature. The atmospheric pressure at the field station was estimated with equation 5-11 using observed values of mean daily atmospheric pressure at sea level obtained from the Surface Airways record for nearby Roosevelt Roads (Figure 3-1).

$$\rho_a = 3.486 \left(\frac{P}{275 + T_a} \right) \quad (5-10)$$

$$P = P_{sl} \left(\frac{293 - 0.00565Z}{293} \right)^{5.256} \quad (5-11)$$

- where P = atmospheric pressure at meteorological sensor (kPa)
 P_{sl} = atmospheric pressure at sea level (kPa)
 Z = elevation of meteorological sensor (m)

Aerodynamic resistance, r_a , is a function of wind speed and of atmospheric turbulence as influenced by roughness characteristics of vegetation. Wind speed measurements for equation 5-12 normally are taken 2 meters above the vegetation canopy. Equation 5-13 was used to correct wind speed measured at 6 meters to an estimated value at 22 meters, two meters above the canopy height (Bras, 1990). The following formulation was used to calculate the resistance (Gash, 1979):

$$r_a = \left(\frac{1}{k^2 u_2} \right) \ln \left(\frac{z_2 - d}{z_o} \right)^2 \quad (5-12)$$

$$\frac{u_1}{u_2} = \frac{\ln(z_1 / z_o)}{\ln(z_2 / z_o)} \quad (5-13)$$

- where k = von Karmans constant (0.41)
 u_1 = wind speed (m s^{-1})
 u_2 = adjusted wind speed (m s^{-1})
 z_1 = measurement height of wind speed (m)
 z_2 = adjusted wind speed height (m)
 z_o = aerodynamic roughness length (m)
 ($0.123 h$ (Shuttleworth, 1993))
 estimated at 0.007 meters for forest clearing (Bras, 1990)
 d = zero plane displacement ($0.67 h$ (Shuttleworth, 1993))
 h = height of vegetation (m)

Selection of Individual Precipitation and Discharge Events

Daily values were derived from the fifteen-minute precipitation records for the Guabá and Icos stations. To maximize the probability of analyzing spatially and temporally uniform storm events, the daily values for the two stations were compared and days for which the coefficient of variation between

stations was 10% or less were selected for further investigation. A period extending two days before and after each candidate day was extracted from the 15-minute precipitation and discharge records. The abstraction model described above, with an initial storage value of 0 mm, was applied to each 5-day period for each event. Precipitation and discharge were graphed for the 5-day period and each precipitation event that was separated from prior and subsequent events by a time period equal to or greater than the duration of the quickflow recession curve was deemed acceptable for further analysis. The corresponding discharge record was examined to assure that both the event and antecedent recession curves registered a continual decline. The point at which 90% of event precipitation had been recorded was assigned as the inception of the quickflow recession curve. This was necessary since minimal, trailing amounts of precipitation were often recorded after the principal mass of a storm event occurred.

Table 5-2 lists the characteristics that were determined for each storm event. To facilitate comparison, both precipitation and runoff rates are expressed as mm/hr and volumes are expressed as an equivalent watershed depth (mm). Guabá station is closest to the center of Icacos basin and, thus, was used to calculate parameters that include precipitation as a component.

Table 5-2: Storm parameters derived for each event.

Parameter	Units
Gross Precipitation	mm
Net Precipitation	mm
Interception	%
Duration of Precipitation	hours
90% Duration of Precipitation	hours
Duration of Quickflow	hours
Total Runoff	mm
Total Runoff as percent of Gross Precipitation	%
Baseflow	mm
Baseflow as percent of Gross Precipitation	%
Quickflow	mm
Quickflow as percent of Gross Precipitation	%
Maximum 15-minute Precipitation Intensity	mm/hr
Peak Instantaneous Runoff Rate	mm/hr
Mean Baseflow	mm/hr
Antecedent Baseflow	mm/hr

Statistical Analysis of Storm Event Descriptors

An inquiry into hydrologic processes should precede any use of statistics to examine potential covariation or causal relationships among hydrologic parameters (Hirsch et al., 1993). The *a priori* examination of basin characteristics permits the development of hypotheses that are more focussed and, thus, more powerful. Prior chapters have: 1) reviewed our current knowledge of runoff generating processes in relation to various physical and climatic characteristics, 2) described the physical and climatic characteristics for a basin located in a humid montane region of Puerto Rico and, 3) provided preliminary conjectures as to what runoff generating mechanisms might be active on the Icacos basin. The following discussion presents predictor and

explanatory variables and the statistical models that are meant to test the runoff processes that are hypothesized to occur on the Iacos basin.

Hydrograph parameters and precipitation characteristics related to a storm event can provide insight into the probable runoff generating mechanisms that are operative within a basin. The various pathways that water follows while en route to a basin outlet will delay and dampen flows by differing degrees and, thus, alter the characteristics of the hydrograph. In particular, contrasting behavior is expected when comparing mechanisms controlled by surface phenomena versus those controlled by subsurface conditions. A strong relationship between the peak instantaneous runoff rate and maximum precipitation intensity is likely to occur in relation to the mechanism of infiltration-excess overland flow (Moore et al., 1986). In contrast, a weak or non-existent relationship can be anticipated when soil moisture status is the critical control (Dunne, 1978). The degree of basin wetness is reflected in measures such as antecedent baseflow or antecedent precipitation. When saturation-excess overland flow predominates, the relative proportion of quickflow to total runoff will be determined, in part, by the degree of basin wetness before and during an event.

A linear model was used to determine whether dependent and explanatory variables were related and, if so, the strength of the relationship (Hirsch et al., 1993). Prior to application of the linear model, the degree of linear association between variables was examined using the Pearson Product-Moment Correlation. Product-moment correlation measures only linear

association and a value of -1 or +1 indicates a perfect linear relationship (Velleman, 1998).

The following steps are prescribed to determine the applicability of a linear model. The normality of each variable is examined and, when necessary, an appropriate transformation is applied. The model is examined graphically to verify whether a linear relationship in fact exists, and to determine whether variance is constant. The slope and intercept parameters are checked to validate the physical veracity of the model. The slope of the model is tested for significance and residuals are plotted and examined for randomness and normality.

The results from the analysis of Icacos basin parameters were compared to results reported for a basin that is well described by the variable source area concept. Geebung Creek is an undisturbed forested basin, 79.6 ha in size, located 30 km from the southeast coast of New South Wales, Australia at an approximate latitude of 37° S (Moore et al., 1986). Basin relief is 174 meters and basin soils, approximately 1 meter deep and underlain by granite, are characterized by high conductivities except where source areas occur, such as along channels. Source areas are fed by rapid subsurface flow from upslope, and no indication exists of infiltration-excess overland flow. Storm event descriptors reported for 20 events that occurred on the Geebung Creek were treated and analyzed in the same manner as were those from Icacos basin.

Topographic Analysis

TOPMODEL, the topography-based hydrologic model, was applied to individual storm events for the Guabá subcatchment (Figure 3-2). The relative small size of the basin, the homogeneity of basin characteristics, and the uniformity of inputs minimizes complicating factors that hinder the parameterization and evaluation of a model. Guabá has an area 1/25th that of the Río Icos basin, which ensures a relatively uniform test case for the model simulations. The basin has one vegetation type (Figure 3-3) and 75% is covered by one soil complex (Figure 3-4), for which information is available from various sources.

The size of Guabá allows greater confidence in the assumption that precipitation, as measured at the basin outlet, is representative of a uniform spatial distribution over the subcatchment. This assumption is further enhanced since the recorded precipitation amounts at Guabá and Icos (Figure 3-2) correlate closely in amount and distribution for the selected storm events. Mean monthly rainfall and runoff totals for concurrent records from Guabá and Icos basin were compared as an additional check on the hydrologic similarity of the two basins.

The storm events selected for simulation were a subset of those extracted for the statistical analysis of storm event parameters, previously described. Two sets of events were selected, one that corresponded to a dry climatic regime, as reflected in the discharge record, and a set that corresponded to a wet climatic

regime. Events were then selected from both sets for model calibration and subsequent validation.

A DEM was constructed for Guabá basin and used to derive the topographic-index distribution function for the basin. A DEM, with a 6-meter resolution, was derived from an USGS digital line graph of hypsography with a 10-meter contour interval. A 6-meter resolution was chosen to adequately characterize the topographic features that control the spatial distribution of hydrologic processes within the basin, while not overly exceeding the inherent accuracy of the DLG. The interpolation from a 10-meter contour interval to a 6-meter resolution DEM should not compromise the representation of basin topography.

The functionality of ARC/INFO (Version 7.2.1, 1998) was used to create the elevation grid (TOPOGRID). Grid cells associated with a stream channel were identified using a contributing area of 7500 m^2 ; the minimum area for perennial flow as determined in the field by Larsen (1997). The computer generated stream network was compared to the stream network that was delineated manually using the crenulation method (Strahler, 1969). The minor discrepancies that existed between the two networks were resolved in favor of, first, the blue line network on the USGS topographic quadrangle and, second, the network created manually. The elevation grid then was processed with the ancillary TOPMODEL program GRIDATB, which derives the topographic-index distribution function (Beven et al., 1995b).

TOPMODEL response is controlled directly by 4 input parameters (Beven et al., 1995a):

1. M - which describes the exponential decay of soil transmissivity with depth (m);
2. T_0 - the lateral transmissivity of the soil profile when saturated (m^2/hr);
3. SRMAX - the maximum storage deficit of the root zone (m);
4. V - the channel routing velocity (m/hr), the importance of which increases with basin size.

TOPMODEL response is sensitive, in particular, to the exponential decay parameter (M). A physical interpretation of M is that it controls the effective depth of the soil profile (Beven et al., 1995a). Values cited in the literature for this parameter range from 0.003 to 0.1 m (Hornberger et al., 1985; Beven, 1997). An initial estimate for M can be obtained from a plot of a recession curve that derives solely from subsurface sources and that is relatively unaffected by evapotranspiration (Beven et al., 1995a; Romanowicz, 1997).

To determine the recession parameter, M , for the Guabá basin, 6 baseflow recession curves were plotted and their slopes ($1/M$) were determined using regression analysis. The recession curves extracted during the baseflow recession analysis (Hydrograph Separation) were utilized to determine a range of values for the M parameter. Three of the recession curves were associated with a relative wet period and 3 with a relative dry period, as determined from a 60-day moving average of basin discharge plotted for the period of record. The

range of values resulting from the analysis was used to guide the calibration of TOPMODEL.

Precise estimates of the saturated transmissivity parameter, T_0 , are difficult to determine and implementations of TOPMODEL often utilize the topographic index rather than the combined soil/topographic index (Hornberger et al., 1985; Durand et al., 1992; Iorgulescu and Jordan, 1994). Another approach, when detailed information on the spatial distribution of soil characteristics is lacking, is to estimate a basin average value for saturated transmissivity. An estimated value for T_0 can be determined by locating a time period within the discharge record during which the basin is saturated and flow derives solely from subsurface drainage. The discharge value, Q_0 , for this period is then inserted into the following equation to derive an estimate of the saturated transmissivity parameter (Romanowicz, 1997):

$$Q_0 = T_0 e^{-\lambda} \quad (5-14)$$

The initial estimate of T_0 for Guabá basin was determined by examining a 60-day moving average of the discharge record and locating extended periods of above average discharge. A higher probability of saturated conditions within the basin is assumed to occur towards the end of an extended wet period and, particularly, after large and prolonged precipitation events. The hydrograph separation technique, described previously, was applied to several events that occurred during wet periods, and the maximum observed value of post-event baseflow discharge was assumed to represent Q_0 in equation 5-14.

TOPMODEL calibration often results in, what appear to be, abnormally high values of saturated transmissivity, T_0 . High values, in some instances, have been attributed to the effects of preferential flow pathways, which are not incorporated into measurements of hydraulic conductivity (Beven et al., 1995a). Values of T_0 cited in the literature range from 0.0007 to 2200 m²/hr, with a median value of 1.9 m²/hr (Beven, 1997).

SRMAX, the maximum storage deficit of the root zone, was determined based on observations made by researchers in Río Icacos basin, and from information published by the National Cooperative Soil Survey (National Soil Survey Center, 1998). McDowell et al. (1992) indicate that vegetation in Icacos basin is shallow-rooted and that the majority of roots are found within 20 cm of the surface. This conforms to observations in other locations of the LEF (Odum, 1970; Frangi and Lugo, 1985). The depth of root zone storage for determination of the TOPMODEL SRMAX parameter was assumed to be equal to 20 cm.

The USACE collected bulk soil samples for three sites located in the Icacos Basin (Figure 3-2) and determined soil moisture contents at 0, 0.06, 0.33, and 15-atm tension for three different soil layers. To calculate SRMAX the moisture content at 0.33-atm was assumed to correspond to field capacity and the 15-atm moisture content to the wilting point. The difference between the moisture content at field capacity and at the wilting point, times the root zone profile depth, provides an estimate of the maximum storage capacity.

Larsen (1997) surveyed cross-sectional and longitudinal profiles for a section of the Icacos River just upstream from the USGS gaging station (Figure

3-2). He calculated average depths and widths at the cross-section for a range of discharges (Table 5-3). The average channel velocity determined from Larsen's figures range from 1080 m/hr at a discharge of 0.09 cms, to 12,927 m/hr at a discharge of 79 cms. These velocity calculations were used to estimate the TOPMODEL parameter V , the channel routing velocity. For each storm event that was simulated, the channel velocity that corresponded to the average event discharge was selected from Table 5-3.

The version of TOPMODEL used in this analysis does not include an interception module. The 15-minute interval net precipitation that was calculated for each storm event was input into TOPMODEL to account for interception and evaporation losses within the forest canopy. Evaporation from root zone storage was modeled with equation 4-10. Estimates for the mean daily potential evapotranspiration at the winter high and the summer low were estimated using published values for locations at elevations similar to that of the Río Icacos basin (EarthInfo, Inc., 1995). The winter high and summer low values were adjusted until the simulated annual total corresponded to 1123 mm, the estimated potential evapotranspiration for Río Icacos basin (Larsen, 1997).

Table 5-3. Cross-sectional area and channel velocity calculations for a range of discharges recorded at the outlet of Río Icacos.

Discharge (cms)	Area (m ²)	Velocity (m/hr)
0.09	0.3	1080
0.10	0.3	1200
0.11	0.3	1320
0.13	0.3	1560
0.14	0.4	1260
0.16	0.4	1440
0.18	0.4	1620
0.20	0.4	1800
0.22	0.4	1980
0.25	0.5	1800
0.28	0.5	2016
0.32	0.5	2304
0.35	0.6	2100
0.40	0.6	2400
0.45	0.6	2700
0.50	0.7	2571
0.56	0.7	2880
0.63	0.8	2835
0.71	0.9	2840
0.79	0.9	3160
0.89	1.0	3204
1.0	1.1	3273
1.1	1.2	3300
1.3	1.3	3600
1.4	1.5	3360
1.6	1.6	3600
1.8	1.7	3812
2.0	1.9	3789
2.2	2.1	3771
2.5	2.3	3913

Discharge (cms)	Area (m ²)	Velocity (m/hr)
2.8	2.5	4032
3.2	2.8	4114
3.5	3.0	4200
4.0	3.3	4364
4.5	3.6	4500
5.0	4.0	4500
5.6	4.3	4688
6.3	4.7	4826
7.1	5.2	4915
7.9	5.8	4903
8.9	6.4	5006
10	7.1	5070
11	7.8	5077
13	8.4	5571
14	9.0	5600
16	9.6	6000
18	10.2	6353
20	10.9	6606
22	11.5	6887
25	12.2	7377
28	12.9	7814
32	13.6	8471
35	14.4	8750
40	15.3	9412
45	16.2	10000
50	17.2	10465
56	18.2	11077
63	19.3	11751
71	20.5	12468
79	22.0	12927

Source: Larsen, 1997

CHAPTER 6

RESULTS AND DISCUSSION

Recession Curve Analysis

The master recession curve for Río Icacos was constructed using six recorded discharge events that exhibited long recession periods uninterrupted by precipitation. The six events ranged in duration from 3 to 7 days and had minimum discharges ranging from 0.09 to 0.34 cms. The master recession curve was derived from a subset of data points that were selected from the recession periods of the six discharge events. The data points were fit to an exponential decay function using linear regression. The analysis yielded a daily recession constant of 0.959 with an R^2 value of 0.99. The recession constant falls within the range commonly associated with baseflow (Nathan and McMahon, 1990).

The master recession curve was applied to 4 independent discharge events in order to determine its utility for demarcating unique storms. The terminal recession segment for each of the discharge events was extracted and subjected to the same procedures utilized to derive the master recession curve. The daily recession constants for the four events, as derived from linear regression, were 0.68, 0.73, 0.83 and 0.93. Only one constant approaches that of the master recession curve.

Several factors may help explain why the recession behavior of common discharge events did not conform to that exhibited by the master recession curve. A more robust and representative portrayal of the master recession curve is obtained when it is constructed from recession segments that are extracted from the full range of discharge stages (Wilson, 1990). Uninterrupted recession segments at higher flow stages, in humid regions, are difficult to encounter and are, thus, underrepresented in the construction of a master curve. All of the recession periods utilized to construct the master recession curve for Icacos basin had base discharges below the average daily discharge for the basin.

The literature indicates that the time period that elapses between peak discharge and the transition point from quickflow to baseflow may be considered a characteristic feature of a basin. A semi-logarithmic plot of recession curves may give an indication of transition points between different discharge components. If each component is assumed to follow a unique exponential decay function, then, a log plot will produce a series of straight lines each with a characteristic slope.

A semi-logarithmic plot of the 6 recession curves extracted for Icacos basin appears to exhibit this behavior (Figure 6-1). Three segments are apparent and they are assumed to conform to quickflow, a transition period between quickflow and baseflow, and to baseflow. The point marking the boundary between the transitional period and baseflow was utilized to determine the time period between peak flow and the inception of pure baseflow. A cursory examination of the plot indicates that the transition point occurs approximately

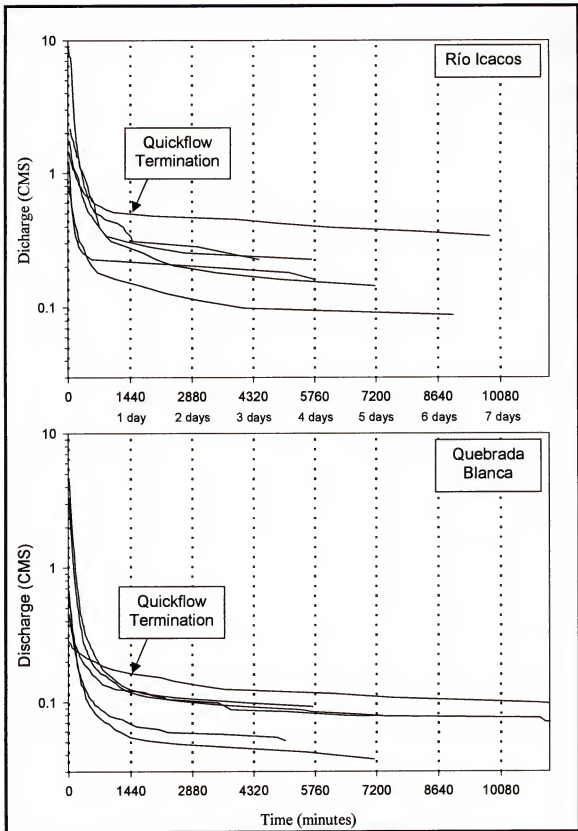


Figure 6-1. Determination of the quickflow termination point using baseflow recession curves from Río Icacos basin and Quebrada Blanca.

one day after peak discharge. This is comparable to the value of 1.05 days that is derived from a widely accepted empirical formulation and was used to define the termination of quickflow (Viessman et al., 1989).

Six additional curves were extracted from a neighboring basin as a check on the results obtained for Icacos basin (Figure 6-1). Quebrada Blanca is an 8.42 km² basin located southwest of Icacos basin at an elevation of 140 m. The basin has a mean annual runoff of approximately 743 mm, which is considerably less than Río Icacos. Longer (6-13 days) and better-behaved recession curves were obtained from the discharge records. The minimum discharge for the 6 curves ranged from 0.04 to 0.09 cms. The results for the Quebrada Blanca correspond with those obtained for Río Icacos (Figure 6-1).

Description of Storm Events

Between water years 1993 through 1997 there were nearly 400 days for which the coefficient of variation was 10% or less for daily precipitation totals recorded at the Icacos and Guabá gages. Further inspection yielded 35 independent storm events that met the criteria for subsequent analysis; a separation from prior and subsequent events by a period of one day or more. The selected events were spread uniformly throughout the year, with each month represented by 2, 3 or 4 events. A subset of the precipitation and discharge descriptors derived for each event are reported in Table 6-1, by date of occurrence. The Guabá precipitation gage is located closest to the basin center and, thus, is more representative of the basin average. Precipitation

Table 6-1. Storm descriptors used in the analysis of 35 events that occurred on Río Icaos basin, 1993-1997.

Date	Precipitation		Runoff				Rates		Basin Wetness	
	Gross (mm)	Net (mm)	Total (mm)	Quick flow (mm)	Quick-flow Prop. (%)	Base-flow (mm)	Max Precip. Intensity (mm/hr)	Peak Instant. Runoff (mm/hr)	Mean Base-flow (mm/hr)	Ant. Base-flow (mm/hr)
11/11/1993	4.6	3.8	3.4	0.4	9.2%	3.0	6.3	0.175	0.122	0.122
11/20/1993	9.1	7.9	8.6	3.3	35.9%	5.3	60.2	1.220	0.208	0.231
11/30/1993	16.0	15.5	11.7	5.6	35.1%	6.1	42.5	1.908	0.232	0.175
1/13/1994	11.7	10.0	7.6	3.3	27.9%	4.4	14.2	0.751	0.123	0.141
1/15/1994	5.3	4.1	3.6	0.7	13.3%	2.9	7.8	0.200	0.115	0.113
2/14/1994	13.5	11.8	5.3	2.5	18.3%	2.8	6.9	0.751	0.097	0.097
2/16/1994	11.4	10.1	5.0	2.2	19.0%	2.8	21.1	0.532	0.106	0.122
3/2/1994	37.3	33.6	17.2	11.7	31.2%	5.5	15.2	1.626	0.113	0.097
3/11/1994	27.7	26.8	12.5	8.3	29.8%	4.3	24.3	1.720	0.129	0.097
6/11/1994	21.8	20.2	10.7	6.4	29.1%	4.4	18.1	0.969	0.131	0.109
7/31/1994	40.4	39.0	26.3	20.6	51.0%	5.7	36.5	4.284	0.147	0.125
8/18/1994	69.6	67.2	38.2	32.2	46.3%	5.9	103.5	10.632	0.134	0.125
9/6/1994	25.9	24.6	16.4	11.9	46.1%	4.5	29.4	2.158	0.138	0.088
9/7/1994	26.7	26.2	23.2	18.6	69.6%	4.6	33.5	7.130	0.161	0.088
12/13/1994	10.2	8.8	11.3	4.1	40.1%	7.2	9.1	0.719	0.210	0.178
12/28/1994	8.9	8.1	9.7	3.5	39.3%	6.2	33.4	0.907	0.250	0.250
2/11/1995	13.2	11.3	12.0	3.8	28.7%	8.2	15.2	1.282	0.242	0.200
3/27/1995	8.9	6.9	8.2	1.2	13.0%	7.0	8.1	0.375	0.245	0.225
4/15/1995	32.3	31.2	17.0	9.5	29.3%	7.5	51.7	1.720	0.249	0.141
7/30/1995	10.2	9.0	11.1	3.5	34.4%	7.6	23.1	0.844	0.281	0.281
8/3/1995	25.4	25.2	22.5	13.8	54.2%	8.8	121.8	4.159	0.344	0.344
9/29/1995	24.1	23.3	19.8	8.8	36.3%	11.0	29.4	1.782	0.355	0.313
11/16/1995	20.6	19.4	18.2	5.9	28.8%	12.3	60.2	2.095	0.469	0.469
1/6/1996	32.0	30.9	20.3	11.3	35.4%	8.9	33.0	1.626	0.266	0.225
1/7/1996	40.4	38.5	32.6	20.5	50.8%	12.1	33.5	4.972	0.302	0.200
3/28/1996	14.5	12.3	11.8	7.3	50.3%	4.5	9.0	0.938	0.131	0.141
4/12/1996	54.4	52.0	32.7	27.6	50.8%	5.1	30.0	2.908	0.123	0.097
7/20/1996	24.9	23.9	19.3	9.0	36.2%	10.3	27.4	1.595	0.344	0.344
10/26/1996	72.9	69.7	57.0	40.9	56.1%	16.1	35.5	6.536	0.328	0.200
10/28/1996	43.7	41.3	47.9	30.5	69.7%	17.5	37.6	6.285	0.375	0.375
2/9/1997	29.0	28.8	45.6	18.0	62.0%	27.7	17.2	5.191	0.774	0.751
5/13/1997	18.3	15.9	20.0	11.5	62.8%	8.6	27.3	3.124	0.263	0.225
5/27/1997	15.0	14.2	14.1	9.2	61.6%	4.8	18.2	3.690	0.195	0.281
6/26/1997	16.5	15.4	14.5	9.1	54.9%	5.5	14.2	1.438	0.168	0.141
8/9/1997	54.1	51.7	53.2	32.3	59.8%	20.9	41.4	3.534	0.489	0.178
Average	25.44	23.90	19.7	11.7	40.5%	8.0	31.3	2.565	0.239	0.208
Maximum	72.90	69.71	57.0	40.9	69.7%	27.7	121.8	10.632	0.774	0.751
Minimum	4.57	3.84	3.4	0.4	9.2%	2.8	6.3	0.175	0.097	0.088

intensities and volumes recorded at Guabá are reported in Table 6-1 and were used in the subsequent analyses.

Gross precipitation amounts for the 35 events ranged from approximately 5 mm to 73 mm. Interception, as a proportion of gross precipitation, averaged 7.6% and ranged from 1% to 18%. The proportion of gross precipitation abstracted due to interception and evaporation tended to increase with smaller storms, as expected, and with longer duration storms. This conforms to expectations since frequent dry periods are interspersed with wet periods during events of longer duration. The 90% duration of precipitation averaged 10.2 hours and ranged from 1 hour to 26.25 hours.

Total runoff for the 35 events averaged approximately 20 mm and ranged from 3 mm to 57 mm. Peak instantaneous runoff rates averaged 2.6 mm/hr and ranged from 0.2 mm/hr to 10.6 mm/hr. These rates are considerably lower than maximum peak rates, of 15 mm/hr to 60 mm/hr, measured on similar sized basins known to be dominated by Hortonian overland flow, but are higher than rates on basins dominated by subsurface flow (Dunne, 1978).

Statistical Analysis

Maximum Precipitation Intensity Versus Peak Instantaneous Runoff Rate

The first analysis conducted was designed to check the strength of the relationship between the maximum precipitation intensity and the peak instantaneous discharge. A strong correlation can be expected between these two parameters in basins that are dominated by infiltration-excess overland flow.

In contrast, negligible correlation is expected in a basin for which subsurface moisture status is the primary control on runoff mechanisms, such as saturation-excess overland flow.

Figures 6-2 and 6-3 contain boxplots and histograms that illustrate the distribution of maximum precipitation intensity values for the 35 storm events. In each figure, and in each subsequent figure of this type, the left-hand plot represents the distribution of the original variable (e.g. maximum precipitation intensity) and the right-hand plot portrays the distribution of a log transformation of the variable. The central box of each boxplot (e.g. Figure 6-2) depicts the range of values between the 25th (low hinge) and 75th percentiles (high hinge) and the horizontal line within the box marks the median value. The whisker that extends below the bottom hinge represents the median value for the range of data between the minimum value and the overall median (Velleman, 1997). The whisker that extends above the top hinge represents the median value for the range of data that extends from the overall median to the maximum value. Outliers, when present, are portrayed as circles, and extreme outliers are portrayed as starbursts. An extreme outlier exceeds the high hinge by three times the height of the central box or is lower than the low hinge by an equal amount.

The median value for the distribution of maximum precipitation intensities was 27.4 mm/hr and the values within the main body (low to high whisker) ranged from 6 to 60 mm/hr (Figure 6-2). Two extreme outliers are evident: 103.5 mm/hr that occurred on 8/18/94 and 121.8 mm/hr that occurred on 8/3/95.

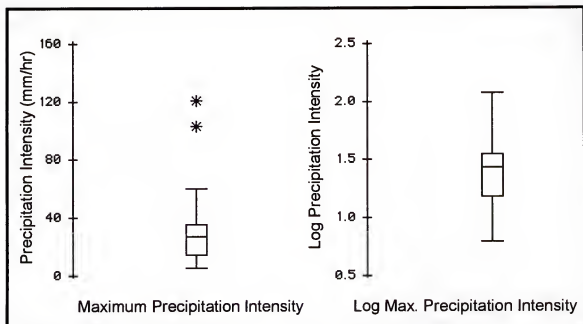


Figure 6-2. Boxplot showing the distribution of maximum precipitation intensity values recorded at Guabá during 35 storm events.

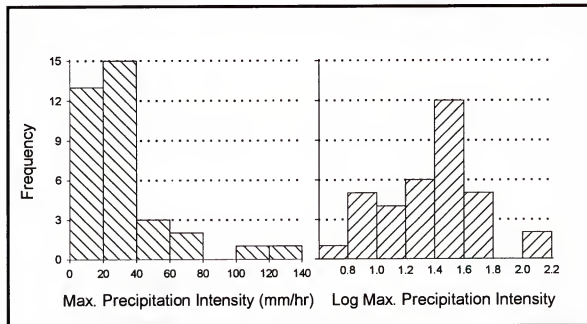


Figure 6-3. Histogram showing the distribution of maximum precipitation intensity values recorded at Guabá during 35 storm events.

Both the boxplot and histogram indicate that the distribution of the maximum precipitation intensities is skewed. The log transformation of the precipitation intensities provides a more symmetrical distribution and, thus, was used in the subsequent analysis.

Figures 6-4 and 6-5 show the distribution of peak instantaneous runoff rate for the 35 storm events. The median peak instantaneous runoff rate is 1.72 mm/hr and the values within the main body of the boxplot range from 0.18 to 7.13 mm/hr. The outlier in Figure 6-4 represents a runoff rate of 10.6 mm/hr that occurred on 8/18/94. Both the boxplot and histogram depict a skewed distribution for peak instantaneous runoff rate. The log transformation provides a more symmetrical distribution and was used in the subsequent analysis.

The Pearson Product-Moment Correlation between the transformed dependent variable, peak instantaneous runoff rate, and the transformed explanatory variable, maximum precipitation intensity, was 0.703 for Icacos basin and 0.310 for Geebung Creek. These results indicate a substantially stronger linear association exists for Icacos than for Geebung Creek. The two variables were fit to the following equation:

$$D = a + bP + \varepsilon$$

where D	= peak instantaneous runoff rate (mm/hr)
P	= maximum precipitation intensity (mm/hr)
a	= intercept coefficient
b	= slope coefficient
ε	= error term

The results of the regression analysis (Figure 6-6 and Table 6-2) demonstrate that Icacos basin exhibits a substantially stronger relationship

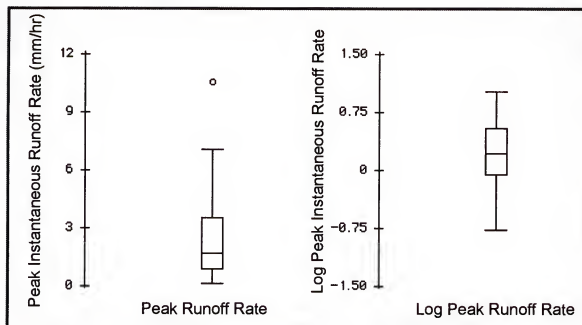


Figure 6-4. Boxplot showing the distribution of peak instantaneous runoff rates recorded for Río Icacos during 35 storm events.

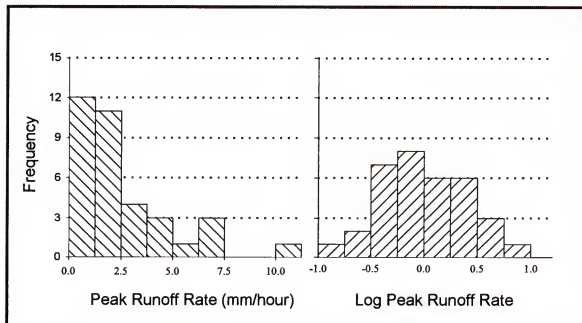


Figure 6-5. Histogram showing the distribution of peak instantaneous runoff rates recorded for Río Icacos during 35 storm events.

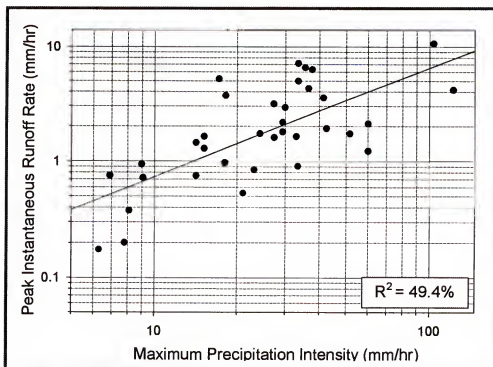


Figure 6-6. Log-Log regression plot of peak instantaneous runoff rate versus maximum precipitation intensity for Río Icacos basin.

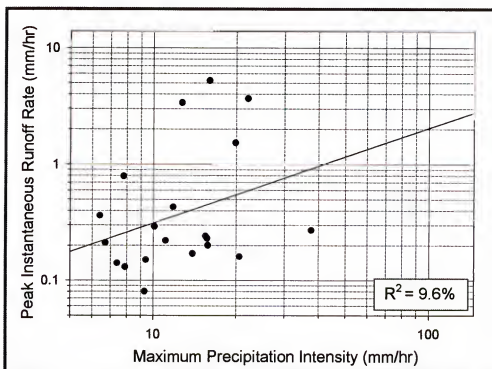


Figure 6-7. Log-Log regression plot of peak instantaneous runoff rate versus maximum precipitation intensity for Geebung Creek.

between maximum precipitation intensity and peak instantaneous runoff rate than does Geebung Creek (Figure 6-7). The regression model for Icacos explained nearly 50% of the variation, compared to approximately 10% for Geebung Creek; and the regression coefficients were significant for Icacos and not for Geebung Creek. The poor correlation in the case of Geebung Creek was attributed to hydrologic behavior that is governed by the subsurface moisture status (Moore et al., 1986). Similar results were anticipated for Icacos, based on the review of site characteristics and climatic controls within the basin and the surrounding region. The disagreement with expectations will be discussed after the remaining analyses are performed.

Table 6-2. Regression results of log peak instantaneous runoff rate versus log maximum precipitation intensity for Río Icacos basin.

R squared = 49.4% S = 0.3047 with 35 - 2 = 33 degrees of freedom				
Source	Sum of Squares	Df	Mean Square	F-ratio
Regression	2.997	1	2.997	32.3
Residual	3.06428	33	0.0928571	
Variable	Coefficient	s.e of Coeff	t-ratio	prob
Constant	-1.07917	0.2367	-4.56	≤ 0.0001
Log Max Precip. Intensity	0.946348	0.1666	5.68	≤ 0.0001

Quickflow Versus Basin Wetness

When subsurface moisture status is the primary control on runoff, it is anticipated that basin wetness will be a strong predictor of the proportion of runoff that is produced as quickflow. This is true particularly for variable source areas, which fluctuate in size and moisture status in relation to basin wetness and, thus, vary in their contribution to runoff. Analyses were conducted using

mean baseflow and antecedent baseflow as indicators of basin wetness. The strength of basin moisture status as a predictor of the relative proportion of storm event quickflow was tested. Gross precipitation was added to the regression analysis to examine its contribution as an explanatory variable.

The range of values for mean baseflow, excluding outliers, was approximately 0.10 to 0.49 mm/hr; and the median value was 0.21 mm/hr. One outlier, with a value of 0.77 mm/hr, occurred on 2/9/97 (Figure 6-8). The boxplot in Figure 6-8 and the histogram in Figure 6-9 indicate a somewhat skewed distribution for mean baseflow and, thus, the transformed distribution was used for subsequent analysis.

The range of values for antecedent baseflow, excluding outliers, was approximately 0.09 to 0.38 mm/hr; and the median value was 0.18 mm/hr. One outlier, with a value of 0.47 mm/hr occurred on 11/16/95. An extreme outlier of 0.75 mm/hr (2/9/97) was not removed in the log transformation of antecedent baseflow and will bear further scrutiny (Figure 6-10). The log transformation of antecedent baseflow was used in the analysis although it did not entirely remove the skewed distribution (Figures 6-10 and 6-11).

The proportion of runoff attributed to quickflow ranged from 9% to 70%, with a median value of 36%. No transformation was necessary as the boxplot and histogram (Figure 6-12) indicate a symmetrical distribution. The range of values for gross precipitation at Guabá, excluding outliers, was approximately 5 to 54 mm; and the median value was 21.8 mm (Figure 6-13). Two outliers

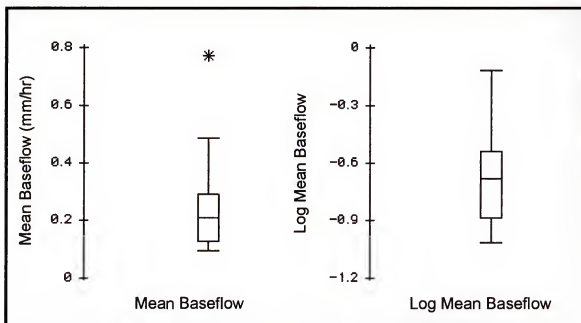


Figure 6-8. Boxplot showing the distribution of mean baseflow values recorded for Río Icacos during 35 storm events.

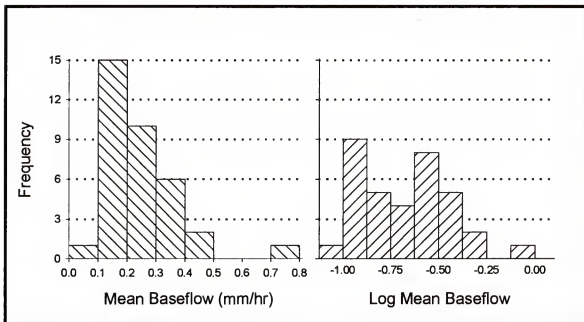


Figure 6-9. Histogram showing the distribution of mean baseflow values recorded for Río Icacos during 35 storm events.

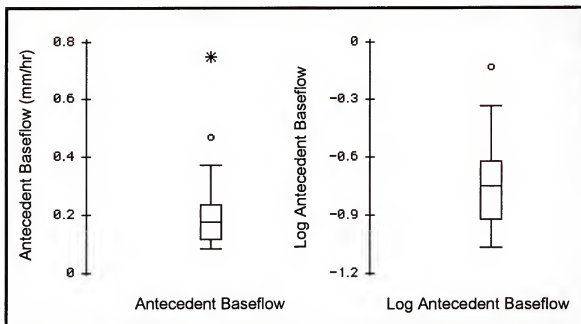


Figure 6-10. Boxplot showing the distribution of antecedent baseflow recorded for Río Icacos prior to 35 storm events.

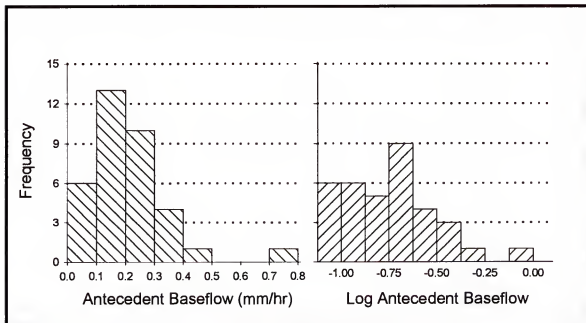


Figure 6-11. Histogram showing the distribution of antecedent baseflow recorded for Río Icacos prior to 35 storm events.

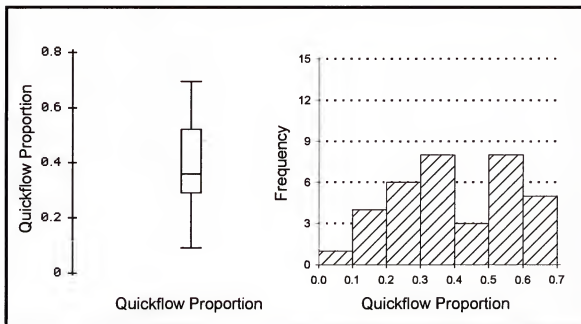


Figure 6-12. Boxplot and histogram showing the distribution of the quickflow proportion recorded for Rio Icaos during 35 storm events.

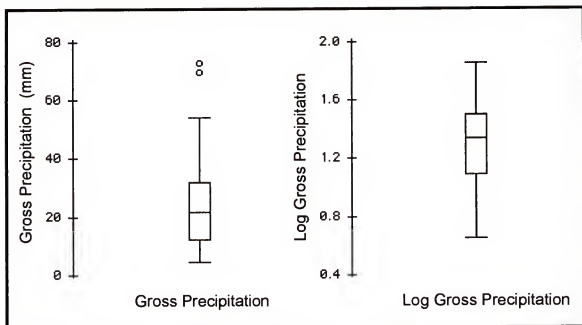


Figure 6-13. Boxplot showing the distribution of gross precipitation values recorded at Guabá during 35 storm events.

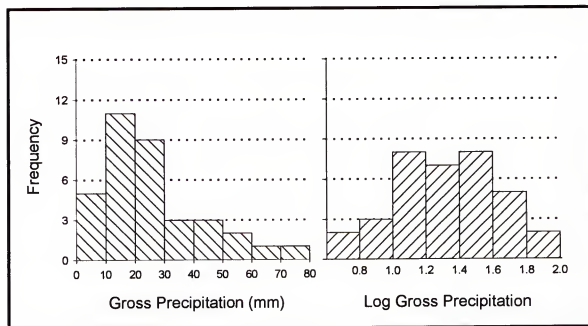


Figure 6-14. Histogram showing the distribution of gross precipitation values recorded at Guabá during 35 storm events.

occurred: 69.6 mm on 8/18/94 and 72.9 mm on 10/26/96. The transformed values were used in the subsequent analysis (Figures 6-13 and 6-14).

Pearson Product-Moment Correlations for quickflow proportion, log mean baseflow, log antecedent baseflow, and log gross precipitation, are presented in Table 6-3 for Icacos and in Table 6-4 for Geebung Creek. In the case of Geebung Creek, a correlation of 0.841 between quickflow proportion and mean baseflow indicates a strong linear association, as was reported by Moore et al. (1986). In contrast, the correlation of quickflow proportion with mean baseflow is only 0.410 in Icacos basin, indicating a weaker relationship. The correlation between quickflow proportion and antecedent baseflow is particularly weak for Icacos. It is noteworthy that, in the case of Icacos, the correlation between quickflow proportion and gross precipitation is greater than is the correlation between quickflow proportion and indicators of the degree of basin wetness.

The variables quickflow proportion, log mean baseflow, and log gross precipitation were fit to the following multiple regression equation. Antecedent baseflow was not included given the low correlation reported in Table 6-3.

$$Q = a + b_1W + b_2P + \varepsilon$$

where Q = quickflow proportion
 W = log mean baseflow
 P = log gross precipitation
 a = intercept coefficient
 $b_{1,2}$ = slope coefficients
 ε = inherent errors

The regression results are presented in Figure 6-15 and Table 6-5. The regression results in Figure 6-15 (Geebung A) clearly demonstrate that mean

Table 6-3. Pearson Product-Moment Correlations for quickflow proportion, mean baseflow, antecedent baseflow, and gross precipitation for Río Icacos basin.

	Quickflow Proportion	Log Mean Baseflow	Log Antecedent Baseflow	Log Gross Precipitation
Quickflow proportion	1.000			
Log Mean Baseflow	0.410	1.000		
Log Antecedent Baseflow	0.265	0.877	1.000	
Log Gross Precipitation	0.597	0.274	0.013	1.000

Table 6-4. Pearson Product-Moment Correlations for quickflow proportion, mean baseflow, antecedent baseflow, and gross precipitation for Geebung Creek.

	Quickflow Proportion	Log Mean Baseflow	Log Antecedent Baseflow	Log Gross Precipitation
Quickflow proportion	1.000			
Log Mean Baseflow	0.841	1.000		
Log Antecedent Baseflow	0.552	0.715	1.000	
Log Gross Precipitation	0.333	0.139	-0.350	1.000

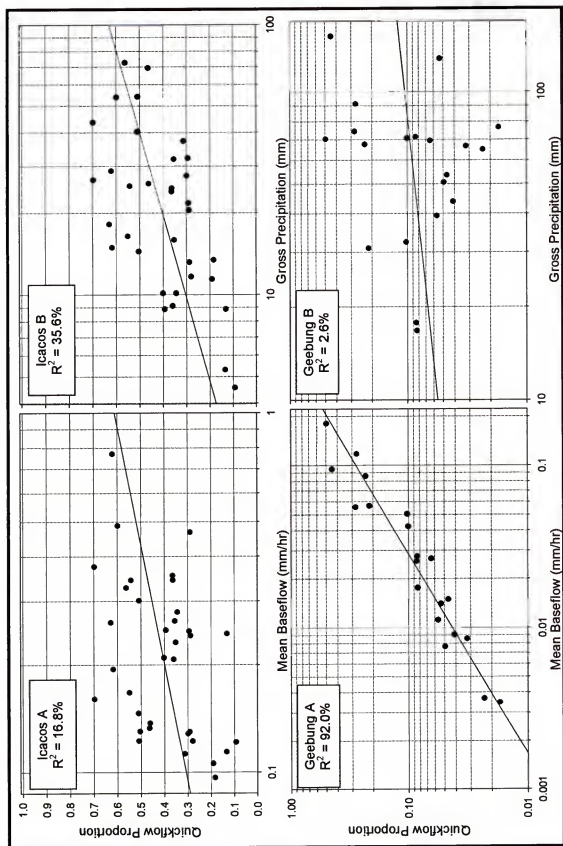


Figure 6-15. Regression plots of quickflow versus mean baseflow and gross precipitation for the Rio Icacos basin and Geebung Creek.

baseflow is a strong predictor of the proportion of storm event quickflow in Geebung Creek. The coefficient of determination is 92.0%, the F-ratio is 207, and the regression coefficients were significant (t-ratio for a = 23.9; t-ratio for b = 14.4). In contrast, Table 6-5 and Figure 6-15 (Icacos A) indicate that mean baseflow is a poor predictor of the proportion of quickflow in Icacos Basin. The regression analysis, with mean baseflow as sole predictor, yields a coefficient of determination of 17%. An R^2 value of 36% (Figure 6-15, Icacos B) indicates that gross precipitation has more value as a predictor of quickflow proportion than does mean baseflow.

Table 6-5. Regression results of quickflow proportion versus log mean baseflow and log gross precipitation for Río Icacos basin.

R squared = 42.2% R squared (adjusted) = 38.5%				
s = 0.1281 with 35 - 3 = 32 degrees of freedom				
Source	Sum of Squares	df	Mean Square	F-ratio
Regression	0.382563	1	0.191281	11.7
Residual	0.524782	32	0.0163994	
Variable	Coefficient	s.e of Coeff	t-ratio	prob
Constant	0.164639	0.1387	1.19	0.2441
Log Mean Baseflow	0.197102	0.1034	1.91	0.0657
Log Gross Precip.	0.285561	0.07626	3.74	0.0007

Discussion of Statistical Analysis

Physical and climatic characteristics suggest that Icacos basin conforms to the concept of variable source areas fed by subsurface flows from upslope. Moore et al. (1986) demonstrated that a similar mechanism occurs on Geebung Creek and provided supporting behavioral evidence. The previous sections

reported and compared the results obtained for Icacos basin with those from Geebung Creek. The results show a significant difference in the hydrologic behavior of the two basins. The following discussion attempts to explain the differences and, based on the statistical analyses and on additional field evidence, describe the hydrologic behavior of Icacos basin and identify runoff generating mechanisms.

Infiltration capacities measured in Icacos were 2-9 cm/minute (McDowell et al., 1992), values which greatly exceed typical rainfall intensities of 80 mm/hr (0.13 cm/minute) reported for the LEF (Brown et al., 1983). Based on the 15-minute or less resolution of the precipitation data used in the current study, the average maximum precipitation intensity for the 35 storm events was 31 mm/hr and, of course, the average precipitation intensity during each storm was considerably lower. The average duration of the storm events was approximately 10 hours and events were often punctuated by frequent intervals of no rain or light rain, during which infiltration capacity recovers. During a year-long field investigation McDowell et al. (1992, p. 64) reported that "although some overland flow was observed in the well fields during intense events, most incoming precipitation quickly entered subsurface flow paths". The measured hydrologic parameters and the experimental observations conducted on Icacos basin appear to rule out overland flow as a significant runoff generating mechanism.

The USACE, in 1962-1963, conducted a trafficability study in Puerto Rico that included 3 sites located within the Icacos basin (Kennedy and Hicks, 1968).

The sites were located on upper slopes and ridges, at elevations of 703, 745 and 774 meters (Figure 3-2, Sites A, B, and C). Accumulated rainfall and the depth to the water table were measured on a daily basis, and monthly measurements of soil moisture were collected over a one-year period at two of the sites (Figure 3-2, sites A and B). Additional information, collected at all 3 locations, included site descriptions and notes on vegetation and soil conditions.

The daily moisture accounting revealed a persistent perched water table, with an approximate average depth of 1 m below the surface, which responded rapidly to rainfall inputs. Soil moisture content was measured on a monthly basis at 3 depth ranges: 0-15 cm, 15-30 cm, and 30-46 cm. The moisture content in each depth range, at both sites, was regularly well above field capacity and averaged 82% of saturation. The average levels of soil moisture reported by the USACE are consistent with observations, in upper soil layers, of moderate to rapid pore-pressure responses during short duration events (Larsen and Torres-Sánchez, 1992). The increases in pore-pressure were greatest in lower sections of concave slopes; topographic features that are commonly associated with source areas.

In a 1988 field study, 11 wells were installed at the stream bank, in the floodplain, and up the adjacent slope next to a tributary of the Icacos River (McDowell et al., 1992). The tributary drains an area of 12.4 ha, the well field is at an approximate elevation of 620 meters, and the wells were 180 and 210 cm deep. Periodic observations revealed that the water table surface was inclined sharply from upslope to stream channel. An average head differential of 2.1

meters over 22 meters indicated strong subsurface flow towards the stream channel. Furthermore, McDowell et al. (1992, p. 64) reported that "Large gradients in water table elevation and moderate to high saturated hydraulic conductivities result in relatively large rapid specific discharges (8.2×10^{-4} to 1.5×10^{-1} m/day at the observed hydraulic gradient)."

Water table depths in the well field were observed to respond "very quickly" (McDowell et al., 1992; p. 64) to precipitation events, in agreement with similar observations reported by the USACE (Kennedy and Hicks, 1968). Figure 6-16 illustrates the rapid water table rise that was recorded, during a storm event, in two wells located in the floodplain (McDowell et al., 1992).

Dunne (1978) reports relationships between lag time and peak runoff rate that were derived from overland flow and subsurface flow hydrographs from numerous basins of varying sizes located in temperate regions. These relationships predict an approximate lag time of 1/2 hour for a basin, similar in size to Icacos, that is subject to infiltration-excess overland flow and 25 hours for a basin subject to subsurface flow. The average lag between maximum precipitation intensity and the peak instantaneous runoff rate for the 35 events on the Icacos basin was approximately 2 hours with a standard deviation of 0.8 hours.

The apparent predominance of subsurface flow in conjunction with relatively short lag times is seemingly incongruous. However, the evidence presented so far indicates that the soils within Icacos basin, though deep, are characterized by a persistent perched water table, above which the soil is near

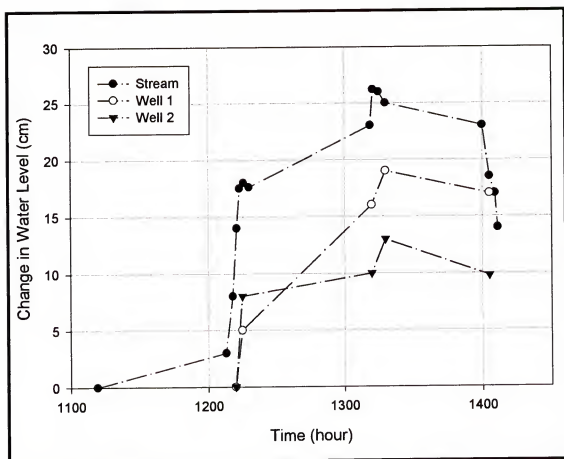


Figure 6-16. Comparison of the water level rise in two floodplain wells with the stream level rise during a storm event (McDowell et al., 1992).

saturation. The fine-textured soils in combination with a low available storage capacity provide for an extremely responsive basin. This is evident in the relatively quick response time of the basin and the relatively high degree of linear association between maximum precipitation intensity and peak instantaneous runoff rate (0.703). The poor correlation between basin wetness and quickflow proportion can be attributed to the persistently high moisture status of the basin.

To investigate further the relationship between basin moisture status and quickflow proportion, the discharge record was examined for extended periods of high and low flows. Figure 6-17 shows a 60-day moving average of daily runoff for Río Icacos between the years 1992 and 1997. An extended period of low flow is apparent from late 1993 through 1994, and there is a prolonged wet period that extends from late 1995 through the middle of 1997. The apparent dry period in Figure 6-17 corresponds to an island-wide drought that affected Puerto Rico from 1994 to 1995 (Larsen, 1997).

The 35 storm events were categorized according to whether they occurred during a wet, dry or normal hydrologic regime (Figure 6-17). The dry hydrologic regime was defined as the period during which the trend line dipped below the long-term median daily runoff for Río Icacos (11 events: 1/13/94-9/7/94). The wet hydrologic regime was defined as the period during which the trend line rose above the long-term mean daily runoff (13 events: 9/29/95-5/27/97).

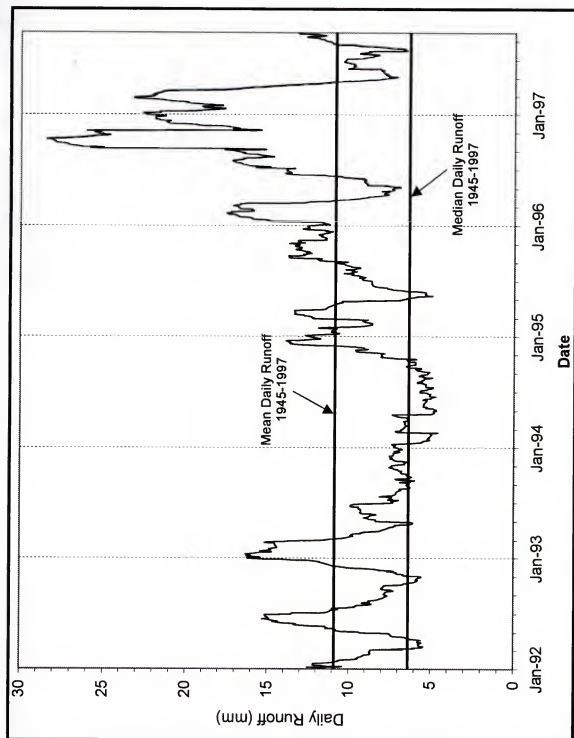


Figure 6-17. Sixty day moving average of daily runoff for Rio Icacos: 1992-1997

Figure 6-18 is a plot of quickflow proportion versus mean baseflow for those events that occurred during the dry hydrologic regime. The degree of association is quite striking, especially when compared to the weak relationship that exists when all events are considered (Figure 6-15, Icacos A). The Pearson Product-Moment Correlation for the two variables is 0.91 and R^2 is 82.7. Figure 6-18 also highlights strong seasonal affects. Dry season (winter/spring) events have a lower mean baseflow and a lower proportion of event runoff that occurs as quickflow than do events that occur during the wet season (summer/fall).

The results correspond to those expected in a basin well described by the variable source area concept, as exemplified by Geebung Creek. The response of Icacos basin would appear to be tied to the floodplain soil and to adjacent topographic features. The next section will investigate this relationship through a topographic analysis of Guabá basin, a subcatchment of Río Icacos. The topography of Guabá will be analyzed and the hydrologic behavior will be tested using a subset of the 35 storm events.

Topographic Analysis

The topography-based simulation model was applied to storm events that occurred on the Guabá subcatchment. Prior to simulation, the hydrologic behavior of the Río Icacos and Guabá basins was compared to check their similarity. Mean monthly precipitation and runoff were analyzed for the period of overlapping record, from 11/93 to 9/97. Months with more than one missing day were not included in the analysis. Figure 6-19 contains two graphs, the top

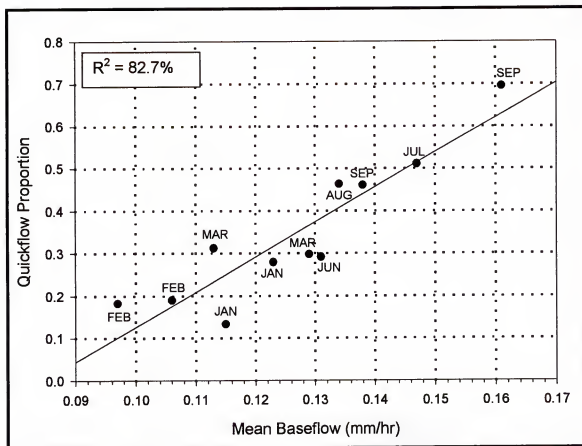


Figure 6-18. Regression plot of quickflow proportion versus mean baseflow for 11 storm events that occurred during a dry hydrologic period on the Río Icaos basin.

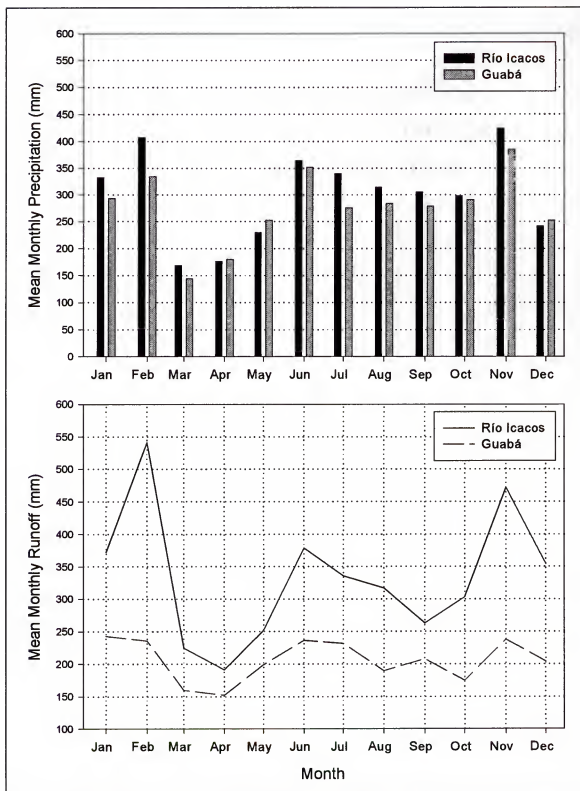


Figure 6-19. Mean monthly precipitation and runoff recorded at the Río Icacos and Guabá basin outlets from 11/1993 to 9/1997.

graph compares the mean monthly precipitation recorded at Guabá and Icacos, while the bottom graph compares mean monthly runoff. The precipitation plot shows close correspondence between the two stations. In contrast, runoff from the Guabá subcatchment appears to be considerably less than that from the entire basin. These results are contrary to expectations, since similar basin characteristics and inputs should result in similar outputs.

To verify the results portrayed in Figure 6-19, the rainfall and runoff records were divided into wet (11/95 - 9/97) and dry periods (1/94 - 9/94) using, as a guide, the 60-day moving average of daily runoff (Figure 6-17). Figure 6-20 depicts the rainfall/runoff relationship for Guabá and Icacos basin during each of these periods. Table 6-6 lists, as an average monthly amount, the rainfall and runoff recorded at the Río Icacos and Guabá outlets during the entire period, and for the wet and dry periods. The relative differences in rainfall and runoff amounts, between stations, and the runoff ratios are listed in Table 6-6 as well.

The differences in runoff amounts, depicted in Figure 6-19, can be partly attributed to the runoff recorded at the Icacos outlet during the wet period. The level of agreement between precipitation (5%) and runoff (< 1%) amounts recorded at the two locations is high during the dry period (Table 6-6). The precipitation amounts recorded at the two stations during the wet period are within 9% and within 7% of each other for the entire period. Except for the runoff ratio for the Icacos wet period (132%), all ratios (77%, 74%, and 80%) agree closely with the runoff ratio, 83%, previously calculated for Río Icacos from long-term records. A review of moderate months, those neither wet nor dry, revealed

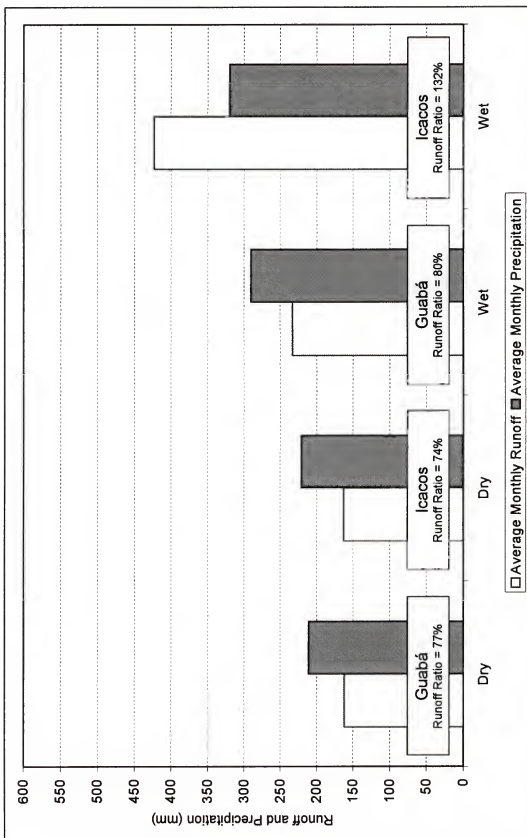


Figure 6-20. Average monthly precipitation and runoff recorded at the Río Icaos and Guabá basin outlets during wet and dry periods: 11/1993 - 9/1997.

Table 6-6. Comparison of average monthly precipitation and runoff at the Río Icacos and Guabá basin outlets during wet and dry periods: 11/1993 – 9/1997.

Station Location	Entire Period 11/93 – 9/97			Wet Period 11/95 – 9/97			Dry Period 1/94 – 9/94		
	Rain (mm)	Runoff (mm)	Runoff Ratio	Rain (mm)	Runoff (mm)	Runoff Ratio	Rain (mm)	Runoff (mm)	Runoff Ratio
Icacos	289	325	113%	320	423	132%	221	163	74%
Guabá	270	203	75%	291	233	80%	211	162	77%
Difference	7%	46%	---	9%	58%	---	5%	<1%	---

more runoff recorded at the Icacos outlet than precipitation, yielding a runoff ratio of 106 percent.

The above results give no clear indication as to why more runoff than precipitation is observed at the Río Icacos outlet during both the wet and moderate periods. A plausible explanation is that basin average rainfall receipts are greater than is indicated by precipitation recorded at Icacos and Guabá. Assuming that the average runoff ratio for the whole basin is 75%, and given the average monthly runoff of 325 mm over the period of record (Table 6-6), the corresponding average monthly rainfall would be 433 mm, or 5200 mm per year. This quantity is approximately 50% more than the average annual amount recorded at Icacos (3468 mm) and Guabá (3240 mm).

Brown et al. (1983) report mean annual precipitation values for 10 stations located within and adjacent to the LEF. La Mina (716 masl), the station with the largest mean annual value (4700 mm), was located between USACE sites C and D (Figure 3-2). The annual precipitation at La Mina, during 8 years of record from the early 1930's to the 1940's, ranged from approximately 3700 to 6450 mm. Brown et al. (1983) report mean annual precipitation of 3600 mm for Pico del Este (1051 masl) for a nine year period during the 1970's. This value compares favorably with the short-term values recorded at the Icacos and Guabá outlets. The mean annual value that was previously reported for the period 1983 to 1995 at Pico del Este was 4318 mm (Figure 3-5). Although the historical precipitation records for La Mina and Pico del Este do not overlap,

long-term stations in their vicinity indicated that annual precipitation followed a fairly uniform trend during the period.

Weaver (1972) measured 8 months of precipitation at Pico del Este (East Peak) and on the windward and leeward slopes adjacent to the peak. Precipitation was consistently higher on the leeward slope (4013 mm) than on both the windward slope (3600 mm) and the peak (3200 mm). The 800 mm of additional precipitation measured on the leeward side versus that measured on the peak is significant, since the eastern half of Río Icacos basin rests on the leeward slope of the same ridge upon which Pico del Este is situated (Figure 3-2). Weaver's study raises the possibility that higher rainfall occurring on leeward slopes is not represented in the amounts measured at the Guabá and Río Icacos outlets.

Cloud moisture interception by vegetation is an additional source of moisture input to consider. The average cloud condensation level within the LEF is at 600 masl, and Río Icacos basin ranges from 616 masl to 840 masl. Weaver (1972) indicates that condensation of cloud droplets on vegetation within the Dwarf forest, which is found adjacent to the Río Icacos basin, is equivalent to approximately 10% of mean annual rainfall. It is logical to expect that cloud condensation provides greater moisture inputs during wet periods than during dry periods. The inputs provided by cloud condensation are not gaged and, thus, the total moisture input to the basin is underrepresented.

Errors within the streamflow record can not be dismissed as a potential contribution to the discrepancy noted in Figure 6-20, particularly during high-flow

wet periods. Errors in streamflow records may stem from instability in the stage-discharge relation, inaccurate measurements of stage, or misinterpretation of records (Díaz et al., 1996). The streamflow records for Guabá and Río Icacos are rated by the USGS as fair, and none of the daily discharge values used to compare Guabá and Icacos were estimated. Based on USGS standards, the daily discharge values measured at Guabá and Río Icacos should be within 15% of their actual value.

The inferences drawn from the above discussion tend to support the premise that precipitation receipts in portions of the Río Icacos basin are considerably greater than in other portions, and that precipitation measured at the Guabá and Icacos outlets underrepresents the basin average. Additionally, a lower accuracy of discharge measurements during periods of high flow likely contributes to errors within the streamflow record.

The comparable amounts of precipitation and runoff recorded at Guabá and Icacos during the dry period, and the similar runoff ratios, indicates that the hydrologic behavior of Guabá likely represents that of the whole basin. This conclusion serves to justify the application of the simulation model to storm events that occurred on the Guabá subcatchment.

TOPMODEL Parameter Determination

Initial estimates of the TOPMODEL parameters for Guabá basin were derived from field observations and from hydrometric records. The analysis of the baseflow recession curves (Figure 6-1) using the technique outlined in Chapter 5, resulted in a TOPMODEL recession parameter, M , that ranged from

0.027 to 0.073 m. The initial estimates fit within the range of values cited in the literature but resulted in a poor fit during model calibration and, thus, were adjusted accordingly. Similar results have been reported in other applications of TOPMODEL (Iorgulescu and Jordan, 1994).

The initial estimate of the basin average saturated transmissivity, T_0 , was derived using equation 5-14. The value of Q_0 , the subsurface drainage when the saturation deficit of the basin is zero, was assumed equal to the largest value of antecedent baseflow recorded for the 35 storm events listed in Table 5-1. The initial estimate of the saturated transmissivity ($0.1729 \text{ m}^2/\text{hr}$) proved to be too low and was revised upward during calibration. The presence of preferential flow may offer a possible explanation for the higher saturated transmissivity (Beven et al., 1995a). The observation by McDowell et al. (1992) that earthworm tubes are common to depths of 30 cm or more, in both the floodplain and upland soils, lends weight to this conjecture. Larsen and Torres-Sanchez (1992) also indicate that the presence of abundant macropores, 2 mm to 2 cm in size, enhances the permeability of LEF soils.

Within the LEF, and in the Río Icacos basin, the majority of roots are found in the top 20 cm of the soil (Frangi and Lugo, 1985; McDowell et al., 1992). The TOPMODEL root zone depth was set to this value. Laboratory analyses of soils within the Río Icacos basin by the USACE (Kennedy and Hicks, 1968) indicated a moisture content of 8.6 cm at field capacity and 3.5 cm at the wilting point, yielding a maximum available storage, SRMAX, of 5.1 cm in the root zone.

Each model run requires an estimate of the initial moisture deficit in the root zone. TOPMODEL is sensitive to this initialization parameter, which is difficult to determine. A value equal to 1/2 the maximum root zone storage was used for events during dry periods, and a value equal to 90% of maximum storage was used for wet period events. Model runs were initialized with input that preceded a target event by several days. Precipitation receipts prior to the target event served to stabilize the root zone storage and eliminate adverse affects on model results due to an inaccurate estimate of the initial root zone deficit.

The mean residence time per unit of storage deficit, t_d , controls the delivery of moisture from the unsaturated zone to the saturated zone (equation 4-11). A series of model runs revealed the relative insensitivity of TOPMODEL to small residence times. A hydrograph simulated for Guabá basin was not affected to a significant degree for values less than 50 hours. Model sensitivity rapidly increased for values greater than 50 hours and the resulting hydrograph was greatly attenuated and delayed, reflecting the response expected from slow-draining subsurface flow.

The residence time for Guabá basin was estimated based on the response of the water table to a precipitation event, as observed in two wells located in Río Icacos basin (McDowell et al., 1992). Figure 6-16 indicates a rapid rise in the water table, which began approximately 1 hour and 20 minutes after the initiation of rainfall. The rapid rise of the water table is characteristic of Icacos basin, as was noted during the year-long study by the USACE (Kennedy

and Hicks, 1968). Based on the water table observations, and bearing in mind the insensitivity of this parameter, the mean residence time was estimated to be 2 hours per unit of storage deficit.

Event Simulation

The initial model calibration was performed on the storm event of September 7, 1994, which occurred during a period of dry climatic conditions. The decay of the receding limb of the simulated hydrograph is less pronounced than that of the observed hydrograph, a discrepancy that was inherent in all model runs (Figure 6-21).

The reoccurrence of the discrepancy might imply that an alternate conceptualization is required for the equation (4-13) that characterizes subsurface flow. A superposed exponential formulation (equation 2-8), which incorporates multiple recession parameters (i.e. M) might be a possible choice. This, of course, introduces more model parameters, increases the model complexity, and increases the difficulty of model parameterization.

Two pronounced peaks occur on the receding limb of the simulated hydrograph, but are much less evident on the observed hydrograph. Model output indicates that the peaks issue from subsurface flow rather than from saturation-excess overland flow. The simulated peaks result from precipitation receipts that enter a root zone storage that is near capacity from preceding precipitation inputs. The portion of incoming moisture that exceeds root zone storage is shunted first to the unsaturated zone storage and, then, to the saturated zone storage. The basin average saturation deficit is decreased and,

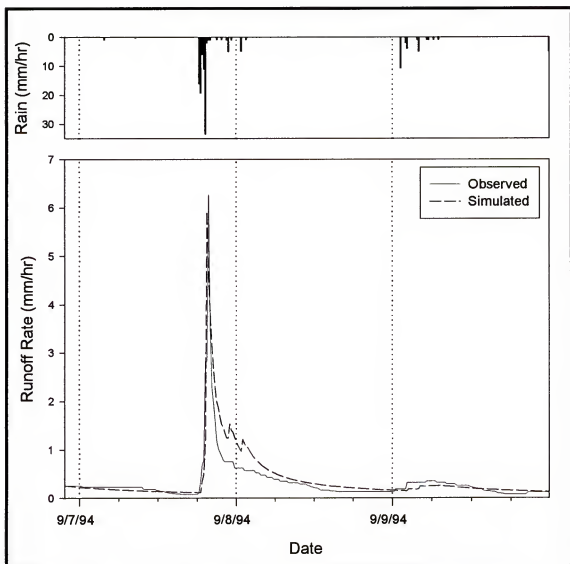


Figure 6-21. September 7, 1994 storm event calibration: observed versus simulated runoff from Guabá basin.

thus, the subsurface drainage increases according to equation 4-13, which results in the simulated peaks.

Model validation was performed on the storm event that occurred on June 11, 1994 (Figure 6-22). The prominent oscillation in runoff that exists at the beginning of the observed hydrograph, and lasts until the inception of the June 11 storm event, was noted to occur frequently in the Guabá discharge record, particularly during low flows and even in the absence of recorded precipitation. The cause is unknown but might be due to the inherent measurement accuracy of the gage at low flows in conjunction with USGS reporting standards.

The decay of the observed hydrograph that occurs prior to the June 11 storm event proceeds at a slower rate than does the decay of the simulated hydrograph. This discrepancy is symptomatic of the same problem that occurred during the calibration event and suggests that one exponential decay parameter is insufficient to characterize the hydrologic behavior of the basin. With a modified exponential parameter the simulated hydrograph would shift upward leading to a greatly improved fit.

Two events were selected from the period of wet climatic conditions and model calibration was performed on the event of October 28, 1996 (Figure 6-23). The only significant parameter adjustment was to raise M from 0.0043, the value during dry period events, to 0.0048. The lack of fit between the simulated and observed recession curves provides additional evidence that the single parameter exponential decay function does not adequately capture the recession characteristics. The time lag between the second observed

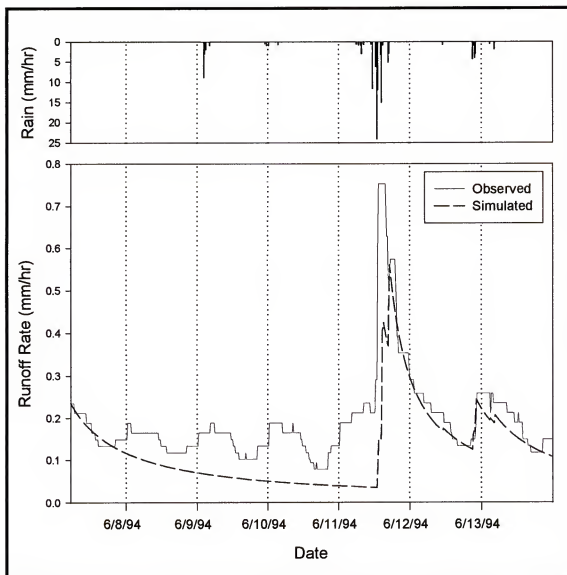


Figure 6-22. June 11, 1994 storm event validation: observed versus simulated runoff from Guabá basin.

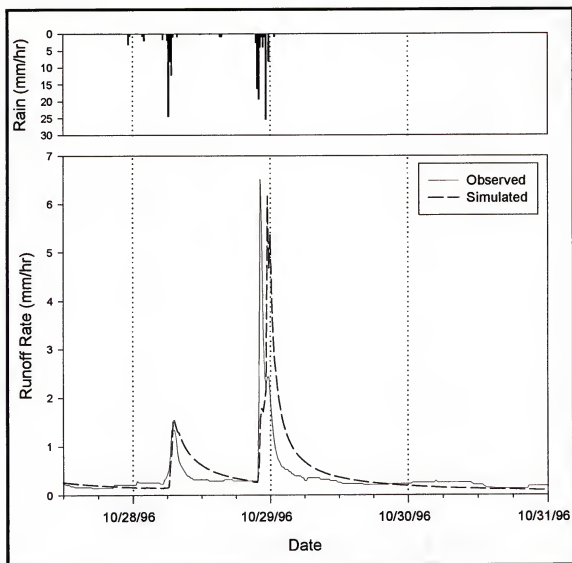


Figure 6-23. October 28, 1996 storm event calibration: observed versus simulated runoff from Guabá basin.

hydrograph peak and the simulated peak reflects the sensitivity of the root zone storage component of TOPMODEL. The depleted root zone storage was replenished with the precipitation inputs that occurred immediately prior to the second peak, which caused the delay.

The results obtained for the validation event of January 7, 1996 were significantly worse than the prior events (Figure 6-24). The initial peak is captured fairly well, but again the recession is poorly represented and the model incorrectly predicts additional peaks on the receding limb.

Areas of saturation were predicted to occur during each of the four simulations. Figure 6-25 illustrates the distribution of slopes and topographic index values in the Guabá subcatchment. Cells with high index values are associated with gentle slopes and/or a larger upslope contributing area and, thus, have a greater probability of reaching saturation. The linear bands of dark cells are associated with the stream channel. The summation of all cells that experienced saturation at any point during a particular storm event ranged from 0.03% of the subcatchment area during the June 11, 1994 event, to 2.5% during the September 7, 1994 event. The predicted contribution to total discharge from saturation-excess overland flow was less than 0.5% for each event. This indicates that, as expected, the major portion of event discharge issued from subsurface flow.

Discussion of TOPMODEL Simulations

The results from the calibration and validation model runs indicate that TOPMODEL can capture the gross hydrologic behavior of Guabá basin. There

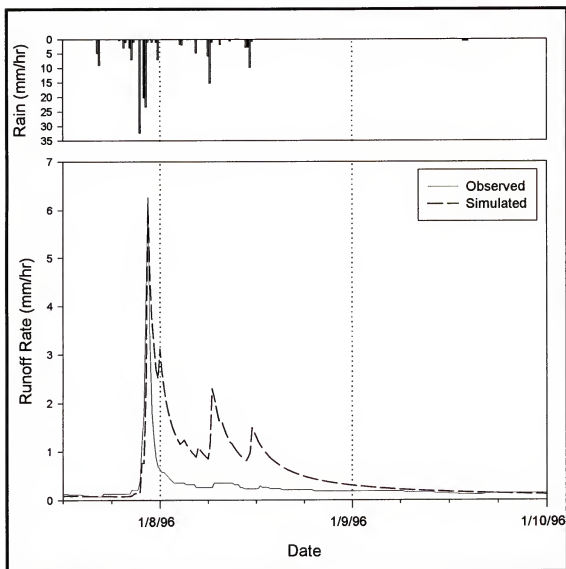


Figure 6-24. January 7, 1996 storm event validation: observed versus simulated runoff from Guabá basin.

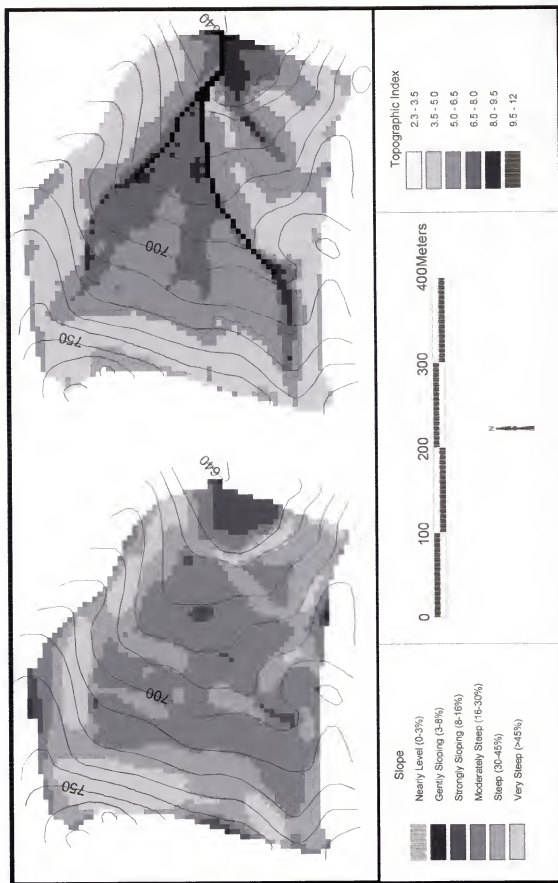


Figure 6-25. Slope ranges, 10-meter contours, and topographic index values for Guabá subcatchment.

are, however, significant departures between the simulated and observed hydrographs that must be explained. The inability of one parameter to capture the recession characteristics of the hydrograph may suggest that an additional moisture store is present in the basin, or that the behavior of the saturated zone does not conform to an exponential model (equation 4-13).

The soils in Río Icaos basin, as noted previously, overlie saprolite and their maximum combined thickness ranges from 10 meters on ridgetops, a few meters on hillslopes, to 24 meters on lower slopes (Larsen, 1997). The water table in several wells established near a basin tributary and on the adjacent slope, at depths of 180 and 210 cm, was observed to occur consistently above the well screens (McDowell et al., 1992). Daily observation of USACE wells, 122 cm deep and located on upland ridges (Figure 3-2), indicated a perched water table that fluctuated, over the course of one year, from approximately 76 cm deep to over 122 cm deep (Kennedy and Hicks, 1968). Both Figures 6-16 and 6-26 demonstrate that this perched water table is highly responsive to precipitation inputs.

Larsen (1997) indicates the presence of a deep water table that lies below the upper, permanent, perched water table. He further indicates that the deeper water table overlies bedrock with a topographic surface that differs significantly from that of the surface topography. Apparently, the deeper water store is buffered by the upper, perched water table and is, most likely, much less responsive. It is postulated that the discrepancies noted in the event simulations can be partly explained by the presence of upper and lower saturated stores, as

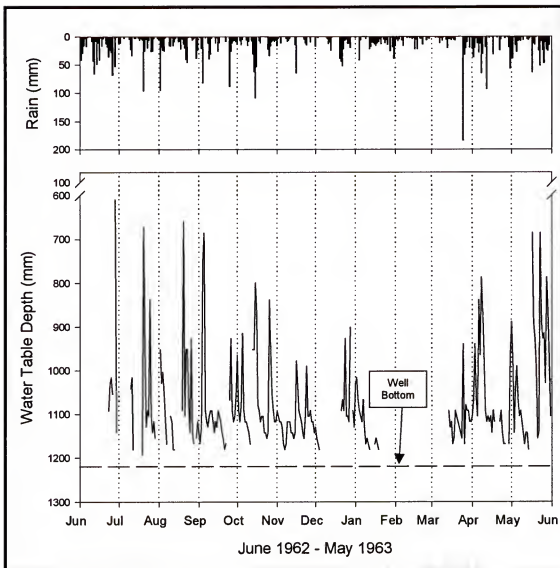


Figure 6-26. Water table response to daily rainfall at USACE site A.
Note: Gaps indicate time periods when the water table fell below the well depth.

represented by the perched water table and the deeper groundwater. The discharge from each of these stores will dominate the hydrograph at different times and will exhibit distinct recession characteristics.

The humid climate of the LEF assures that basin soils are maintained at high levels of moisture content and that the permanent perched water table is continually recharged. The dynamic and highly responsive nature of the upper, perched water table, as demonstrated in Figures 6-16 and 6-26, suggests that groundwater ridging may be a potential mechanism of streamflow generation within the Icacos basin. Groundwater ridging is associated with a zone of tension saturation (capillary fringe) that extends from the water table to, or near, the ground surface. Laboratory and field studies have demonstrated that, under the above conditions, small precipitation inputs can cause immediate and rapid water table rise, the magnitude of which is greater than that expected for a given input (Abdul and Gillham, 1984; Abdul and Gillham, 1989). The theory holds that the water table rise in the vicinity of the stream channel could result in a rapid increase in the hydraulic gradient and, thus, a rapid increase in subsurface discharge to the stream.

An examination of water table elevations and daily rainfall records from USACE site A (Figure 3-2) reveals an indirect relationship between the water table response to recharge volumes as reflected in daily precipitation amounts. Figure 6-27 illustrates changes in water table elevation as a function of precipitation receipts and of the depth to the water table prior to recharge. The top graph shows that, in general, the water table response per unit of

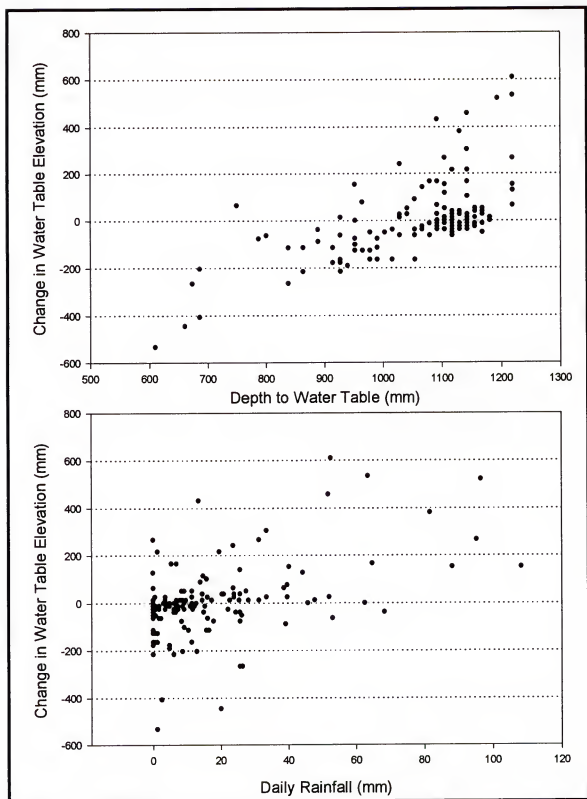


Figure 6-27. Change in water table elevation at USACE site A with respect to the initial water table depth and the daily rainfall.

precipitation was greater when the initial water table elevation was lower. This behavior might be related to a capillary fringe that is truncated as the water table rises. The Pearson Product-Moment Correlation is 0.62 for elevation change and the initial depth to the water table, and 0.49 between elevation change and daily precipitation. Together, precipitation receipts and depth to the water table explain 61% of the variation in changes in water table elevation. Figure 6-26 shows also that changes in water table elevation are more dynamic and of greater magnitude during the summer months.

The model results and the above discussion suggest that the hydrologic behavior of Río Icacos basin is more complex than can be handled by TOPMODEL. The version of TOPMODEL utilized in this study is optimized for an exponential saturated zone store and a water table that is quasi-parallel to the surface topography (Beven et al., 1995a). Furthermore, the model conceptualization does not account for the dynamic and variable water table response revealed by separate well studies conducted in the Río Icacos basin. Additionally, while TOPMODEL is able to model subsurface flow, its strength lies in the simulation of saturation-excess overland flow from variable source areas. The results indicate that basic model assumptions are violated and imply that modifications to TOPMODEL are needed to adequately capture the hydrologic behavior of both Guabá and Río Icacos basin.

CHAPTER 7

SUMMARY AND CONCLUSIONS

The objectives of this research were to 1) associate known runoff generating mechanisms with the physical and climatic characteristics of a site or region, 2) assess the hydrologic behavior of a humid montane watershed in Puerto Rico based on site specific characteristics, 3) conjecture as to the prevailing runoff mechanisms within the study basin, 4) analyze statistical relationships among storm event parameters and compare results with a similar basin for which runoff generating mechanisms are well described and, 5) assess the ability of topographic analysis to model and predict runoff generating mechanisms within the study basin.

Río Icacos, a 3.26 km² undisturbed forested basin, located in the Luquillo Experimental Forest of Puerto Rico was chosen for the research. The basin is relatively well instrumented, with a set of precipitation and discharge gages at the outlet and a set located in Guabá, an interior subcatchment of 0.13 km². Several field investigations have been conducted in the basin and considerable research has occurred in surrounding areas. The literature review, the characteristics of Río Icacos basin, and field observations suggested that the primary runoff mechanism within the basin consists of variable source areas primarily fed by subsurface flow. Hydraulic characteristics of basin soils and

field observations indicate that Infiltration-excess overland flow is limited to extreme events that occur infrequently. Saturation-excess overland flow, less common than subsurface flow, likely occurs on floodplains, adjacent to stream channels, during periods of prolonged precipitation.

Thirty-five distinct storm events were extracted from the 15-minute precipitation and discharge records. The events selected for analysis had similar volumes and temporal patterns, as reflected in the rainfall records from three local stations. Precipitation during each event was assumed to be uniformly distributed over the Río Icacos basin. Statistical tests were performed on precipitation and discharge parameters, extracted for each event, to test for the runoff processes hypothesized to occur on the basin. The correlation of the peak instantaneous runoff rate with the maximum precipitation intensity was stronger than expected for a basin that is dominated by subsurface flow. The relationship between quickflow and mean baseflow, a measure of basin wetness, was weaker than expected.

Further analysis on a subset of events specific to a dry climatic period, yielded a coefficient of correlation of 82.7, which is indicative of the strong linear relationship expected between measures of basin wetness and quickflow. The strength of the relationship conforms to expectations for a basin dominated by subsurface flow. The results suggest that, during wet periods, the basin experiences a persistently high moisture status, whereas during dry periods the soil has a greater capacity to buffer incoming precipitation receipts and, thus, modify the basin response.

An examination of rainfall/runoff characteristics and a review of historical rainfall records indicate that the upper reaches of the Río Icacos basin receives more precipitation than does the lower portion, particularly during wet periods. The spatial variability in rainfall distribution was not apparent during a dry climatic period, as reflected in a comparison of 15-minute discharge and precipitation records. The inability to adequately capture the variation in precipitation receipts, and the likelihood that precipitation recorded at Guabá and Icacos stations is less than the basin average, probably biased the results of the statistical analysis of storm event parameters. A better representation of basin precipitation during the storm events, particularly those that occurred during the wet period, likely would have resulted in higher peak rainfall intensities and greater volumes. The discrepancy noted between the wet and dry periods lends additional weight to the strong correlation between quickflow and basin wetness obtained for the 11 dry period events.

The Guabá subcatchment exhibited uniform rainfall and runoff characteristics during both wet and dry periods. It is recommended that the statistical methods be applied to the Guabá subcatchment to further corroborate the statistical results obtained for the Río Icacos basin. Discharge events for Guabá basin are more difficult to isolate due to the flow regime, and several events selected for Río Icacos were poorly represented in the Guabá record. Application of the methodology will require the extraction of additional events from the precipitation and discharge records. To obtain an adequate sample size of events additional years of record may be required.

A subset of storm events for the Guabá subcatchment was subjected to an analysis using a topography-based hydrologic model. TOPMODEL is a physically based, semi-distributed model that has been applied widely and requires few field measurements. The model is based on simplifying assumptions that relate the spatial variability of soil water content and lateral drainage to soil and topographic characteristics of the basin. The simple structure of the model and the need for few parameters make it an attractive alternative for data-poor areas. The model was selected because the hydrologic behavior of the study basin was believed to conform to the assumptions that underlie the model structure.

The simulated hydrographs conformed, in a general fashion, to the observed hydrographs for Guabá basin. However, the results did reveal hydrologic behavior that appears to violate some model assumptions. TOPMODEL simulates recession behavior with an exponential saturated zone store, while the basin hydrograph exhibited nonlinear behavior. The characteristic shape of the basin recession may be attributed to the presence of a deep groundwater store below an upper, permanent perched water table. The upper water table is quasi-parallel to the topographic surface and responds quickly to precipitation inputs. In contrast, the deeper water table reflects the bedrock topography, which does not conform to that of the surface. The differing characteristics inherent to the two stores result in the nonlinear recession behavior of the basin.

An additional complication stems from the upper, perched water table that responds in a dynamic and variable manner and, thus, contrasts with the relatively simple conceptual moisture stores contained in the TOPMODEL version utilized in the study. The behavior of the perched water table exhibits characteristics similar to those associated with the phenomena of groundwater ridging. Frequent precipitation inputs and nearly saturated soils likely are conducive to a rapid increase in the hydraulic gradient adjacent to streams and, thus, an increased subsurface flow and seepage into channels. Changes in water table elevation do not correspond directly to precipitation inputs but, rather, more strongly correlate with the initial water table depth. This behavior may offer a possible explanation for the lack of agreement between observed and simulated secondary peaks on some hydrographs.

The application of the topography-based hydrologic model has provided useful insights into the hydrologic behavior of the Río Icacos basin. The results from the modelling exercise indicate that, with modification, a topography-based hydrologic model, with minimal parameters, could provide an important management tool in humid montane watersheds. A logical follow-up is to incorporate the postulated mechanisms and then, for verification, re-apply the model to the storm events.

This research has provided new insights into the hydrologic behavior of a humid montane watershed located in the tropics. The study also highlights the inherent variability of physical and climatic characteristics within the Luquillo Experimental Forest, a relatively small area. The large degree of variability

dictates that the application of research results and conclusions to other locales must proceed with caution. The high natural variation within the humid montane region underscores the need for a denser instrumentation network to quantify the spatial and temporal variability of hydrologic processes. Long-term monitoring of soil moisture status and fluxes in relation to rainfall and runoff would provide important information with which to discern runoff mechanisms and hydrologic behavior. The strong research programs presently conducted by various entities within the LEF make the forest an ideal location for a hydrologic laboratory. The results from any long-term program, together with the results of the current study, are a step towards a more comprehensive assessment of hydrologic behavior in humid montane regions, as represented by the Río Icacos basin.

LIST OF REFERENCES

- Abdul, A. S. and R. W. Gillham. 1984. Laboratory studies of the effects of capillary fringe in stormflow generation. Water Resources Research 20: 691-8.
- _____. 1989. Field studies of the effects of the capillary fringe on streamflow generation. Journal of Hydrology 112: 1-18.
- Anderson, M. G. and T. P. Burt. 1978a. The role of topography in controlling throughflow generation. Earth Surface Processes 3: 331-44.
- _____. 1978b. Toward a more detailed field monitoring of variable source areas. Water Resources Research 14, no. 6: 1123-31.
- _____. 1990a. Process studies in hillslope hydrology: an overview. In Process studies in hillslope hydrology, ed. M. G. Anderson and T. P. Burt, 1-8. Chichester, UK: John Wiley & Sons.
- _____. 1990b. Subsurface runoff. In Process studies in hillslope hydrology, ed. M. G. Anderson and T. P. Burt, 365-400. Chichester, UK: John Wiley & Sons.
- ARC/INFO Version 7.2.1. 1998. Environmental Systems Research Institute, Inc., Redlands, CA.
- Arnold, J. G., P. M. Allen, R. Muttiah, and G. Bernhardt. 1995. Automated base flow separation and recession analysis techniques. Ground Water 33, no. 6: 1010-8.
- Augelli, J. P. 1951. Geography of agriculture and settlement in interior Puerto Rico: problems of upper Loiza Basin. Ph.D. diss., Harvard University.
- Bako, M. D. and D. A. Hunt. 1988. Derivation of baseflow recession constant using computer and numerical analysis. Hydrological Sciences - Journal 33, no. 4: 357-67.
- Barnes, B. S. 1939. The structure of discharge-recession curves. Transactions - American Geophysical Union 20: 721-5.
- Bedient, P. B. and W. C. Huber. 1989. Hydrology and floodplain analysis. Reading, MA: Addison-Wesley Publishing Company.

- Beinroth, F. H. 1969. An outline of the geology of Puerto Rico. Río Piedras, Puerto Rico: University of Puerto Rico, Agricultural Experiment Station, Bulletin 213.
- Betson, R. P. 1964. What is watershed runoff? Journal of Geophysical Research 69, no. April: 1541-52.
- Betson, R. P. and J. B. Marius. 1969. Source areas of storm runoff. Water Resources Research 5: 574-82.
- Beven, K. J. 1978. The hydrological response of headwater and sideslope areas. Hydrological Sciences Bulletin 23: 419-37.
- Beven, K. J. 1984. Infiltration into a class of vertically non-uniform soils. Hydrological Sciences - Journal 29, no. 4: 425-34.
- Beven, K. J. 1997. TOPMODEL: A critique. In Distributed hydrological modelling: Applications of the TOPMODEL concept, ed. K. J. Beven, 1-17. Chichester, UK: John Wiley & Sons.
- Beven, K. J. 1998. Welcome to the TOPMODEL/GLUE web pages. [<http://es-sv1.lancs.ac.uk/es/research/hfdg/topmodel.html>].
- Beven, K. J. and M. J. Kirkby. 1979. A physically-based variable contributing area model of basin hydrology. Hydrological Sciences Bulletin 24, no. 1: 43-69.
- Beven, K. J. and E. F. Wood. 1983. Catchment geomorphology and the dynamics of runoff contributing areas. Journal of Hydrology 65: 139-58.
- Beven, K. J., M. J. Kirkby, N. Schofield, and A. F. Tagg. 1984. Testing a physically-based flood forecasting model (TOPMODEL) for three U.K. catchments. Journal of Hydrology 69: 119-43.
- Beven, K. J., R. Lamb, P. Quinn, R. Romanowicz, and J. Freer. 1995a. TOPMODEL. In Computer models of watershed hydrology, ed. V. P. Singh, 627-68. Englewood, CO: Water Resources Publications.
- Beven, K. J., P. Quinn, R. Romanowicz, J. Freer, J. Fisher, and R. Lamb. 1995b. TOPMODEL. A users guide to the distribution version for DOS (95.02). Lancaster, UK: Centre for Research on Environmental Systems and Statistics, Lancaster University.
- Boccheciamp, R. A. 1977. Soil survey of the Humacao area of eastern Puerto Rico. Washington, DC: U.S. Department of Agriculture, Soil Conservation Service.

- Bonell, M. and J. Balek. 1993. Recent scientific developments and research needs in hydrological processes of the humid tropics. In Hydrology and water management in the humid tropics, ed. M. Bonell, M. M. Hufschmidt, and J. S. Gladwell. Cambridge: Cambridge University Press.
- Bonell, M. and D. A. Gilmour. 1978. The development of overland flow in a tropical rain-forest catchment. Journal of Hydrology 39: 365-82.
- Bonell, M., D. A. Gilmour, and D. G. Sinclair. 1981. Soil hydraulic properties and their effect on surface and subsurface water transfer in a tropical rainforest catchment. Hydrological Sciences Bulletin 26, no. 1/3: 1-18.
- Bras, R. L. 1990. Hydrology: An introduction to hydrologic science. Reading, MA: Addison-Wesley Publishing Company, Inc.
- Briscoe, C. B. 1966. Weather in the Luquillo mountains of Puerto Rico. Washington, DC: U.S. Department of Agriculture Forest Service, Research Paper ITF-3.
- Brown, S., A. E. Lugo, S. Silander, and L. Liegel. 1983. Research history and opportunities in the Luquillo experimental forest. U.S. Forest Service, Southern Forest Experiment Station, General Technical Report SO-44.
- Bruijnzeel, L. A. 1983. Evaluation of runoff sources in a forested basin in a wet monsoonal environment: A combined hydrological and hydrochemical approach. Hydrology of humid tropical regions: Aspects of tropical cyclones, hydrological effects of agriculture and forestry practice; Proceedings of a symposium held during the XVIIIth General Assembly of the International Union of Geodesy and Geophysics at Hamburg, Federal Republic of Germany, 15-27 August 1983, edited by R. Keller, 165-74. Washington, DC: International Association of Hydrological Sciences.
- Brutsaert, W. and J. L. Nieber. 1977. Regionalized drought flow hydrographs from a mature glaciated plateau. Water Resources Research 13, no. 3: 637-43.
- Burt, T. P. 1986. Runoff processes and solutional denudation rates on humid temperate hillslopes. In Solute processes, ed. S. T. Trudgill. Chichester, UK: John Wiley & Sons.
- _____. 1989. Storm runoff generation in small catchments in relation to the flood response of large basins. In Floods: Hydrological, sedimentological and geomorphological implications, ed. K. Beven and P. Carling, 11-35. Chichester, UK: John Wiley & Sons.

- Calvesbert, R. J. 1980. Climate of Puerto Rico and the U.S. Virgin Islands. Climatology of the United States, no. 60. Asheville, NC: National Oceanic and Atmospheric Administration, Environmental Data Service, National Climatic Data Center.
- Carson, M. A. and M. J. Kirkby. 1972. Hillslope form and process. Cambridge: Cambridge University Press.
- Carter, M. M. and J. B. Elsner. 1996. Convective rainfall regions of Puerto Rico. International Journal of Climatology 16: 1033-1043.
- Chorley, R. J. 1978. The hillslope hydrological cycle. In Hillslope hydrology, ed. M. J. Kirkby, 1-42. New York: John Wiley.
- Chow, V. T., D. R. Maidment, and L. W. Mays. 1988. Applied hydrology. New York: McGraw-Hill, Inc.
- Crossley, D. A. and W. T. Swank. 1988. Forest hydrology and ecology at Coweeta. New York: Springer-Verlag.
- Díaz, P. L., Z. Aquino, C. Figueroa-Alamo, R. J. Vachier, and A. V. Sánchez. 1997. Water resources data. Puerto Rico and the U.S. Virgin Islands, Water Year 1996. San Juan, Puerto Rico: U.S. Department of the Interior, Geological Survey, U.S. Geological Survey Water-Data Report PR-96-1.
- Dingman, S. L. 1984. Fluvial hydrology. New York: W.H. Freeman and Company.
- Dunne, T. 1978. Field studies of hillslope flow processes. In Hillslope hydrology, ed. M. J. Kirkby, 227-93. New York: John Wiley & Sons.
- _____. 1983. Relation of field studies and modelling in the production of storm runoff. Journal of Hydrology 65: 25-48.
- Dunne, T. and R. D. Black. 1970. An experimental investigation of runoff production in permeable soils. Water Resources Research 6: 478-90.
- Dunne, T., T. R. Moore, and C. H. Taylor. 1975. Recognition and prediction of runoff-producing zones in humid regions. Hydrological Sciences Bulletin 20, no. 3: 305-27.
- Durand, P., A. Robson, and C. Neal. 1992. Modelling the hydrology of submediterranean montane catchments (Mont-Lozère, France) using TOPMODEL: initial results. Journal of Hydrology 139: 1-14.
- EarthInfo, Inc. 1995. Climatedata. EarthInfo, Inc., Boulder, CO.

- EarthInfo, Inc. 1996. CD² USGS daily values. EarthInfo, Inc., Boulder, CO.
- Frangi, J. L. and A. E. Lugo. 1985. Ecosystem dynamics of a subtropical floodplain forest. Ecological Monographs 55: 351-69.
- Freeze, R. A. 1972. Role of subsurface flow in generating stream runoff. 2. Upstream source areas. Water Resources Research 8: 1273-83.
- _____. 1974. Streamflow generation. Reviews of Geophysics and Space Physics 12, no. 4: 627-47.
- García-Martinó, A. R., G. S. Warner, F. Scatena, and D. L. Civco. 1996. Rainfall, runoff and elevation relationships in the Luquillo Mountains of Puerto Rico. Caribbean Journal of Science 32, no. 4: 413-24.
- Gash, J. H. C. 1979. An analytical model of rainfall interception by forests. Quarterly Journal of the Royal Meteorological Society 105: 43-55.
- Gilmour, D. A. and M. Bonell. 1979. Runoff processes in tropical rainforests with special reference to a study in north-east Australia. In Geographical approaches to fluvial processes, ed. A. J. Pitty. Norwich, UK: GeoBooks.
- GTCO Corporation. 1986. DIGI-PAD type 5A user's manual. Columbia, MD: GTCO Corporation.
- Guzmán-Rios, S. 1989. Suspended sediment data in the Upper Río Grande de Loíza basin, Puerto Rico. Denver, CO: U.S. Department of the Interior, Geological Survey, Open-File Data Report 88-324.
- Hall, F. R. 1968. Base flow recessions-a review. Water Resources Research 4, no. 5: 973-83.
- Hewlett, J. D. 1961. Soil moisture as a source of base-flow from steep mountain watersheds. USDA, FS, SEFES, Station Paper. 132.
- Hewlett, J. D. and A. R. Hibbert. 1967. Factors affecting the response of small watersheds to precipitation in humid areas. In Forest hydrology: proceedings of a National Science Foundation advanced science seminar held at The Pennsylvania State University, University Park, Pennsylvania August 29-September 10 1965, edited by W. E. Sopper and H. W. Lull, 275-298. Oxford: Pergamon Press.
- Hewlett, J. D. and W. L. Nutter. 1972. Varying source area of streamflow from upland basins. Proceedings of the symposium on interdisciplinary aspects of watershed management, August 3-6 1970, Montana State University, Bozeman, Montana, by the American Society of Civil Engineers, 65-83. New York: American Society of Civil Engineers.

- Hirsch, R. M., D. R. Helsel, T. A. Cohn, and E. J. Gilroy. 1993. Statistical treatment of hydrologic data. In Handbook of hydrology, ed. D. R. Maidment, 17.1-17.55. New York: McGraw-Hill, Inc.
- Hornberger, G. M., K. J. Beven, B. J. Cosby, and D. E. Sappington. 1985. Shenandoah watershed study: calibration of a topography-based, variable contributing model to a small forested catchment. Water Resources Research 21: 1841-50.
- Horton, R. E. 1933. The role of infiltration in the hydrologic cycle. Transactions - American Geophysical Union 17: 296-302.
- Hromadka, T. V. 1987. Complex watershed models in flood control: Questions of credibility. Computational Hydrology 87: Proceedings of the 1st International Conference, Anaheim, California, U.S.A., July 1987, edited by T. V. Hromadka and R. H. McCuen, A34-A37. Mission Viejo, CA: Lighthouse Publications.
- Institute for Tropical Ecosystem Studies. 1997. Luquillo Experimental Forest LTER. [<http://sunceer.upr.clu.edu/index.htm>].
- Iorgulescu, I. and J. P. Jordan. 1994. Validation of TOPMODEL on a small Swiss catchment. Journal of Hydrology 159: 255-73.
- Jordan, C. F. 1970. Flow of soil water in the lower montane tropical rain forest. In A tropical rain forest, ed. H. T. Odum and R. F. Pigeon, H199-H200. Springfield, Virginia: National Technical Information Service.
- Kennedy, J. G. and T. E. Hicks. 1968. Trafficability predictions in tropical soils. Report 6, Puerto Rico study no. 2 (March 1962-Nov. 1963). Vicksburg, MS: U.S. Army Engineer Waterways Experiment Station, Corps of Engineers.
- Kirkby, M. 1975. Hydrograph modelling strategies. In Processes in physical and human geography, ed. R. Peel, M. Chisholm, and P. Haggett, 69-90. London: Heinemann Educational Books.
- Kirkby, M. J. 1988. Hillslope runoff processes and models. Journal of Hydrology 100: 315-39.
- Kirkby, M. J. and R. J. Chorley. 1967. Throughflow, overland flow, and erosion. Bulletin of the International Association of Scientific Hydrology 12: 5-21.
- Larsen, M. C. 1997. Tropical geomorphology and geomorphic work: A study of geomorphic processes and sediment and water budgets in montane humid-tropical forested and developed watersheds, Puerto Rico. Ph.D. diss., University of Colorado.

- Larsen, M. C., P. D. Collar, and R. F. Stallard. 1992. Research plan for the investigation of water, energy, and biogeochemical budgets in the Luquillo Mountains, Puerto Rico. U.S. Geological Survey, Open-File Report 92-150.
- Larsen, M. C. and A. J. Torres-Sánchez. 1992. Landslides triggered by the rainfall associated with Hurricane Hugo, eastern Puerto Rico, September 1989. Caribbean Journal of Science 28, no. 3-4: 113-20.
- Linsley, R. K., M. A. Kohler, and J. L. H. Paulhus. 1982. Hydrology for engineers. 3d ed. New York: McGraw-Hill.
- Lugo, A. E. 1986. Water and the ecosystems of the Luquillo Experimental Forest. New Orleans, LA: U.S. Department of Agriculture, Forest Service, Southern Forest Experiment Station.
- Lugo, A. E. and F. N. Scatena. 1992. Epiphytes and climate change research in the Caribbean: a proposal. Selbyana 13: 123-30.
- Lugo-López, M. A., J. Juárez Jr., and J. A. Bonnet. 1968. The relative infiltration rate of Puerto Rican soils. Journal of Agriculture of the University of Puerto Rico 53, no. 3: 233-40.
- Lugo-López, M. A., J. M. Wolf, and R. Pérez-Escobar. 1981. Water loss, intake, movement, retention and availability in major soils of Puerto Rico. Río Piedras, Puerto Rico: University of Puerto Rico, Agricultural Experiment Station, Bulletin 264.
- McDowell, W. H., W. B. Bowden, and C. E. Asbury. 1992. Riparian nitrogen dynamics in two geomorphologically distinct tropical rain forest watersheds: Subsurface solute patterns. Biogeochemistry 18: 53-75.
- Meyerhoff, H. A. 1933. Geology of Puerto Rico. Río Piedras, Puerto Rico: University of Puerto Rico.
- Monroe, W. H. 1980. Some tropical landforms of Puerto Rico. U.S. Department of Interior, Geological Survey Professional Paper 1159.
- Moore, I. D., R. B. Grayson, and A. R. Ladson. 1991. Digital terrain modelling: A review of hydrological, geomorphological and biological applications. Hydrological Processes 5: 3-30.
- Moore, I. D., S. M. Mackay, P. J. Wallbrink, G. J. Burch, and E. M. O'Loughlin. 1986. Hydrologic characteristics and modelling of a small forested catchment in southeastern New South Wales. Pre-logging condition. Journal of Hydrology 83: 307-35.

- Musk, L. F. 1988. Weather systems. Cambridge Topics in Geography: Second Series. Cambridge: Cambridge University Press.
- Nash, J. E. and J. V. Sutcliffe. 1970. River flow forecasting through conceptual models. Part 1 - A discussion of principles. Journal of Hydrology 10: 282-90.
- Nathan, R. J. and T. A. McMahon. 1990. Evaluation of automated techniques for base flow and recession analysis. Water Resources Research 26, no. 7: 1465-73.
- National Resources Conservation Service, Caribbean Area. 1998. [<http://www.ga.nrcs.usda.gov/mlra15/cbsoilnt/prmptxt.html>].
- National Soil Survey Center. 1998. National Soil Data Access Facility. [<http://www.statlab.iastate.edu/soils/nsdaff/>].
- Odum, H. T. 1970. Rain forest structure and mineral-cycling homeostasis. In A tropical rain forest, ed. H. T. Odum and R. F. Pigeon, H3-H52. Springfield, VA: National Technical Information Service.
- Odum, H. T., G. Drewry, and J. R. Kline. 1970. Climate in El Verde. In A tropical rain forest, ed. H. T. Odum and R. F. Pigeon, B347-B418. Springfield, VA: National Technical Information Service.
- O'Loughlin, E. M. 1986. Prediction of surface saturation zones in natural catchments by topographic analysis. Water Resources Research 22, no. 5: 794-804.
- Pearce, A. J., M. K. Stewart, and M. G. Sklash. 1986. Storm runoff generation in humid headwater catchments. 1. Where does the water come from? Water Resources Research 22, no. 8: 1263-72.
- Pethick, J. P. 1984. An introduction to coastal geomorphology. London: Edward Arnold.
- Picó, R. 1974. The geography of Puerto Rico. Chicago: Aldine Publishing Company.
- Pierson, T. C. 1980. Piezometric response to rainstorms in forested hillslope drainage depressions. Journal of Hydrology 19: 1-10.
- Pilgrim, D. H. 1966. Radioactive tracing of storm runoff on a small catchment, I. Experimental technique. Journal of Hydrology 4: 209-305.
- Ponce, V. M. 1989. Engineering hydrology: Principles and practices. Englewood Cliffs, NJ: Prentice-Hall.

- Quinn, P. F. and K. J. Beven. 1993. Spatial and temporal predictions of soil moisture dynamics, runoff, variable source areas and evapotranspiration for Plynlimon, Mid-Wales. Hydrological Processes 7: 425-48.
- Quinn, P. F., K. J. Beven, and R. Lamb. 1995. The $\ln(a/\tan\beta)$ index: How to calculate it and how to use it within the TOPMODEL framework. Hydrological Processes 9: 161-82.
- Rawitz, E., E. T. Engman, and G. D. Cline. 1970. Use of the mass balance method for examining the role of soils in controlling watershed performance. Water Resources Research 6, no. 4: 1115-23.
- Riggs, H. C. and M. G. Wolman. 1990. Introduction. In The geology of North America, Volume D-1, Surface water hydrology, ed. M. G. Wolman and H. C. Riggs, 1-10. Boulder, CO: The Geological Society of America.
- Romanowicz, R. 1997. A MATLAB implementation of TOPMODEL. In Distributed hydrological modelling: Applications of the TOPMODEL concept, ed. K. J. Beven, 107-22. Chichester, UK: John Wiley & Sons.
- Rutter, A. J., K. A. Kershaw, P. C. Robins, and A. J. Morton. 1971. A predictive model of rainfall interception in forests. I. Derivation of the model from observations in a stand of Corsican pine. Agricultural Meteorology 9: 367-84.
- Scatena, F. N. 1989. An introduction to the physiography and history of the Bisley experimental watersheds in the Luquillo Mountains of Puerto Rico. New Orleans, LA: U.S. Department of Agriculture, Forest Service, Southern Experiment Station, S0-72.
- _____. 1990. Watershed scale rainfall interception on two forested watersheds in the Luquillo Mountains of Puerto Rico. Journal of Hydrology 113: 89-102.
- Sherman, L. K. 1932. Streamflow from rainfall by the unit hydrograph method. Engineering News Record 108: 501-5.
- Shuttleworth, W. J. 1993. Evaporation. In Handbook of hydrology, ed. David R. Maidment, 4.1-4.53. New York: McGraw-Hill, Inc.
- Singh, V. P. 1988. Hydrologic systems-volume I. Rainfall-runoff modeling. Englewood Cliffs, NJ: Prentice Hall.
- Sklash, M. G. and R. N. Farvolden. 1979. The role of groundwater in storm runoff. Journal of Hydrology 43: 45-65.

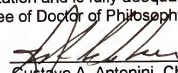
- Sklash, M. G., R. N. Farvolden, and P. Fritz. 1976. A conceptual model of watershed response to rainfall, developed through the use of oxygen-18 as a natural tracer. Canadian Journal of Earth Sciences 13: 271-83.
- Sklash, M. G., M. K. Stewart, and A. J. Pearce. 1986. Storm runoff generation in humid headwater catchments 2. A case study of hillslope and low-order stream response. Water Resources Research 22, no. 8: 1273-82.
- Soil Survey Division staff. 1993. Soil Survey Manual. United States Department of Agriculture Handbook No. 18. Washington, DC: U.S. Department of Agriculture.
- Strahler, A. N. 1969. Physical geography. 3rd ed. New York: John Wiley.
- Szilagyi, J. and M. B. Parlange. 1998. Baseflow separation based on analytical solutions of the Boussinesq equation. Journal of Hydrology 204: 251-60.
- Tallaksen, L. M. 1995. A review of baseflow recession analysis. Journal of Hydrology 165: 349-70.
- Tischendorf, W. G. 1969. Tracing stormflow to varying source areas in a small forested watershed in the southeastern Piedmont. Ph.D. diss., University of Georgia.
- Trewartha, G. T. and L. H. Horn. 1980. An introduction to climate. 5th ed. New York, NY: McGraw-Hill, Inc.
- U.S. Geological Survey. 1990. Digital elevation models, Data users guide 5. Reston, VA: U.S. Department of the Interior.
- U.S. Geological Survey. 1998. Puerto Rico NWIS-W data retrieval. [<http://waterdata.usgs.gov/nwis-w/PR/>].
- Van de Griend, A. A. and E. T. Engman. 1985. Partial area hydrology and remote sensing. Journal of Hydrology 81: 211-51.
- Veen, A. W. L. and A. J. Dolman. 1989. Water dynamics of forests: One-dimensional modeling. Progress in Physical Geography 13: 471-506.
- Velleman, P. F. 1997. DataDesk Version 6.0: Statistics Guide. Ithaca, NY: Data Description, Inc.
- Viessman, W., G. L. Lewis, and J. W. Knapp. 1989. Introduction to hydrology. 3rd ed. New York: Harper & Row, Publishers, Inc.
- Wadsworth, F. H. 1951. Forest management in the Luquillo Mountains. I. The setting. Caribbean Forester 12: 93-114.

- Wadsworth, F. H. and J. A. Bonnet. 1951. Soil as a factor in the occurrence of two types of montane forest in Puerto Rico. Caribbean Forester 12: 67-70.
- Weaver, P. L. 1972. Cloud moisture interception in the Luquillo mountains of Puerto Rico. Caribbean Journal of Science 12(3-4): 129-44.
- Weaver, P. L. 1986. Hurricane damage and recovery in the montane forests of the Luquillo mountains of Puerto Rico. Caribbean Journal of Science 22, no. 1-2: 53-70.
- Weyman, D. R. 1970. Throughflow on hillslopes and its relation to the stream hydrograph. Bulletin of the International Association of Scientific Hydrology 15, no. 3: 25-33.
- _____. 1973. Measurement of the downslope flow of water in a soil. Journal of Hydrology 20: 267-88.
- Whipkey, R. Z. 1965. Subsurface stormflow from forested slopes. Bulletin of the International Association of Scientific Hydrology 10, no. 2: 74-85.
- Wilson, E. M. 1990. Engineering hydrology. 4th ed. Basingstoke, UK: Macmillan.

BIOGRAPHICAL SKETCH

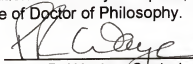
Robert Swett was born June 16, 1954 in Fort Lee, Virginia. He attended high school in Maine and, upon graduation, served in the United States Navy as an electronics technician. He received a Bachelor of Science in forest management from the University of Maine at Orono. Upon graduating with distinction he served three years as a Peace Corps volunteer in Guatemala, where he established a forest nursery and initiated several conservation projects in the rural highlands. Robert received a Master of Arts degree in Latin American studies from the University of Florida. His thesis research focused on an assessment of fuelwood needs and was conducted in Honduras. While enrolled in the Ph.D. program at the University of Florida, Robert has worked as a research associate and as the manager of the Cartographic Research Laboratory in Applied Geography. He has been married to Maria Antonieta Leiva of San Nicolás, Honduras, for thirteen years and they have three children, Miguel, Elizabeth, and Christopher.

I certify that I have read this study and that in my opinion it conforms to acceptable standards of scholarly presentation and is fully adequate, in scope and quality, as a dissertation for the degree of Doctor of Philosophy.



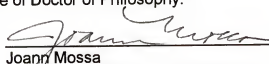
Gustavo A. Antonini, Chair
Professor of Geography

I certify that I have read this study and that in my opinion it conforms to acceptable standards of scholarly presentation and is fully adequate, in scope and quality, as a dissertation for the degree of Doctor of Philosophy.



Peter R. Waylen, Cochair
Professor of Geography

I certify that I have read this study and that in my opinion it conforms to acceptable standards of scholarly presentation and is fully adequate, in scope and quality, as a dissertation for the degree of Doctor of Philosophy.

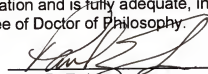


Joann Mossa
Associate Professor of Geography

I certify that I have read this study and that in my opinion it conforms to acceptable standards of scholarly presentation and is fully adequate, in scope and quality, as a dissertation for the degree of Doctor of Philosophy.

Kenneth L. Campbell
Professor of Agricultural and
Biological Engineering

I certify that I have read this study and that in my opinion it conforms to acceptable standards of scholarly presentation and is fully adequate, in scope and quality, as a dissertation for the degree of Doctor of Philosophy.



Paul D. Zwick
Associate Professor of
Urban and Regional Planning

This dissertation was submitted to the Graduate Faculty of the Department of Geography in the College of Liberal Arts and Sciences and to the Graduate School and was accepted as partial fulfillment of the requirements for the degree of Doctor of Philosophy.

May, 1999

Dean, Graduate School